Exploring the ecophysiology of anaerobic communities of methanotrophic archaea and sulfate-reducing bacteria

Peer H. A. Timmers

Propositions

1. When studying anaerobic methanotrophy, one should always consider methanogenesis.

(this thesis)

2. Expecting that phylogenetically unrelated methanotrophic clades are metabolically similar is not even close to 'comparing apples and pears'.

(this thesis)

3. Social media could be used as a platform that substitutes scientific publication as we know it.

4. A critical and open-minded view on fairly unknown topics is essential for scientific progress.

5. Apples and pears can be compared since they do belong to the same subfamily and some pears even look like apples (e.g. *Pyrus pyrifolia*).

6. People that do not believe in natural selection are subjected most to it.

7. Concerns about privacy continue to be raised, whereas concerns about indoctrination by global commercial radio are never heard.

Exploring the ecophysiology of anaerobic communities of methanotrophic archaea and sulfate-reducing bacteria

Peer H.A. Timmers

Thesis committee

Promotor
Prof. Dr Alfons J.M. Stams
Personal chair at the Laboratory of Microbiology
Wageningen University

Co-promotor
Dr Caroline M. Plugge
Associate Professor, Laboratory of Microbiology
Wageningen University

Other members
Prof. Dr Albert J.H. Janssen, Wageningen University
Dr Katharina F. Ettwig, Radboud University Nijmegen, The Netherlands
Prof. Dr Gerard Muyzer, University of Amsterdam, The Netherlands
Prof. Dr Stefan Schouten, Royal Netherlands Institute for Sea Research (NIOZ), Den Burg, The Netherlands

Exploring the ecophysiology of anaerobic communities of methanotrophic archaea and sulfate-reducing bacteria

Peer H.A. Timmers

Thesis

submitted in partial fulfilment of the requirements for the degree of doctor

at Wageningen University

by the authority of the Rector Magnificus

Prof. Dr A.P.J. Mol,

in presence of the

Thesis Committee appointed by the Academic Board

to be defended in public

on Friday 4 December 2015

at 4 p.m. in the Aula.

Voor Arie

Table of Contents

CHAPTER 1

GENERAL INTRODUCTION AND THESIS OUTLINE

Methane oxidation in marine sediments

Atmospheric methane (CH_4) is together with carbon dioxide (CO_2) a most important greenhouse gas on earth and it accounts for 20% of all the infrared radiation captured in the atmosphere (Dale et al 2006). The specific infrared capture of methane is 21 times higher than of CO_2. Methane is biologically produced in anoxic environments such as swamps, tundra's, rice paddy fields, intestinal systems, landfills, anoxic wastewater treatment facilities and anoxic freshwater and marine sediments. Marine sediments produce most methane, making them the largest methane reservoirs on earth, with estimates of around 3 times the terrestrial biomass (Dale et al 2006). The main sources of methane in marine sediments are biogenic methane formation (i.e. organic matter degradation) and to a lesser extent abiotic methane formation (i.e. thermogenic and geochemical processes) (Reeburgh 2007, Thauer et al 2008). The produced methane only partly reaches the water column through seeps, vents and mud volcanoes or via diffusion from anoxic sediments and dissolution of methane clathrate hydrates.

In seeps, hydrothermal vents and mud volcanoes, methane extrudes with high flux from deep layers and the upper layer of the sediment is therefore rich in methane (>80 mM). In these environments, organic matter is readily available and can have a high abundance of chemosynthetic communities, such as at the seeps of Hydrate Ridge (Boetius and Suess 2004) and at the Gulf of Mexico (Joye et al 2004). In gassy coastal sediments and diffusive sediments, methane only derives from *in situ* organic matter degradation, and a so called sulfate-methane transition zone (SMTZ) exists where methane from deeper layers diffuses upwards and meets sulfate that diffuses downwards from the sea water (Fig 1) (Bussmann et al 1999, Harrison et al 2009, Krüger et al 2005, Martens and Berner 1974, Murray et al 1978, Niewöhner et al 1998, Reeburgh 1976, Thomsen et al 2001, Treude et al 2005a, Treude et al 2005b, Wu et al 2006).

In gassy coastal sediments, this SMTZ is typically shallow, with decimeters to meters below the sediment surface. These sediments are rich in organic matter that fuels high methane production rates and release methane gas bubbles to the hydrosphere due to super saturation (Martens et al 1998). In diffusive sediments that are low in organic matter, methane concentrations are lower ($\pm$1mM), sulfate concentrations are lower than the overlying seawater and most organic matter is already degraded at this level. Here, the SMTZ is lowered to some meters below the sea floor and methane does not escape to the hydrosphere since production rates are low (Iversen and Jørgensen 1985). These sediments are therefore coined 'diffusive' or 'quiescent sediments' as compared to the high microbial activity and competition in non-diffusive systems (Alperin and Hoehler 2010). In this thesis, studies were mainly performed with a gassy coastal sediment from Eckernförde Bay, Germany (Treude et al 2005b).
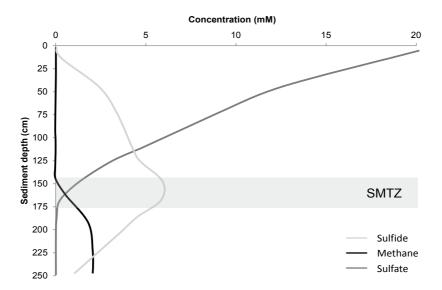
Figure 1 Methane, sulfate and sulfide (mM) profiles in a typical marine sediment. The profile shows the sulfate-methane transition zone (SMTZ, grey area). The picture was adapted from actual measurements performed in a sediment core taken from station M1 at Arhus Bay, Denmark.

When the SMTZ was firstly studied, it was postulated that this typical profile was due to competition of sulfate-reducing bacteria (SRB) and methanogenic archaea for mutual substrates such as H_2/CO_2 (Martens and Berner 1974). It was, however, also speculated that methane was produced at the same rate throughout the sediment column, but was consumed by SRB where sulfate and methane intersect according to reaction 1.

$$CH_4 + SO_4^{2-} + 2H^+ \rightarrow H_2S + CO_2 + 2\,H_2O \quad (1)$$

This theory was supported by other sediment profile studies and laboratory incubations (Barnes and Goldberg 1976, Martens and Berner 1977, Murray et al 1978, Panganiban et al 1979, Reeburgh 1976). Radiotracer studies revealed for the first time that methane was indeed oxidized anaerobically and that this activity was highest at the peak of the SMTZ where methane and sulfate intersect (Reeburgh 1980). More radiotracer studies and stable carbon isotopic data showed *in situ* $^{13}CH_4$ enrichment which is typical for biological methane oxidation since $^{12}CH_4$ is oxidized faster than $^{13}CH_4$. This results in a higher percentage of heavy $^{13}CH_4$ in the environment (Alperin et al 1988) and in ^{13}C-depletion in specific lipids unique for archaea and sulfate-reducing bacteria (reviewed in Valentine and Reeburgh 2000, Hinrichs and Boetius 2002). With increasing evidence for sulfate-dependent anaerobic oxidation of methane (AOM) in different marine sediments, it was estimated that more than 90% of the annually produced methane was consumed in anoxic marine sediments before it could reach the hydrosphere (reviewed in Hinrichs and Boetius 2002, Knittel and Boetius 2009, Reeburgh 2007).

AOM coupled to sulfate reduction (SR) thus occurs *in situ* at the SMTZ. Moreover, *ex situ* experiments with specific inhibitors for both methanogenesis and SR showed that both AOM and SR are interdependent (Hansen et al 1998, Hoehler et al 1994, Krüger et al 2003, Nauhaus et al 2005). *In vitro* studies showed no sulfide production in the absence of methane (Nauhaus et al 2002) and no AOM without sulfate addition (Nauhaus et al 2005), indicating that AOM and SR are directly coupled. Therefore, it was considered that AOM coupled SR is a syntrophic process that involved methanogens acting in reverse together with SRB that are metabolically interdependent on each other.

Trace methane oxidation and anaerobic methane oxidation

Pure strains of methanogens were found to be able to oxidize methane, but only during net methane production (Zehnder and Brock 1979). This process was demonstrated by labelled methane addition to pure cultures of methanogens that showed production of labelled CO_2 during net methane production. This characteristic was confirmed in studies on other pure cultures (Harder 1997, Moran et al 2005, Moran et al 2007), granular sludge (Harder 1997, Meulepas et al 2010a, Zehnder and Brock 1980), and on freshwater and terrestrial environments (Blazewicz et al 2012, Zehnder and Brock 1980). The process was later called 'trace methane oxidation' (TMO), since the CO_2 is formed in trace amounts from methane during net methane production (Moran et al 2005). In anoxic sludge, endogenous CO_2 production coincides with hydrogen production from organic matter degradation (Demirel 2014). In a closed system with a mixed community, methane production from H_2/CO_2 will therefore decrease in time when endogenous substrates are depleted, and thus TMO and methanogenesis will decrease proportionally (Fig 2). TMO was thought of to be an active metabolic process and not an enzymatic back flux, since the amount of methane oxidation was different between different species of methanogens grown on the same methanogenic substrate and was different within the same species when grown on different substrates (Moran et al 2005). During hydrogenotrophic and methylotrophic methanogenesis, TMO mainly produced CO_2 from labeled methane. When grown on acetate, *M. acetivorans* produced no CO_2 but instead produced solely labeled acetate (methyl position) from labeled methane and when grown on carbon monoxide, it produced both labeled acetate and methyl sulfides from labeled methane (Moran et al 2007).

In AOM, methane oxidation is not coupled to methanogenesis. Methane production is lower in presence of sulfate and when hydrogen concentrations and methanogenesis drop during incubation in a closed system during organic matter degradation, AOM continues to increase in presence of excess methane (Fig 2). The process of methane oxidation coupled to sulfate reduction is at the limit of what is energetically possible for sustaining life, with estimates of a Gibbs free energy yields between -18 to -25 kJ mol^{-1} for non-seep and -35 kJ mol^{-1} for seep sediments (Alperin and Hoehler 2009, Caldwell et al 2008, Thauer 2011, Valentine and

Reeburgh 2000, Wang et al 2010) and doubling times of the microorganisms between 1.1 and 7.5 months (Girguis et al 2005, Krüger et al 2008a, Meulepas et al 2009a, Nauhaus et al 2007). Since this process operates close to its thermodynamic equilibrium, the commonly known phenomenon of reversibility of individual enzymes becomes substantial. This leads to measurable back flux of methane oxidation coupled to sulfate reduction, producing methane (3-7% of AOM) and sulfate (5.5-13% of SR) during AOM coupled to SR (Holler et al 2011a). This was observed before *in situ* (Orcutt et al 2005) and in sediment slurries, with methanogenesis around 10% of AOM (Orcutt et al 2008, Treude et al 2007) or even as high as 50% (Seifert et al 2006). When sulfate becomes depleted, Gibbs free energy yields become even lower (less negative) and the enzymatic back flux becomes even more apparent, up to 78% of net AOM (Yoshinaga et al 2014). Previous measurements of ^{13}C depletion below the SMTZ that were thought to be indicative for methanogenesis, were therefore attributed to the back flux of methane oxidation. This broadened the range of methane oxidation activity below and above the SMTZ (Yoshinaga et al 2014).
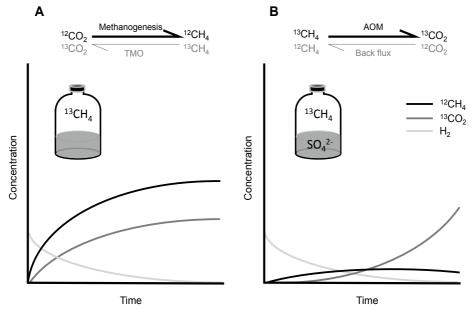
Figure 2 Typical $^{12}CH_4$, $^{13}CO_2$ and H_2 profiles (mM) during incubation in closed systems when either trace methane oxidation (TMO) (A) or sulfate-dependent anaerobic methane oxidation (AOM) (B) is the dominant process. In TMO, the $^{13}CO_2$ production from $^{13}CH_4$ is coupled to the H_2 concentration and methane production ($^{12}CH_4$) whereas in AOM, the $^{13}CO_2$ production is not coupled to net methane production. In presence of sulfate, the methane production is drastically lower when competitive endogenous substrates are present. During AOM, a back flux also occurs, producing CH_4 from CO_2.

Due to competition for certain substrates between methanogens and sulfate reducers, sulfate addition results in a decrease of methanogenesis and thus of TMO (Meulepas et al 2010a) whereas in AOM, sulfate stimulates methane oxidation. However, it was shown that in digested sludge, TMO was stimulated at high methane partial pressure and by manganese dioxide

and ferrous sulfate addition, reaching concentrations up to 98% of the methane produced (Zehnder and Brock 1980). Increasing the methane partial pressure of a closed system more often led to increased TMO rates (Smemo and Yavitt 2007, Zehnder and Brock 1980) due to repression of methanogenesis via product inhibition. This subsequently positively affects SR for competitive substrates when sulfate is present (Meulepas et al 2010a). Thus, a high methane partial pressure has a stimulating effect on $^{13}CO_2$ production and endogenous SR, unrelated to AOM. Methane-dependent SR is therefore not necessarily an effect of AOM. Therefore, when studying AOM, TMO and AOM back flux should be considered carefully in the interpretation of measurements. When experiments are performed with 100% $^{13}CH_4$ as sole energy and carbon source, methanogenesis produces $^{12}CH_4$ from endogenous substrates already present in the inoculum while TMO produces $^{13}CO_2$ from the overabundant $^{13}CH_4$ (Fig 2). Therefore, $^{13}CO_2$ accumulates in parallel with $^{12}CH_4$ production during TMO. If AOM is the dominant process, $^{13}CO_2$ is also produced from the overabundant $^{13}CH_4$. During AOM back flux, both $^{13}CO_2$ or $^{12}CO_2$ can be converted to $^{13}CH_4$ or $^{12}CH_4$, respectively, depending which isotope is more abundant. If $^{12}CO_2$ is preferred, also here $^{13}CO_2$ accumulates in parallel with $^{12}CH_4$. The only difference between TMO and AOM back flux would then be either net methanogenesis or net methane oxidation, respectively. The finding that organisms performing AOM possibly could also perform net methanogenesis (Bertram et al 2013, Lloyd et al 2011), and thus TMO, makes it even more complicated.

Microbes involved in anaerobic methane oxidation

The first evidence that methanogen-related archaea perform AOM through reverse methanogenesis came from investigation of methane-seep communities, and the archaea were named ANaerobic MEthanotrophc archaea (ANME) (Hinrichs et al 1999). ANME archaea appeared to form aggregates with sulfate-reducing bacteria belonging to the *Deltaproteobacteria* in zones where sulfate-dependent AOM occurred (Boetius et al 2000). Direct secondary ion mass spectrometry (SIMS) coupled to fluorescence *in situ* hybridisation (FISH) showed highly depleted ^{13}C inside the ANME cells, indicating assimilation of isotopically light methane (Orphan et al 2001a). Metagenomic analysis revealed that these ANME archaea possess most genes involved in the methanogenesis pathway (Hallam et al 2004, Meyerdierks et al 2005, Meyerdierks et al 2010), which was also confirmed with meta proteomics (Stokke et al 2012). More recently, all genes were confirmed to be present in a member of an ANME subgroup (Wang et al 2014). The methyl-coenzyme M reductase likely involved in reverse methanogenesis was purified and characterized and the nickel cofactor F_{430} showed to be of a higher molecular mass than the one in methanogens (Friedrich 2005, Krüger et al 2003, Mayr et al 2008).

So far, three distinct archaeal groups were classified to be methanotrophic, named ANME-1 (subcluster a and b), ANME-2 (subcluster a/b and c) and ANME-3. The ANME-1 cluster is

related to *Methanomicrobiales* and *Methanosarcinales* but forms a separate cluster (Hinrichs et al 1999), the ANME-2 cluster is related to cultivated members of the *Methanosarcinales* (Hinrichs 2002) and ANME-3 are more related to *Methanococcoides* spp. (Knittel et al 2005). Subcluster ANME-2a/b was previously separated in a and b, but with more sequences recovered, these were later found to be monophyletic (Fig 3). The different ANME clades are not monophyletic and phylogenetic distance between all subgroups is large, with rRNA gene sequence similarity of 75-92% (Knittel and Boetius 2009). The clades were found to co-occur in many different marine environments, except for ANME-3 that was mainly found in mud volcanoes and some seep sediments (Knittel and Boetius 2009, Lösekann et al 2007, Niemann et al 2006). From the phylogenetic divergence between the groups, one would expect ecophysiological differences between the clades and subclusters. Indeed, in core samples from marine sediments, a distinct zonation occurs of ANME-2a/b dominating upper layers whereas ANME-2c and/or ANME-1 abundance increases with increasing depth (Nunoura et al 2006, Orcutt et al 2005, Orphan et al 2004, Pachiadaki et al 2011, Roalkvam et al 2012, Yanagawa et al 2011). ANME-1 seemed to exist in environments with low methane concentrations (Blumenberg et al 2004) or even without methane (Bertram et al 2013), and in environments with low sulfate concentrations (Vigneron et al 2013a, Yanagawa et al 2011) and high sulfide levels (Biddle et al 2012, Knittel et al 2005).

Recently, evidence emerged that a fourth subcluster of methanotrophic archaea exists in freshwater environments which belonged to the previously named AOM-associated archaea (AAA) (Knittel and Boetius 2009). A member of this subcluster was shown to couple AOM to nitrate reduction and was named "*Ca.* Methanoperedens nitroreducens" and the overarching subcluster was named ANME-2d (Haroon et al 2013). This subcluster was already found in a nitrate-dependent AOM enrichment (Raghoebarsing et al 2006) but was lost when nitrite was fed as sole electron acceptor (Ettwig et al 2008), suggesting that these archaea might use nitrate. The name 'ANME-2d' was proposed before for a marine subcluster that was thought to be involved in AOM (Mills et al 2003), which was later renamed to 'GOM Arc I' since it was argued that it did not form a monophyletic cluster with other ANME-2 subclusters (Fig 3) and no AOM activity was shown yet (Lloyd et al 2006). Since proof exists that AOM was performed by "*Ca.* Methanoperedens nitroreducens" and with recent 16S rRNA sequence data, phylogenetic analysis shows that the GoM Arc I cluster is monophyletic with "*Ca.* Methanoperedens nitroreducens" and other AAA sequences, but distinct from other ANME-2 subclusters (Fig 3). The name 'ANME-2d' is therefore appropriate for this cluster.

Besides the ecophysiological information currently known on the ANME archaea, less is known about the sulfate-reducing bacterial partners. Mostly, the associated bacteria of ANME-2 belong to the *Desulfosarcina/Desulfococcus* cluster (DSS) of the *Deltaproteobacteria* (Boetius et al 2000, Orphan et al 2001a), which was later narrowed down to a specific cluster named 'SEEP-SRB1' (Knittel et al 2003), and appeared to be highly adapted to a symbiotic relationship with ANME-2 (Schreiber et al 2010). However, other SRB were also postulated to
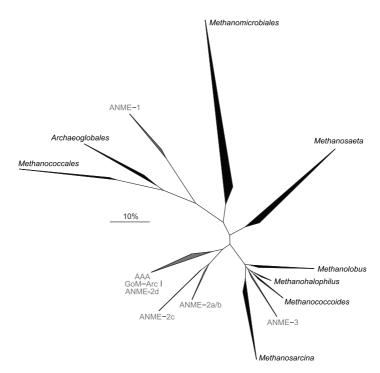
Figure 3 Phylogenetic tree of archaeal full length 16S rRNA sequences showing all archaeal methanotrophic clades so far described (grey) and the related methanogenic clades (black). The tree was constructed with the ARB software package (version arb-6.0.1.rev12565) (Ludwig et al 2004) using 2800 sequences from the SILVA SSURef NR 99 database (release 119.1) (Pruesse et al 2007). Trees were calculated by maximum likelihood analysis (RAxML, PHYML) and the ARB neighbor-joining method with terminal filtering and the Jukes-Cantor correction. Resulting trees were compared manually and a consensus tree was constructed. *Sulfolobales* as out-group was removed after tree calculations. The scale bar represents the percentage of changes per nucleotide position.

be involved in AOM, directly or indirectly (Orphan et al 2001b). In many other studies, different archaeal-bacterial associations and even single cells or aggregates of solely ANME archaea were found (Blumenberg et al 2004, Holler et al 2011b, Kleindienst et al 2012, Knittel et al 2005, Lösekann et al 2007, Orphan et al 2001b, Orphan et al 2002, Orphan et al 2004, Pernthaler et al 2008, Treude et al 2007, Vigneron et al 2013a, Vigneron et al 2013b). This indicates that the syntrophic association is possibly not fixed to a certain phylogenetic cluster but is flexible and dependent on yet-unknown factors. The finding of single cells or aggregates of solely ANME archaea in sediment samples even questions the theory that AOM is an obligate syntrophy (Schreiber et al 2010). Figure 4 shows some examples of typical FISH pictures made from seep sediment and diffusive sediment samples. Fluorescent oligonucleotide probes showed individual cells of ANME-1 (Fig 4, A) and cell aggregates of ANME-1/*Bacteria* (Fig 4, B), cluster of ANME-3 cells (Fig 4, C), different aggregates of ANME-2/*Bacteria* (Fig 4, D1-D6), and small mono-specific ANME-2 aggregates (Fig 4, E1-E4). In diffusive sediments, aggregates of ANME-2 are mostly very small and form mono-culture aggregates (Fig 4, E1-E4), but can

also occur as single cells or are loosely associated with SRB (Alperin and Hoehler 2009, Treude et al 2005b), even in reactor enrichments derived from these sediments (Jagersma et al 2009). In seep sediments, ANME-2 were mostly found in association with SRB and form big aggregates (Fig 4, D1-D6). In many cases, these aggregates have a shell type structure where ANME-2 archaea form the inner core with SRB forming the outer shell, in a ratio of 1:2, respectively (Fig 4, D1-D4) (Boetius et al 2000). In some cases, the aggregates are of a mixed-type where ANME-2 and the SRB are mixed throughout the aggregate (Fig 4, D5-D6). In a methane seep microbial mat, ANME-1 archaea were surrounding the bacteria (Fig 4, D7). Although it seemed that ANME-2c mainly form the shell type structures and ANME-2a/b form the mixed type aggregates (Knittel et al 2005), the ecophysiological reasons for these morphological differences are not understood. The finding of ANME-1 cells without a bacterial partner is reported frequently (Blumenberg et al 2004, Knittel et al 2005, Orphan et al 2002, Orphan et al 2004) and their occurrence in other zones of sediments not belonging the SMTZ gives indication of other metabolic properties besides AOM coupled SR. It was postulated that ANME-1 could oxidize methane without a bacterial partner (Maignien et al 2013, Orphan et al 2002, Pachiadaki et al 2011) or perform methanogenesis (Lloyd et al 2011), as was also described for ANME-2 (Bertram et al 2013).
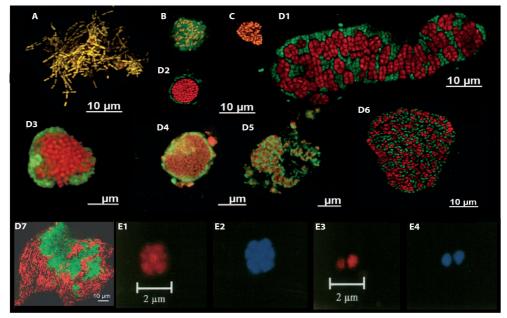
Figure 4 Fluorescent in-situ hybridisation (FISH) pictures from cold seep sediment samples (A-D7) and a diffusive sediment sample (E1-E4) showing single ANME-1 archaeal rod-shaped cells in yellow (A), aggregations of ANME-1 in yellow with *Bacteria* in green (B), cluster of ANME-3 cells in orange (C) and shell type aggregates of ANME-2 in red with *Bacteria* in green (D1-D4) and in mixed type aggregates (D5-D6), aggregates of ANME-1 in red surrounding sulfate-reducing bacteria in green (D7), small mono-aggregates of ANME-2 in red (E1, E3) and stained with DAPI (E2, E4). The picture was adapted from Vigeneron et al., 2013a, Treude et al., 2005b, Boetius et al., 2000, Knittel et al., 2005 and Michaelis et al., 2002.

Interspecies electron transfer

Considering the low energetic yield of AOM coupled to SR, it is essential that the products of methane oxidation are kept low enough by the sulfate-reducing partner to make AOM thermodynamically feasible as was also described for many other syntrophic associations (Stams and Plugge 2009). It is however still not known which product is formed in methane oxidation that acts as interspecies electron carrier (IEC). The product of methane oxidation that is transferred to the sulfate-reducing partner is either a less reduced compound that acts as IEC or electrons are transferred directly (through nanowires or pili) or indirectly (through extracellular quinones). For IECs, only pore water hydrogen concentrations are in range with thermodynamic requirements for AOM (Hoehler et al 1994). Model predictions show that interspecies hydrogen, formate, or acetate transfer are consistent with measured rates (Alperin and Hoehler 2009). However, laboratory experiments have excluded these compounds as IEC since these compounds did not affect AOM or stimulated sulfate reduction (Meulepas et al 2010b, Nauhaus et al 2002, Nauhaus et al 2005, Orcutt et al 2008, Treude et al 2007). Also, the distance between the cell walls of the producer and consumer of the IEC is too high to allow diffusion of any IEC compound other than formate (Sørensen et al 2001). Moran *et al* (2008) argued for methyl sulfides as IEC since methanethiol actually inhibited AOM, while the other conventional methanogenic compounds did not. However, toxicity effects cannot be excluded, as was also the case for carbon monoxide (Meulepas et al 2010b). The possibility of electron transfer via an external acceptor was tested for phenazines, AQDS (anthroquinone disulfonate) and humic acids, but none of these increased AOM rates (Nauhaus et al 2005). Valentine and Reeburgh (2000) speculated that the ANME archaea produce acetate and hydrogen from 2 molecules of methane. Stams and Plugge (2009) also speculated on multiple intermediates such as hydrogen and acetate and postulated that methane will be converted to methyl coenzyme M, but the subsequent steps to form acetate and CO_2 will go through the acetate and hydrogen pathway, respectively. Another possibility is that a single microorganism oxidizes methane and reduces sulfate, as described for an enrichment from a seep sediment. Here, the ANME archaea oxidize methane and reduce sulfate to sulfur, which is used by the sulfate-reducing partner after chemical conversion to polysulfide (Milucka et al 2012).

Project goal and thesis outline

AOM coupled SR is a process that is interesting for application in certain wastewater streams. Biological SR is used for removal and recovery of oxidized sulfur compounds and metals from process water (Meulepas et al 2010c). In this process, conventional electron donors such as hydrogen or ethanol are currently used. For example, at the zinc refinery of Nyrstar in Budel (the Netherlands), hydrogen is produced from natural gas or biogas via a steam reforming process which is rather costly. Directly using natural gas or biogas for biological sulfate reduction would drastically reduce costs and CO_2 emission and would simplify the

1

process design (Meulepas et al 2010c) (Fig 5).

The major bottle-neck for application of AOM is the low activity and growth rates of anaerobic methanotropic communities. Previous research at the Laboratory of Microbiology and the Sub-department of Environmental Technology (WUR) resulted in multiple active submerged membrane bioreactors (MBR) inoculated with Eckernförde bay sediment from the Baltic Sea (Meulepas et al 2009a). One reactor, reactor R3, showed a maximum AOM rate of 286 µmol/$g_{dry\ weight}$/day and an estimated doubling time of 3.8 months (Meulepas et al 2009a). Reactor R3 was enriched in ANME-2a/b archaea and SRB belonging to the *Desulfococcus/Desulfosarcina* cluster (Jagersma et al 2009).

Different electron acceptors such as sulfite, thiosulfate and sulfur affected AOM and SR rates. Most sulfate reducers can also use thiosulfate and sulfite as electron acceptors and the Gibbs free energy changes for methane oxidation with these electron acceptors are also higher (more negative) than that for sulfate. Only thiosulfate had a positive effect on AOM, whereas sulfite and sulfur were toxic or could not be utilized, respectively (Meulepas et al 2009b). Methanogenic substrates such as methanol, H_2/CO_2, formate, carbon monoxide, methanethiol and acetate did not show a substantial effect on AOM and SR (Meulepas et al 2010b). Optimal conditions for several environmental parameters were also determined and showed an optimal temperature of 20°C, a salinity of 30 ‰ and a pH of 7.5 for the AOM and SR performing enrichment (Meulepas et al 2009b). Substrate concentration experiments showed a positive linear correlation of methane partial pressure with AOM and SR rates, while AOM coupled to SR did not occur below 2 mM sulfate (Meulepas et al 2009b). Product inhibition only occurred with sulfide and not with CO_2, and AOM was completely and reversibly inhibited at 2.5 mM free sulfide (H_2S) (Meulepas et al 2009b).

Although rates of the reactor R3 enrichment were the highest reported so far at that time, conversion rates that are 100 times higher are necessary for an economically attractive application for different process water streams. We therefore applied multiple strategies to obtain higher AOM rates and/or faster growth rates of the responsible organisms, such as higher methane partial pressure and alternative substrates besides methane. We also investigated the effect of substrate and product concentration on AOM and we searched for the presence of low salinity AOM in the environment.

$$SO_4^{2-} + 4H_2 + H^+ \longrightarrow HS^- + 4H_2O$$
$$Zn^2 + HS^- \longrightarrow ZnS + H^+$$
$$2HS^- + O_2 + 2H^+ \longrightarrow 2S^° + 2H_2O$$

$$SO_4^{2-} + CH_4 + H^+ \longrightarrow HS^- + CO_2 + 2H_2O$$
$$Zn^2 + HS^- \longrightarrow ZnS + H^+$$
$$2HS^- + O_2 + 2H^+ \longrightarrow 2S^° + 2H_2O$$
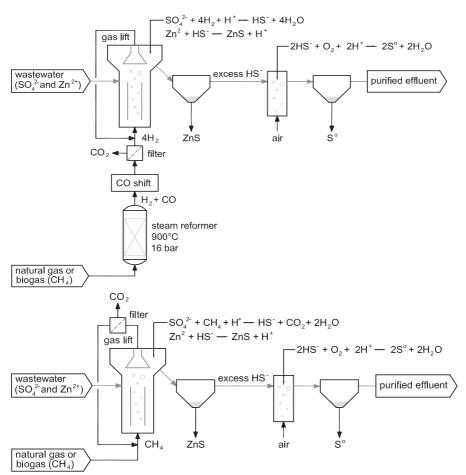
Figure 5 Simplified scheme of the wastewater treatment process operating at Nyrstar zinc refinery in Budel, The Netherlands (top) and a wastewater treatment process proposed when methane is directly used as electron donor (bottom). Scheme was adapted from Meulepas et al., 2010c.

Chapter 2: Methane partial pressure

One major bottle-neck for AOM is the low methane solubility at ambient pressure in seawater (Yamamoto et al 1976). Elevated methane pressure yields higher maximum dissolved methane concentrations and thus increases methane availability for the microbes. It was indeed shown that higher methane partial pressures increase AOM activity (Kallmeyer and Boetius 2004, Krüger et al 2005, Meulepas et al 2009b, Nauhaus et al 2002); microorganisms are clearly limited in growth and activity at atmospheric methane pressure. We performed incubations at high methane partial pressure (10.1 MPa) in a membrane-capsule bioreactor to assess growth and activity of methanotrophic communities. The AOM activity and ANME/ SRB growth is described in chapter 2.

Chapter 3: AOM at low salinity

Process waters with heavy metal and high sulfate content normally derive from freshwater systems. Sulfate-dependent AOM has only been well described in marine environments and previously described high rate enrichments originated from marine sediments. The previous enrichment from reactor R3 with Eckernförde bay sediment showed an optimum salinity at 30 ‰, while no AOM activity was observed at 4 ‰. Due to the high salinity requirement of the biomass, process streams low in salts other than sulfate cannot be treated with this biomass, unless salt addition is considered. Indications exist that sulfate-dependent AOM occurs in non-marine environments and ANME archaea have been detected, but growth and activity of ANME organisms was not proven. In chapter 3, we describe AOM activity and the presence of ANME archaea in association with SRB in a freshwater environment.

Chapter 4: Enrichments with alternative substrates

Besides increasing the methane partial pressure, enrichment of the responsible microorganisms with alternative substrates is another possible strategy to enrich AOM biomass. Since the consortia are syntrophic, "pushing" the reaction by stimulating growth of the archaeal or "pulling" the reaction by stimulating growth of the bacterial partner could stimulate growth of the consortia as a whole. Since the bacterial partner is related to sulfate-reducing bacteria, we aimed to enrich them by addition of canonical substrates for sulfate-reduction. In chapter 4, we enriched sulfate-reducing bacteria using methanol, formate, H_2/CO_2, butyrate, lactate, acetate, propionate and pyruvate, as well as possible IECs in AOM such as methanethiol and polysulfide. As inoculum, we used a highly enriched methanotrophic sample from reactor R4 (Meulepas et al 2009a). We used the last dilution that showed AOM activity from a dilution series from this sample to minimize presence of sulfate-reducing bacteria not involved in AOM. Although previous research showed that thiosulfate could be used as alternative electron acceptor in an enrichment coupling AOM to SR, we performed all incubations with sulfate to minimize enrichment of SRB that dismutate thiosulfate. We successfully enriched for different sulfate-reducing bacteria related to SRB involved in AOM, but we could not demonstrate their role in AOM.

Chapter 5: Primers and probes for ANME archaea

Since the discovery that AOM was performed by ANME archaea in consortia with SRB, different probes for FISH and primers for both qualitative and quantitative detection were developed. In this chapter, we evaluate existing probes and primers for detection of the ANME clades and subclusters and we optimized protocols for specific quantitative detection of ANME-2a/b, ANME-2c and ANME-1 using quantitative PCR. These were used in chapter 2, 3 and 6 for quantitative detection of ANME subclusters.

Chapter 6: ANME ecophysiology

In order to be able to enrich for ANME archaea in bioreactor studies, understanding the factors that determine maximum AOM activity and growth of different ANME clades is essential. In previous studies with Eckernförde bay sediment, the highly active reactor R3 enrichment was completely inhibited at very low levels of sulfide (Meulepas et al 2009a) which is not desired for broad application. In studies done by others, inhibition started at much higher sulfide concentrations. We therefore went back to the original Eckernförde bay sediment to assess growth and activity of different ANME subclusters under different sulfate and sulfide concentrations, with and without the addition of methane.

Chapter 7: General discussion

In the general discussion, results obtained in this thesis are combined with the knowledge obtained so far in other studies. Methane oxidation and methanogenesis are discussed in an integrative way and the differences between diffusive and non-diffusive sediments are addressed which potentially have an effect on the mechanisms of AOM.

Chapter 2

Growth of anaerobic methane oxidizing archaea and sulfate-reducing bacteria in a high pressure membrane-capsule bioreactor

Peer H. A. Timmers, Jarno Gieteling, H. C. Aura Widjaja-Greefkes, Caroline M. Plugge, Alfons J. M. Stams, Piet N. L. Lens and Roel J. W. Meulepas

Abstract

Anaerobic methane oxidizing communities of archaea (ANME) and sulfate-reducing bacteria (SRB) grow slowly, which limits physiological studies. High methane partial pressure was previously successfully applied to stimulate growth, but it is not clear how different ANME clades and associated sulfate-reducing bacteria (SRB) are affected by it. Here, we report on the growth of ANME/SRB in a membrane-capsule bioreactor inoculated with Eckernförde Bay sediment that combines high pressure incubation (10.1 MPa methane) and thorough mixing (100 rpm) with complete cell retention by a 0.2 µm pore-size membrane. The results were compared to previously obtained data from an ambient-pressure (0.101 MPa methane) bioreactor inoculated with the same sediment. Labelled-methane oxidation rates were not higher at 10.1 MPa, likely because measurements were done at ambient pressure. The subcluster ANME-2a/b was abundant in both reactors, but subcluster ANME-2c was only enriched at 10.1 MPa. SRB at 10.1 MPa mainly belonged to the SEEP-SRB2, Eel-1 group and *Desulfuromonadales* and not to the typically found SEEP-SRB1. The increase of ANME-2a/b occurred in parallel with the increase of SEEP-SRB2 which was previously found to be associated only with ANME-2c. Our results imply that the syntrophic association is flexible and that methane pressure and sulfide concentration influence growth of different ANME-SRB consortia. We also studied the effect of elevated methane pressure on methane production and oxidation by a mixture of methanogenic and sulfate-reducing sludge. Here, methane oxidation rates decreased and were not coupled to sulfide production, indicating trace methane oxidation during net methanogenesis and not anaerobic methane oxidation, even at high methane partial pressure.

Introduction

Anaerobic oxidation of methane (AOM) coupled to sulfate reduction (SR) is a process influenced by the CH_4 partial pressure. The SR rate of sediment from Hydrate Ridge was significantly higher at elevated CH_4 partial pressure (Krüger et al 2008a, Nauhaus et al 2002). Between 0 and 0.15 MPa, there is a positive linear correlation between the CH_4 partial pressure and the AOM and SR rates of an anaerobic methanotrophic enrichment obtained from Eckernförde Bay sediment (Meulepas et al 2009b). The methane-dependent sulfide production by microbial mats from the Black Sea increased 10 to 15-fold after increasing the methane partial pressure from 0.2 to 10.0 MPa (Deusner et al 2010). The affinity constant (K_m) for methane of anaerobic methanotrophs from Gulf of Cádiz sediment is around 37 mM which is equivalent to 3 MPa CH_4 (Zhang et al 2010). Because of the more negative Gibbs free energy change (ΔG) at elevated CH_4 partial pressures, growth of the anaerobic methanotrophs might be faster when the CH_4 partial pressure is increased (Fig S1). Bioreactor studies with high methane pressure have been performed (Deusner et al 2010, Zhang et al 2010), but it is not clear how the different ANME clades and associated SRB are affected by the methane pressure. This information would contribute to the understanding of the process of AOM coupled to SR and would help in further attempts to cultivate the responsible organisms.

In this study, we investigated the effect of the CH_4 partial pressure on methane oxidation and methane production rates in Eckernförde Bay sediment from the Baltic Sea. We also studied the effect of long-term (240-days) incubation under a high methane pressure (10.1 MPa CH_4) on the activity of this sediment ('reactor HP-1'). These results, together with the results of microbial community analysis, were compared with data from a bioreactor at ambient pressure ('reactor AP') (Jagersma et al 2009, Meulepas et al 2009a) inoculated with the same sediment as reactor HP-1 and with the original Eckernförde Bay sediment (EB). We also investigated the effect of the CH_4 partial pressure on methane oxidation and methane production rates in mixed methanogenic and sulfate-reducing granular sludge, both in short and long-term incubation ('reactor HP-2'). This was done to evaluate the capacity of methanogenic and sulfate-reducing communities to perform methane oxidation under favorable conditions. A summary of the experimental set-up is given in Fig 1.

Materials and methods

Origin of the inocula

The samples of the Eckernförde Bay sediment used for the initial activity assays and to inoculate reactor HP-1 were taken at Eckernförde Bay (Baltic Sea) at station B (water depth 28 m; position 54º31'15N, 10º01'28E) during a cruise of the German research vessel *Littorina* in June 2005. This sampling site has been described by Treude *et al* (2005b). Sediment samples were taken with a small multicore sampler based on the construction described
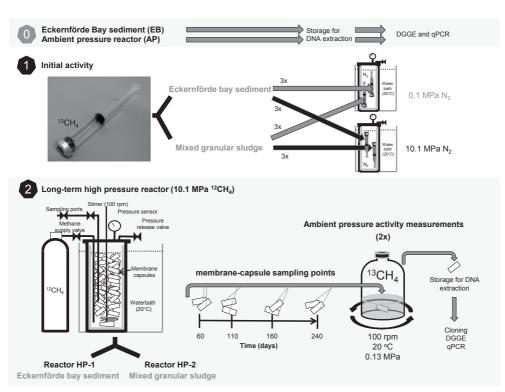
Figure 1 Schematic representation of the different experiments performed in this study. Experiment 0 represents the study of reactor AP published previously (Jagersma et al 2009, Meulepas et al 2009a) and the original Eckernförde Bay sediment (EB) of which samples were stored and analyzed in this study. Experiment 1 and 2 were fully conducted in this study. The piston picture was modified with permission from Meulepas et al. 2010 (Meulepas et al 2010a).

previously (Barnett et al 1984). The cores had a length of 50 cm and reached 30-40 cm into the sediment bed. Immediately after sampling, the content of the cores was mixed in a large bottle, which was made anoxic by replacing the headspace by anoxic artificial seawater. Back in the laboratory, the sediment was homogenized and transferred into 1L bottles in an anoxic chamber. The 1-L bottles were closed with butyl rubber stoppers and the headspace was replaced by CH_4 (0.15 MPa).

The mixed sludge used for the initial activity assays and to inoculate reactor HP-2 was sampled at two full-scale mesophilic upflow anaerobic sludge blanket reactors: a methanogenic reactor treating wastewater from paper mills (Industriewater Eerbeek, Eerbeek, the Netherlands, June 2005) and a sulfate-reducing reactor fed with ethanol (Emmtec, Emmen, the Netherlands, May 2006). The two sludge types were crushed by pressing them sequentially through needles with diameters of 1.2, 0.8 and 0.5 mm, mixed and transferred into anaerobic bottles.

The bottles with sediment and sludge were stored in the dark at 4ºC until the experiments were started.

Medium preparation

The basal marine medium used for the incubations with Eckernförde sediment was made as described previously (Meulepas et al 2009a). The basal fresh water medium used for the incubations with mixed sludge was made according to Meulepas *et al* (2010a). Both media were minimal media and did not contain any carbon source and no other electron acceptor than sulfate. The media were boiled, cooled down under a nitrogen (N_2) flow and transferred into stock bottles with a N_2 headspace until use. The final pH of the media was 7.2. The phosphate provided buffering capacity to maintain a neutral pH value.

Effect of the CH_4 partial pressure on the initial activity

The effect of the CH_4 partial pressure on the CH_4 oxidation and methane production rate of both the Eckernförde Bay sediment and the mixed sludge was assessed in triplicate incubations with 0.02 gram volatile suspended solids (g_{VSS}) at atmospheric (0.101 MPa) and elevated (10.1 MPa) methane pressure (Fig 1, experiment 1). These tests were performed in glass tubes (18 ml), sealed with a butyl rubber stopper and capped at one side and equipped with a piston at the opposite side (De Glasinstrumentenmakerij, Wageningen, The Netherlands; Meulepas et al 2010a). The glass tubes were filled with sediment or mixed sludge and filled with 9 ml marine medium or freshwater medium, respectively. Then, tubes were closed and flushed with N_2. After removing the N_2 gas with a syringe and needle, 3 ml $^{13}CH_4$ (purity 5.5) was added. The glass tubes were incubated statically at 20ºC in a non-pressurized incubator or in a 2.0 L pressure vessel (Parr, Moline, IL) filled with 1.8 L water. The vessel was pressurized with N_2 gas. The pH, liquid volume, gas volume and gas composition in the tubes were measured weekly. To do so, the pressure vessel had to be depressurized. Both pressurization and depressurization were done gradually over a period of two hours.

Effect of long-term high-pressure incubation

Two high-pressure vessels (Parr, Moline, IL) were controlled at 20 (±1)ºC and equipped with a stirrer controlled at 100 rpm (Fig 1, experiment 2). One vessel was filled with 1.8 L marine medium and inoculated with 25 membrane capsules, each containing 0.038 (±0.003) g_{VSS} Eckernförde Bay sediment (reactor HP-1). The other vessel was filled with 0.5 L freshwater medium and inoculated with 25 membrane capsules, each containing 0.072 (±0.006) g_{VSS} mixed sludge (reactor HP-2). The membrane capsules were cylindrically shaped, 14 mm in diameter, 20 mm long and had a membrane surface of 840 mm^2. The polysulfone membranes (Triqua BV, Wageningen, The Netherlands) had a pore size of 0.2 μm to retain microorganisms. The filled capsules were slightly lighter than water, which made them float when the stirrer was turned off. During inoculation, the lid of the vessel was removed in an anaerobic glove box containing 90% N_2 and 10% H_2. Afterwards, the high-pressure vessel was connected to a bottle with pressurized CH_4 (purity 5.5). The vessel was flushed with approximately 10 L CH_4 (the gas entered the vessel at the bottom to remove any dissolved gas) and subsequently

slowly pressurized to 10.1 MPa. At four time points (at 60, 110, 160 and 240 days), the pressure was gradually released and the vessel was opened in an anaerobic glove box to replace the medium and to sample two membrane capsules per reactor. Subsequently, the vessel was closed, flushed and pressurized again with CH_4 gas as described above. The high-pressure vessels were equipped with sampling ports for liquid phase sampling just before depressurization for sulfide determination. For activity determination, the sampled membrane capsules were incubated in 25-ml serum bottles at ambient pressure, closed with butyl rubber stoppers and filled with 20 ml medium. The 5 ml headspace was filled with pure ^{13}C-labeled CH_4 (0.13 MPa). The serum bottles were incubated at 20°C in orbital shakers (100 rpm). For around 30 days, weekly the pH, liquid and gas volume, pressure, gas composition and sulfide concentration in the serum bottles was measured. After these assays, the two membrane capsules per sampling point were frozen at -20°C for subsequent DNA extraction for molecular analysis. From the last sampling point at 240 days, only one membrane capsule was taken.

Geochemical analyses

Total dissolved sulfide species (H_2S, HS^- and S^{2-}) were measured photometrically using a standard kit (LCK 653) and a photo spectrometer (Xion 500) both from Hach Lange (Dusseldorf, Germany).

Gas composition was measured on a gas chromatograph-mass spectrometer (GC-MS) from Interscience (Breda, The Netherlands). The system was composed of a Trace GC equipped with a GS-GasPro column (30 m by 0.32 mm; J&W Scientific, Folsom, CA), and a Ion-Trap MS. Helium was the carrier gas at a flow rate of 1.7 mL min^{-1}. The column temperature was 30°C. The fractions of $^{13}CH_4$, $^{12}CH_4$, $^{13}CO_2$ and $^{12}CO_2$ were derived from the mass spectrum as described (Shigematsu et al 2004), with a retention time for CH_4 at 1.6 min in the gas chromatogram and 1.8 min for CO_2.

The pressure in the bottles and tubes was determined using a portable membrane pressure unit, WAL 0–0.4 MPa absolute (WalMess- und Regelsysteme, Oldenburg, Germany).

The pH was checked by means of pH paper (Macherey-Nagel, Dűren, Germany).

Calculations

For explanation on calculations of total $^{13}CO_2$, $^{12}CO_2$, $^{13}CH_4$ and $^{12}CH_4$, see supplementary information and Table S1.

DNA extraction

DNA was extracted from the membrane capsules using the Fast DNA Kit for Soil (MP Biomedicals, Santa Ana, CA) according to the manufacturer's protocol with two 45-second beat beating steps using a Fastprep Instrument (MP Biomedicals). In parallel, DNA was extracted from stored samples of reactor AP and from the original Eckernförde bay sediment (EB) (Fig 1, experiment 0).

Clone library construction

Extracted DNA from the last sampling point at 240 days was used for clone library construction. To amplify almost full-length bacterial 16S rRNA genes for cloning, primers 27F (5'-AGAGTTTGATCCTGGCTCAG-3') and 1492R (5'-GYTACCTTGTTACGACTT-3') (Lane 1991) were used. The archaeal 16S rRNA genes were amplified using primers A109f (ACKGCTCAGTAACACGT) (Grosskopf et al 1998) and universal reverse primer 1492R. PCR amplification was done with the GoTaq Polymerase kit (Promega, Madison, WI) using a G-Storm cycler (G-storm, Essex, UK) with a pre-denaturing step of 2 min at 95ºC followed by 35 cycles of 95ºC for 30 s, 52ºC for 40 s and 72ºC for 1.5 min. Lastly, a post-elongation step of 5 min at 72ºC was done. PCR products were pooled and purified using the PCR Clean & Concentrator kit (Zymo Research Corporation, Irvine, CA) and were ligated into a pGEM-T Easy plasmid vector (Promega) and transformed into *E. coli* XL1-Blue Competent Cells (Stratagene/Agilent Technologies, Santa Clara, CA). Both ligation and transformation were performed according to the manufacturer's instructions.

DGGE analysis

Extracted DNA from the membrane capsules at every sampling point was used for DGGE analysis, as well as DNA from reactor AP and from EB. The V3 region of the archaeal 16S rRNA sequences was amplified with primers GC-ARC344f (5'-ACGGGGYGCAGCAGGCGCGA-3') and ARC519r (5'-GWATTACCGCGGCKGCTG-3') (Yu et al 2008) using the GoTaq Polymerase kit (Promega, Madison, WI). PCR reactions were performed in a G-Storm cycler (G-storm, Essex, UK) with a pre-denaturing step of 5 min at 94ºC followed by 10 cycles of 94ºC for 10 s, 61ºC for 10 s (-0.5ºC/cycle), 72ºC for 40 s and 25 cycles of 94ºC for 10 s, 56 ºC for 20 s, 72ºC for 40 s and a post-elongation step of 30 min at 72ºC. Bacterial 16S rRNA V6-V8 regions were amplified using Phire Hot start II Polymerase (Thermo Scientific, F-122L, Waltham, MA) with the DGGE primer pair F-968-GC (5'-AACGCGAAGAACCTTAC-3') and R-1401 (5'-CGGTGTGTACAAGACCC-3') (Nubel et al 1996). Bacterial amplicons were produced with a G-Storm cycler (G-storm, Essex, UK) using a pre-denaturing step of 30 s at 98ºC followed by 35 cycles of 98ºC for 10 s, 56ºC for 10 s, 72ºC for 30 s and a post-elongation step of 1 min at 72ºC. Forward primers had a GC clamp of 40 bp attached to the 5' end as used by Yu *et al* (2008). DGGE analysis was performed as previously described (Martin et al 2007, Muyzer et al 1993) in a Dcode system (Bio-Rad Laboratories, Hercules, CA) at 60ºC for 16 hours with a denaturing gradient of 30-60% for bacterial profiles and a 40-60% denaturing gradient for archaeal profiles, as recommended (Yu et al 2008).

To clarify which of the most intense DGGE bands correspond to an OTU found in the clone library, clones were subjected to PCR-DGGE after cell lysis, using the same primer pairs that were used for previous DGGE profiling. One clone of every OTU was loaded on a DGGE gel parallel to the last sample (240 days) of reactor HP-1. Clones that corresponded to bands of the DGGE pattern of reactor HP-1 were annotated as such using the Bionumerics software

V4.61 (Applied Maths NV, Belgium).

Phylogenetic analysis

For the archaeal and bacterial clone library, 75 and 82 picked white colonies were sent for sequencing respectively, with the primer pair SP6 (5'- ATTTAGGTGACACTATAGAA-3') and T7 (5'- TAATACGACTCACTATAGGG-3') to GATC Biotech (Konstanz, Germany). All reverse and forward sequenced overlapping reads were trimmed of vector and bad quality sequences, and were assembled into contiguous reads using the DNA baser software (Heracle BioSoft S.R.L., Pitesti, Romania). After assembly, possible chimeras were removed using the Greengenes Bellerophon Chimera check (http://greengenes.lbl.gov) (DeSantis et al 2006). Whole 16S rRNA sequences were checked with BlastN. Sequences were aligned using the SINA online alignment tool version 1.2.11 (Pruesse et al 2012). Phylogenetic trees were constructed after merging aligned sequences with the Silva SSU Ref database release 111 (Quast et al 2013) by use of the ARB software package version 5.3-org-8209 (Ludwig et al 2004). Phylogenetic trees were calculated by the ARB neighbor-joining algorithm.

Quantitative real-time PCR

Extracted DNA from the membrane capsules at every sampling point was used for qPCR analysis, as well as DNA from reactor AP and from EB. The DNA concentration was determined with the Qubit 2.0 fluorometer (Thermo Fisher Scientific, MA). Amplifications were done in triplicate in a BioRad CFX96 system (Bio-Rad Laboratories) in a final volume of 25 µl using iTaq Universal SYBR Green Supermix (Bio-Rad Laboratories)**,** 5 ng of template DNA and primers with optimal concentrations and annealing temperatures for highest efficiency and specificity (Table S2), all according to the manufacturer's recommendations. New primer sets were designed using the ARB software package version 5.3-org-8209 (Ludwig et al 2004). Triplicate standard curves were obtained with 10-fold serial dilutions ranged from 2×10^5 to 2×10^{-2} copies per µl of plasmids containing 16S rRNA archaeal inserts of ANME-2a/b and ANME-2c and bacterial inserts of SEEP-SRB2 and Eel-1 group. The efficiency of the reactions was up to 100% and the R^2 of the standard curves were up to 0.999. All used primers were extensively tested for specificity with cloned archaeal inserts of ANME-1, ANME-2a/b, ANME-2c, *Methanococcoides* and *Methanosarcinales* and bacterial inserts of SEEP-SRB1, SEEP-SRB2, Eel-1 group, *Desulfuromonadales*, *Desulfosarcina* and *Myxococcales* and with genomic DNA of *Methanosarcina mazei* TMA (DSM-9195) and *Desulfovibrio* sp. G11 (DSM-7057). PCR conditions consisted of a pre-denaturing step for 5 min at 95°C, followed by 5 touch-down cycles of 95°C for 30 s, annealing at 60°C for 30 s with a decrement per cycle to reach the optimized annealing temperature (temperatures are shown in Table S2), and extension at 72°C (times are shown in Table S2). This was followed by 40 cycles of denaturing at 95°C for 15 s, 30 s of annealing and extension at 72°C. PCR products were checked for specificity by a melting curve analysis (72-95°C) after each amplification step and by gel electrophoresis**.** Quantification of specific archaeal and bacterial groups was expressed as

total 16S rRNA gene copies per g_{vss} extracted from the capsules.

Nucleotide sequences

Nucleotide sequence data reported are available in the DDJB/EMBL/GenBank databases under the accession numbers HF922229 to HF922386.

2

Results

Effect of the CH_4 partial pressure on the initial activity

The results of the initial activity experiment (Fig 1, experiment 1) are shown in Table 1 which presents the effect of an elevated $^{13}CH_4$ partial pressure on the oxidation of $^{13}CH_4$ to $^{13}CO_2$ and the $^{12}CH_4$ production of Eckernförde Bay sediment and mixed sludge. In both incubations with Eckernförde Bay sediment and mixed sludge, we observed $^{12}CH_4$ production and $^{13}CO_2$ production. Since no other carbon source than $^{13}CH_4$ was added, the $^{12}CH_4$ must have been produced from endogenous organic matter. At 0.101 MPa CH_4, both Eckernförde Bay sediment and mixed sludge showed $^{13}CO_2$ production during net methanogenesis. At 10.1 MPa, the Eckernförde Bay sediment showed no methane production and 4 times higher oxidation rates of $^{13}CH_4$ to $^{13}CO_2$ than at 0.101 MPa. The oxidation of $^{13}CH_4$ to $^{13}CO_2$ by the mixed sludge was approximately 2 times higher at 10.1 MPa CH_4 than at 0.1 MPa CH_4 but still showed net methane production.

Table 1 $^{13}CO_2$ and $^{12}CH_4$ production rates by EB and mixed sludge at 0.101 and 10.1 MPa $^{13}CH_4$ in the initial activity experiment.

	Production rate[a] (μmol g_{VSS}^{-1} day^{-1})			
	EB		Mixed sludge	
Molecule produced	0.101 MPa $^{13}CH_4$	10.1 MPa $^{13}CH_4$	0.101 MPa $^{13}CH_4$	10.1 MPa $^{13}CH_4$
$^{13}CO_2$	5.8 (±0.3)	20.9 (±4.5)	8.6 (±0.9)	16.3 (±6.2)
$^{12}CH_4$	8.5 (±1.4)	0.0 (±0.1)	47.1 (±1.9)	36.6 (±7.3)

[a]Standard deviations represent biological triplicates of 0.02 g_{vss} inoculum per glass tube.

Effect of long-term high-pressure incubation

The long-term effects of an elevated methane partial pressure were tested in reactors with either Eckernförde Bay sediment or mixed sludge (Fig 1, experiment 2). At 10.1 MPa CH_4, the methane oxidation rate in reactor HP-1 increased from 0.006 mmol g_{VSS}^{-1} day^{-1} to 0.024 mmol g_{VSS}^{-1} day^{-1} during the 240-day incubation (Fig 2A and Table S3). The $^{12}CO_2$ production rate on the other hand decreased, likely because the available endogenous organic matter was depleted. After 240 days, $^{13}CO_2$ production was faster than the endogenous $^{12}CO_2$ production. Initially the SR rate by reactor HP-1 also decreased, but from day 110 onwards the SR rate was correlated to the methane oxidation rate. During long-term incubation of the mixed sludge, methane oxidation and sulfide production in reactor HP-2 did not increase, nor were they coupled during the 160-day incubation at 10.1 MPa CH_4. The total CO_2 and sulfide production rates decreased during the reactor run (Fig 2B and Table S3).
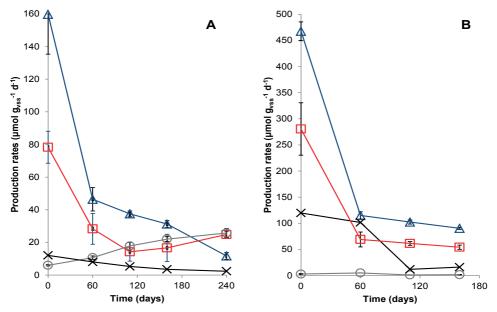

Figure 2 The $^{13}CO_2$ (○), $^{12}CO_2$ (Δ), $^{12}CH_4$ (x) and sulfide (□) production rates derived from the ambient pressure activity measurements with $^{13}CH_4$ of sampled capsules of reactor HP-1 (A) and reactor HP-2 (B) after different periods of incubation at 10.1 MPa $^{12}CH_4$ and 20ºC. Error bars represent standard deviations from independent measurements.

Microbial community of Eckernförde Bay sediment reactor

An archaeal clone library of a sample taken from reactor HP-1 at 240 days of incubation shows that the total of 75 sequences are dominated by different clades of ANME archaea (Fig 3 and Table S4). The highest percentage of ANME clones belonged to the ANME-2a/b group (56% of all sequences), followed by ANME-2c (19%) and ANME-1b (4%). Other clones with relatively high frequency in the clone library cluster with the Miscellaneous Crenarchaeotal Group 15 (MCG-15) (9%) and the Marine benthic group D (MBG-D) (8%). Archaeal DGGE

profiling of membrane capsule DNA from reactor HP-1 at all sampling points was done to see initial community changes. Afterwards, PCR-DGGE of cloned inserts with known composition revealed that bands belonging to ANME-2a/b and ANME-2c were increasing in intensity (Fig S2). qPCR analysis of the same samples with specific 16S rRNA primers for ANME-2a/b, ANME-2c and total Archaea are shown in Fig 4. A significant increase (2-tailed t-test with unequal variance p<0.05) of both ANME-2a/b and ANME-2c 16S rRNA gene copies at 110 days of incubation is observed, confirming initial DGGE results. The increase of ANME continued throughout reactor run and coincided with an increase of AOM and SR rates (Fig 2A and Table S3). The ANME-2a/b subcluster comprised a major fraction of total Archaea whereas ANME-2c abundance was much lower during reactor operation (Fig 4). However, ANME-2c 16S rRNA gene copies showed a faster increase than ANME-2a/b between 160 and 240 days.
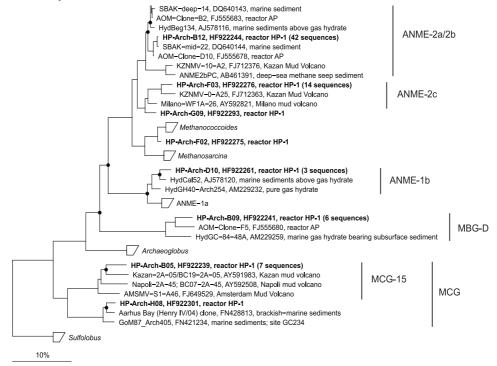
Figure 3 Phylogenetic tree of 16S rRNA gene sequences from an archaeal clone library constructed of a sample taken at 240 days of incubation of reactor HP-1. The tree was constructed with the ARB neighbor-joining method with terminal filtering and jukes-cantor correction using almost full length 16S rRNA sequences. Clones detected in this study are indicated in bold. The numbers in parenthesis indicate the number of sequences found of each phylotype. Closed circles represent bootstrap values >70% (1000 replicates). The scale bar represents the percentage of changes per nucleotide position.
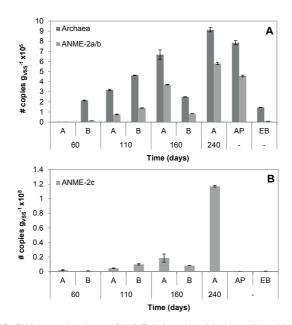
Figure 4 Absolute 16S rRNA gene abundance of ANME-2a/b and total Archaea (A) and ANME-2c (B) in reactor HP-1 sampled in duplicate (A and B) at 60, 110 and 160 days, except at 240 days. Results are compared to the ambient pressure reactor (AP) and the Eckernförde bay sediment inoculum (EB). Standard deviations represent triplicate analysis.

A bacterial clone library of 82 sequences of reactor HP-1 at 240 days of incubation shows a high bacterial diversity (Fig 5 and Table S4). All but two sequences within the clone library showed 97% or less similarity to known cultivated members. From the *Deltaproteobacteria*, the most common phylotypes recovered belonged to the methane-seep associated 'Eel-1' (6% of all sequences) and 'Eel-2' (13%) clades as described by Orphan *et al* (2001b) of which the Eel-2 clade clusters within the SEEP-SRB2 group. We also found sequences that are affiliated with the order *Desulfuromonadales* (7%). Members of the *Desulfobacteriaceae* were least abundant and only 2% belonged to the *Desulfosarcinales/Desulfococcus* cluster SEEP-SRB1. Some sequences found belonged to the *Myxococcales* group. The remaining bacterial phyloptypes were very diverse and many groups are also found previously in sediments and reactor systems with AOM activity. Some are only represented by one phylotype derived from the clone library (Table S4).

qPCR analysis results of membrane capsule DNA from reactor HP-1 at all sampling points with 16S rRNA primers for total Bacteria, specific primers for SEEP-SRB2 and the newly designed specific primers for Eel-1 are shown in Fig 6. An 8-fold increase of SEEP-SRB2 16S rRNA gene copies was observed at 160 days of incubation, and Eel-1 16S rRNA gene copies increased 4-fold. The abundance of Eel-1 decreased slightly in parallel with total Bacteria after 160 days of incubation whereas SEEP-SRB2 continued to slightly increase. This results in a relative increase of SEEP-SRB2 throughout the reactor run whereas Eel-1 remained at
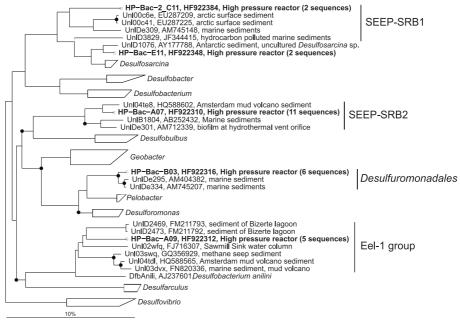
Figure 5 Phylogenetic tree of 16S rRNA gene sequences from a bacterial clone library constructed of a sample taken at 240 days of incubation of reactor HP-1. The tree shows only the canonical sulfate-reducing bacterial phylotypes found. The tree was constructed with the ARB neighbor-joining method with terminal filtering and jukes-cantor correction using almost full length 16S rRNA sequences. Clones detected in this study are indicated in bold. The numbers in parenthesis indicate the number of sequences found of each phylotype. Closed circles represent bootstrap values >70% (1000 replicates). The tree outgroup *Clostridium* was removed after tree construction. The scale bar represents the percentage of changes per nucleotide position.

a constant 2.5% of total Bacteria. From the qPCR results, we also calculated the ratios of ANME-2a/b and ANME-2c over Eel-1 and SEEP-SRB2 copy numbers. We observed that only ANME-2a/b and SEEP-SRB2 were detected in a constant ratio of around 1:2 throughout reactor operation and in EB (Fig 6C). In reactor AP, much more ANME-2a/b copies were detected as compared to SEEP-SRB2. The Eel-1 copies did not show a constant ratio with any ANME clade. We could not analyze *Desulfuromonadales* within the reactor as we were not able to design specific primers for this clade.

Microbial community of mixed sludge reactor

Microbial community analysis of the mixed sludge reactor HP-2 was restricted to archaeal and bacterial DGGE analysis (Fig S2 and S3) as no increase in methane oxidation was observed. On both the archaeal and bacterial DGGE profile, we did not see any community changes during reactor run.
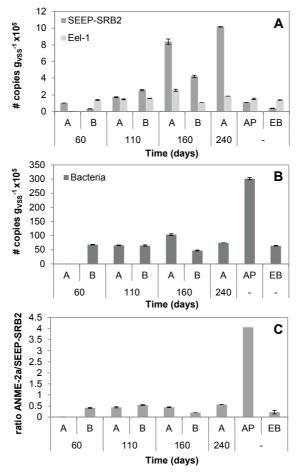
Figure 6 Absolute 16S rRNA gene abundance of SEEP-SRB2 and Eel-1 group (A) and total Bacteria (B) with standard deviations representing triplicate analysis and the ratio of ANME-2a/b and SEEP-SRB2 (C) with combined standard deviations calculated as described (Ku 1966). Reactor HP-1 was sampled in duplicate (A and B) at 60, 110, 160 days, except at 240 days and was compared to the ambient pressure reactor (AP) and the Eckernförde bay sediment inoculum (EB).

Discussion

Activity of Eckernförde Bay sediment

Our initial activity experiments showed that the Eckernförde Bay sediment performed trace methane oxidation (TMO) during net methanogenesis at 0.101 MPa CH_4 and net anaerobic oxidation of methane (AOM) at 10.1 MPa CH_4 without methane production (Table 1). Because the $^{13}CO_2$ production rate was also 4 times higher at 10.1 MPa CH_4 as compared to 0.101 MPa CH_4, we expect that the AOM activity of Eckernförde Bay sediment is stimulated by the higher methane partial pressure, although the sediment originates from relative shallow waters of 28 m depth (Treude et al 2005b). The AOM activity in reactor HP-1 did however not increase

faster than the reported AOM activity of the same Eckernförde Bay sediment in reactor AP at 0.101 MPa CH_4. In reactor HP-1, the AOM rate increased from 0.006 to 0.025 mmol g_{VSS}^{-1} d^{-1} over 240 days (Fig 2A and Table S3) and in reactor AP, the AOM rate increased from 0.003 to 0.55 mmol g_{VSS}^{-1} day^{-1} in 842 days (Meulepas et al 2009a).

Despite the good mixing of reactor HP-1, the increase of the AOM rate could have been limited by the larger diffusion distances. In reactor HP-1 the biomass was present in membrane capsules with a diameter of 14 mm, whereas reactor AP was a membrane bioreactor (MBR) where the biomass was present as 0.1-mm flocks that were directly in contact with the bioreactor medium (Meulepas et al 2009a). In reactor HP-1 at day 240, the average methane flux though the membranes was 0.11 µmol cm^{-2} d^{-1} (which is equal to 0.025 mmol g_{VSS}^{-1} day^{-1} x 0.038 g_{VSS} / 8.8 cm^2). At this flux, the change in the CH_4 concentration ($\Delta[CH_4]/\Delta x$, where Δx is the difference in distance), is 16 mM cm^{-1}, according to Fick's first law of diffusion ([CH_4 flux = - $\emptyset D_{methane}$ ($\Delta[CH_4]/\Delta x$)], where $\emptyset D_{methane}$ is the average porosity [88%] multiplied by the molecular diffusion coefficient of methane) (see Table S1 for nomenclature). At 10.1 MPa CH_4 and 20ºC, the CH_4 concentration in the bulk liquid was approximately 152 mM. The average CH_4 concentration near the microorganisms was therefore only marginally lower than in the bulk liquid and cannot explain the slow activity increase.

A more plausible explanation for the slow activity increase could be related to the method of measuring activity of the high pressure reactor samples. Sampled membrane capsules were incubated in 25-ml serum bottles at ambient pressure, using 0.13 MPa of pure $^{13}CH_4$ (Fig 1, experiment 2). Activity measurement at ambient pressure previously showed decreased AOM activity as compared to high pressure measurements (Bowles et al 2011) but also the microorganisms could have adapted to the higher pressure and will be less active when incubated at ambient pressure as shown for true piezophiles (Vossmeyer et al 2012). Indeed, the doubling times calculated from the exponential increase in AOM rate in both reactors was 3.8 months (R^2=0.98, N=12) for reactor AP and 3.9 months (R^2=0.90, N=15) for reactor HP-1. The doubling time calculated from qPCR analysis was 1.5 months for ANME-2a/b, 1.1 months for ANME-2c and 1.4 months for SEEP-SRB2. This indicates that high methane partial pressure had a positive effect on the AOM mediating microorganisms, which was not reflected in AOM activity measurements.

A less likely explanation could be that reactor HP-1 was operated in fed-batch mode. Here, sulfide and bicarbonate accumulated until the medium was replaced. Sulfide levels during the first (days 0-60) and the last (days 160-240) incubation periods reached 2.7 mM (Table 2). This could have been limiting the overall activity of the AOM mediating microorganisms as 2.4 (±0.1) mM sulfide was found to completely inhibit AOM and SR in reactor AP (Meulepas et al 2009a). In reactor AP, sulfide levels were below 1.5 mM in the first 800 days of the reactor run, reaching only 1.9 mM in the last 7 day period.

Table 2 Sulfide concentration in reactor HP-1 inoculated with EB

Time (days)	Sulfide conc. (mM)
0	-
60	2.7
110	1.5
160	2.1
240	2.7

Microbial community of Eckernförde Bay sediment reactor

Increase in 16S rRNA gene copies of ANME-2c archaea was only observed in the high pressure reactor HP-1. In the ambient pressure reactor AP, only ANME-2a/b was present (Jagersma et al 2009), which was verified by DGGE and qPCR (Fig 4). ANME-2a/b also showed growth at high pressure, indicating that both phylotypes could grow at high methane partial pressure. Previous studies showed predominance of ANME-2c archaea at high methane partial pressure (Schreiber et al 2010), in interior of hydrates (Mills et al 2005), and showed a transition of ANME-2a/b to ANME-2c sequence abundance with increasing sediment depth and sulfide concentration (Roalkvam et al 2011). Also, ANME-2a/b archaea seem to exist in sediments with little or no free sulfide (Biddle et al 2012). Because ANME-2c archaea were not present in reactor AP at atmospheric pressure and lower sulfide concentration, it is likely that these methanotrophs do not grow at low methane pressure and that they have higher sulfide tolerance. This could have resulted in higher growth rates than for ANME-2a/b. Indeed, ANME-2c showed faster growth at the end of the run of reactor HP-1 as compared to ANME-2a/b (Fig 4) and a shorter doubling time of 1.1 months vs. 1.5 months in the exponential phase. An eventual predominance of ANME-2c in reactor HP-1 after prolonged incubation time is therefore plausible. ANME-1b archaea were the least abundant methanotrophs in both AOM-SR reactors, which could be explained by the continuous high sulfate and low sulfide concentrations that seems to preferentially select for ANME-2 archaea. Several studies showed a dominance of ANME-1 archaea in environments with low sulfate concentrations (Vigneron et al 2013a) together with high sulfide concentrations (Biddle et al 2012) and it was suggested that ANME-1 could perform AOM independent of sulfate-reducing bacteria (Maignien et al 2013, Orphan et al 2002, Pachiadaki et al 2011) or even perform methanogenesis (Lloyd et al 2011).

Archaeal DGGE bands that were intense throughout incubation of reactor HP-1 belong to the MCG-15 and MBG-D (Fig S2). The MBG-D represent 8% of our clone library sequences and have been found in many cold marine (deep sea) sediments (Kendall et al 2007, Orphan et al

2001b, Vetriani et al 2003) and were consistently found in bioreactors (Meulepas et al 2009a, Zhang et al 2011). These archaea are related to the sulfur-reducing order *Thermoplasmatales,* and appear to include methanogens named "*Methanoplasmatales"* (Paul et al 2012). The MCG that were present until the end of the reactor run are abundant in marine deep subsurface sediments (Inagaki et al 2003). One hypothesis is that MCG archaea are heterotrophic anaerobes (Teske and Sørensen 2008) and carbon-isotopic signatures and polar lipid analysis also indicated an organic carbon metabolism in sediments dominated by MCG sequences (Biddle et al 2006). Recently, it was found with single cell genomic sequencing that the MCG and MBG-D archaea could play a role in protein degradation (Lloyd et al 2013). The batch mode of operation of our reactor implies long retention time of products of endogenous activity that could function as potential new substrates. This may have led to less selective enrichment and could explain the richness in archaeal diversity in our reactor.

Deltaproteobacteria of the Eel-1 and the SEEP-SRB2 clade were present during run of reactor HP-1, as qPCR and clone library results showed. Eel-1 members are closely related to the marine sulfate reducer *Desulfobacterium anilini* (Schnell et al 1989). Most members of the SEEP-SRB2 are related to *Dissulfuribacter thermophilus* (92% similarity) and *Desulfobulbus propionicus* DSM 2032 (89% similarity), both sulfur disproportionating bacteria (Lovley and Phillips 1994, Slobodkin et al 2013). Sequences related to *Desulfuromonadales* sequences were as abundant as the Eel-1 group in the clone library and clustered closely to sequences of the *Pelobacter* genus. *Pelobacter* is distinguished from *Desulfuromonas* species by being able to ferment specific hydrocarbons and being unable to reduce Fe(III) and/or elemental sulfur (Evers et al 1993). Both the SEEP-SRB2 and the Eel-1 group had increased in 16S rRNA gene copies at 160 days but Eel-1 decreased in abundance with reactor time, in parallel with total Bacteria (Fig 6). The Eel-1 group was previously hypothesized to be *in situ* directly or indirectly involved in AOM (Orphan et al 2001b). We however found that only growth of ANME-2a/b coincided with growth of SEEP-SRB2 with a stable ratio of around 1:2 (Fig 6C), excluding at least the direct involvement of Eel-1 members in AOM. This ratio has been found before in AOM performing consortia (discussed in chapter 1). This finding, together with the observed similar doubling times, could indicate that ANME-2a/b is growing in consortia with SEEP-SRB2, which to our knowledge has not been shown before. ANME-2c archaea could have been paired with the other most abundant *Desulfuromonadales*. This SRB group was previously found in AOM mediating enrichments (Schreiber et al 2010) and in cold seep sediment (Orcutt et al 2010, Roalkvam et al 2011). However, as with the Eel-1 group, abundance is not an indication for the involvement in AOM-SR. It could be that ANME-2c is actually forming consortia with SEEP-SRB2 as well, but a strong correlation was not found because ANME-2c copies were very low at the start of the reactor run and increased most between 160 and 240 days. A stronger correlation between ANME-2c and SEEP-SRB2 may have been found if the reactor would have been monitored longer.

Only 2% of the sequences in the clone library of reactor HP-1 belong to the SEEP-SRB1 clade. In previous research on different AOM sediments, cloning results show a co-occurrence of ANME-2 archaea and SEEP-SRB1. In contrast, when there is presence of ANME-1 archaea, the Eel-1 and SEEP-SRB2 group seem to be more abundant (Table 3). With microscopy techniques, other researchers recently found ANME-2c to be associated with SEEP-SRB2 (Kleindienst et al 2012), or other ANME-2 partners, such as *Desulfobulbus* spp. related SRB (Pernthaler et al 2008, Vigneron et al 2013b), and unidentified bacteria (Orphan et al 2002). Other ANME clades besides ANME-2 were also found to aggregate with SEEP-SRB1 (Knittel et al 2005, Lösekann et al 2007). Recently, a novel bacterial partner named 'HotSeep-1' was found in thermophilic AOM (Holler et al 2011b) and ANME-1a was even found at 90ºC in absence of SRB (Wankel et al 2012). Our findings clearly indicate that the syntrophic relationship between different clades of ANME and SRB is flexible and dependent on environmental factors. It was suggested before that syntrophy in AOM depends on the metabolism or ecological niche of the SRB (Kleindienst et al 2012, Vigneron et al 2013b) and nitrate was suggested as the basis for niche differentiation between some groups of SRB (Green-Saxena et al 2014). Uncultivated SRB belonging to SEEP-SRB2 are dominating seep habitats and are believed to be able to use non-methane hydrocarbons (Green-Saxena et al 2014, Kleindienst et al 2012). We observed growth of SEEP-SRB2 in reactor HP-1, indicating that this clade is indeed involved in AOM and does not need other non-methane hydrocarbons for growth. More likely, environmental parameters such as methane partial pressure and sulfide concentration play a key role in growth of SEEP-SRB2 and ANME-2c. This could explain the lack of ANME-2c and SEEP-SRB2 in reactor AP at ambient methane pressure and low sulfide levels and the lack of SEEP-SRB1 at high pressure and increased sulfide levels in reactor HP-1. Further studies are however needed to clarify which environmental parameters are crucial and which mechanism underlies the syntrophic interaction between ANME and SRB. A continuous flow bioreactor which mimics *in situ* conditions with little disturbance, already showed differential growth dynamics between ANME-1 and ANME-2 populations dependent on altering pore water flow rates (Girguis et al 2005). Similar studies where only the methane partial pressure or sulfide concentration is the varying factor could also give more insight into the differential growth and activity of ANME-2a/b and ANME-2c phylotypes and the associated SRB.

Activity and microbial community of mixed sludge

Our initial activity experiments showed that mixed sludge performs TMO during net methanogenesis at both 0.101 MPa CH_4 and 10.1 MPa CH_4 (Table 1). Where reactor HP-1 showed increasing AOM activity during long term incubation, reactor HP-2 did not. The total CO_2 and sulfide production decreased during the reactor run as endogenous substrates became depleted. Microbial analysis was restricted to DGGE profiling which did not show major community changes as observed in reactor HP-1 performing net AOM (Fig S2 and S3). This demonstrates that even at 10.1 MPa CH_4, the anaerobic community in granular

Table 3 Overview of archaeal and bacterial 16S rRNA genes detected in different studies on AOM-mediating marine sediments[b]

Sampling site	Eel River Basin			Hydrate Ridge *Beggiatoa* Mat	Santa Barbara	Gulf of Mexico	Guaymas Basin		Santa Barbara	HR	Isis	Eckernförde Bay	
												Reactor AP	Reactor HP
	0-4 cm	20-22 cm	4-7 cm		139 cm	15-18 cm	Core A	Core C	13-16 cm				
Reference	Orphan et al 2011b			Knittel et al, 2003; Knittel et al 2005	Harrison et al 2009	Lloyd et al 2006	Teske et al 2002		Orphan et al 2001b	Schreiber et al 2010		Jagersma et al 2009	This study
Archaea													
ANME-1	++	++	+	+	+	+	+	-	-	-	-	-	+
ANME-2	+	+	++	++			-	+	+	+	+	+	++
Bacteria													
SEEP-SRB1	+	+	+	++	+	++	-	+	+	++	++	++	+
SEEP-SRB2	+	+	-	+	-		+	-	-	-	-	+	‡
SEEP-SRB3	+	-	+	+			+		-				-
SEEP-SRB4				+				+					-
Eel-1	+	+	-	-	++	+	-	-	-	-	-	+	+
Eel-3	+	-	-						+				-

[b] Symbols represent presence (+), dominance (++) or absence (-) of 16S rRNA gene sequences. HR = Hydrate ridge, Isis = Isis mud volcano

sludge was not able to utilize the available energy for AOM coupled to SR during 160 days of incubation or that it does not have the metabolic flexibility to do so. This is in agreement with previous findings that granular sludge mediates TMO during net methanogenesis (Meulepas et al 2010a, Zehnder and Brock 1980), which results in much higher $^{13}CO_2$ production rates from $^{13}CH_4$ than the reported carbon back flux (Holler et al 2011a). In contrast, Eckernförde Bay sediment showed a clear uncoupling between the methane oxidation and the endogenous methanogenic activity and a coupling of $^{13}CO_2$ and sulfide production after 110 days of incubation. The production of $^{12}CO_2$ dropped to around 37 µmol g^{-1} d^{-1} when AOM started to occur and kept on decreasing whereas the sludge reactor never reached less than 90 µmol g^{-1} d^{-1} $^{12}CO_2$ production during the 160 days of reactor run. According to Hoehler *et al* (1994), the hydrogen concentration must be low enough for AOM to occur. Assuming that $^{12}CO_2$ production coincides with hydrogen production from organic matter degradation in anoxic sludge (Demirel 2014), then the hydrogen concentration was probably low enough in the Eckernförde Bay sediment reactor at 110 days, but too high in the mixed sludge reactor. If we would have allowed $^{12}CO_2$ production to drop as low as 37 µmol g^{-1} d^{-1} in the sludge reactor, it maybe could have allowed AOM to occur. It was shown recently that in anaerobic digestion of a diverse mixture of samples, the chemical oxygen demand also drastically drops in the first 150 days of reactor incubation and reaches steady state at around 160 days (Vanwonterghem et al 2014). Long term incubation is therefore indispensable to distinguish between labeled-methane oxidation during net methanogenesis (TMO) or net anaerobic methane oxidation (AOM).

Acknowledgements

Supplementary information

Calculations

For each time the tubes or bottles used for the activity assays were sampled, the total amount of $^{13}CO_2$, $^{12}CO_2$, $^{13}CH_4$, $^{12}CH_4$ and sulfide was calculated. The following equations were used for the calculations:

$$^{13}CO_2 \quad = f^{13}CO_2 \times P \times \left(\frac{V_{gas}}{R \times T} + \frac{V_{liquid}}{k_{CO_2}} \times \left(1 + \frac{K_{a,CO_2}}{[H^+]} \right) \right)$$

$$^{12}CO_2 \quad = f^{12}CO_2 \times P \times \left(\frac{V_{gas}}{R \times T} + \frac{V_{liquid}}{k_{CO_2}} \times \left(1 + \frac{K_{a,CO_2}}{[H^+]} \right) \right)$$

$$^{13}CH_4 \quad = f^{13}CH_4 \times P \times \left(\frac{V_{gas}}{R \times T} + \frac{V_{liquid}}{k_{CH_4}} \right)$$

$$^{12}CH_4 \quad = f^{12}CH_4 \times P \times \left(\frac{V_{gas}}{R \times T} + \frac{V_{liquid}}{k_{CH_4}} \right)$$

$$\text{Sulfide} \quad = [sulfide] \times V_{liquid}$$

The $^{13}CO_2$, $^{12}CH_4$ and sulfide production rates were obtained by dividing the increase of the total amount by the number of days and by the biomass content in tube or serum bottle in g_{VSS}:

$^{13}CO_2$ production rate = $(\Delta^{13}CO_2/\Delta t)/X$

The $^{13}CO_2$ production rate can be considered a good and direct measure for the methane oxidation rate, since the headspace of the activity assays contains initially 100% pure $^{13}CH_4$.

$^{12}CH_4$ production rate = $(\Delta^{12}CH_4/\Delta t)/X$

The $^{12}CH_4$ production rate can be considered a good measure for the methane production from endogenous organic matter, since 98.9% of the natural carbon is ^{12}C-carbon.

Sulfide production rate = $(\Delta sulfide/\Delta t)/X$

For explanation of the nomenclature, see Table S1.
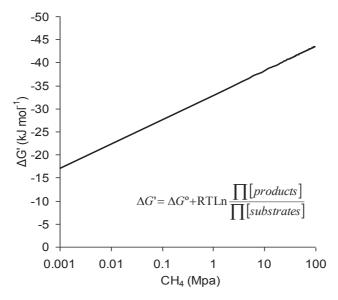
Figure S1 The influence of the CH_4 partial pressure on the Gibbs Free Energy yield (ΔG in kJ mol^{-1}) of AOM coupled to SR. Calculations assume the following conditions: temperature = 4°C, pH = 7.2, [HCO_3^-] = 17 mM, [HS^-] = 2.5 mM, [SO_4^{2-}] = 5 mM.
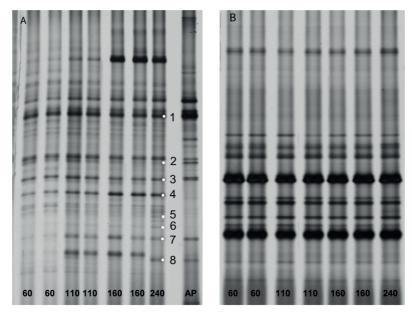
Figure S2 Archaeal DGGE profiles of the high pressure EB sediment reactor HP-1 (A) as compared to the ambient pressure reactor (AP) and mixed granular sludge reactor HP-2 (B). The high pressure reactors were sampled in duplicate at 60, 110, 160 and 240 days. Band numbers represent clones that were subjected to PCR-DGGE. 1: MBG-D, 2: ANME-1, 3: MCG-15, 4: MCG-15 & Other MCG, 5: ANME-2c (clone F07), 6: ANME-2c (clone G09), 7: ANME-2a/b, 8: ANME-2a/b.
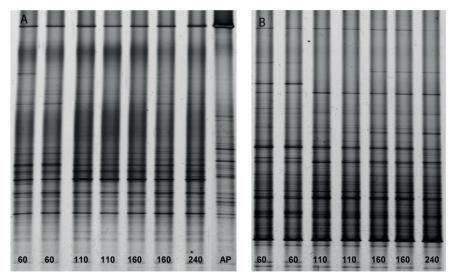
Figure S3 Bacterial DGGE profiles of the high pressure EB sediment reactor HP-1 (A) as compared to the ambient pressure reactor (AP) and mixed granular sludge reactor HP-2 (B). The high pressure reactors were sampled in duplicate at 60, 110, 160 and 240 days.

Table S1 Nomenclature

Symbol	Description
Ø	average porosity: 88% (Treude et al 2005b)
$D_{methane}$	molecular diffusion coefficient of CH_4: 7.5 cm d^{-1} (Treude et al 2005b)
f	fraction
k_{CO2}	Henry's law constant for CO_2 at sampling temperature (20ºC): 0.0388 mol L^{-1} atm^{-1}
k_{CH4}	Henry's law constant for CH_4 at sampling temperature (20ºC): 0.00153 mol L^{-1} atm^{-1}
$K_{a,CO2}$	dissociation constant of dissolved CO_2 + H_2O: 4.5 10^{-7} (pK_a: 6.9)
P	pressure
R	gas constant: 8.314 J^{-1} mol^{-1} K^{-1}
t	time
T	temperature in °K
V_{gas}	gas volume in tube or serum bottle for activity assay
V_{liquid}	liquid volume in tube or serum bottle for activity assay
VSS	volatile suspended solids
X	biomass content in tube or serum bottle in g_{VSS}
x	distance

Table S2 Primers used for qPCR in this study with the corresponding annealing temperatures and concentrations

Target	Primer name	Sequence (5'-3')	Annealing temp (°C)	Extension time (s)	Amplicon size (bp)	Primer conc. (mM)	Reference
Archaea	Arch-787f	ATT AGA TAC CCS BGT AGT CC	55.4	40	272	1	Yu et al 2005
	Arch-1059r	GCC ATG CAC CWC CTC				1	
ANME-2a/b	ANME2a-426F*	TGT TGG CTG TCC GGA TGA	60	40	833	1	Miyashita et al 2009
		TGT TGG CTG TCC AGA TGA					
		TGT TGG CTG TCC AGA TGG					
	ANME2a-1242R	AGG TGC CCA TTG TCC CAA				1	
ANME-2c	ANME-2cF	TCG TTT ACG GCT GGG ACT AC	60	40	221	1	Vigneron et al 2013a
	ANME-2cR	TCC TCT GGG AAA TCT GGT TG				1	
Bacteria	BACT_1369F	CGG TGA ATA CGT TCY CGG	55.5	30	123	1	Suzuki et al 2001
	PROK_1492R	GGW TAC CTT GTT ACG ACT T				1	
SEEP-SRB2	SRB2-649F	ACT TGA GTA CCG GAG AGG GA	53.3	30	180	1	Vigneron et al 2013b
	SRB2-808R	CCT AGT GCC CAT CGT TTA GG				1	
Eel-1 group	Eel-1-732F	GAC TCT CTG GAC CAA TAC	50.4	30	106	1	This study
	Eel-1-838R	CCG CTA CAC CTA GTT CTC				1	

*These primers are a mixture of each taxonomic group targeted primers at an equimolar amount, as described (Miyashita et al 2009).

2

Table S3 Production rates of $^{13}CO_2$, $^{12}CO_2$, $^{12}CH_4$ and sulfide (µmol g_{vss}^{-1} d^{-1}) in both high pressure reactors HP-1 (inoculated with Eckernförde sediment) and HP-2 (inoculated with mixed methanogenic and sulfate-reducing granular sludge) during incubation.

HP-1	Production rates	(µmol g_{vss}^{-1} d^{-1})		
Time (days)	$^{13}CO_2$	$^{12}CO_2$	$^{12}CH_4$	Sulfide
0	6.015 (±0.4)	159.7 (±24.4)	12.1	78.3 (±9.8)
60	10.71 (±1.05)	46.43 (±7.14)	8.07	28.34 (±9.4)
110	17.86 (±2.38)	37.5 (±1.79)	5.33	14.28 (±5.7)
160	22.06 (±1.47)	31.25 (±2.13)	3.56	16.66 (±8.3)
240	25.78 (±2.78)	11.72 (±2.08)	2.37	24.89 (±1.8)
HP-2	**Production rates**	**(µmol g_{vss}^{-1} d^{-1})**		
Time (days)	$^{13}CO_2$	$^{12}CO_2$	$^{12}CH_4$	Sulfide
0	2.914 (±1.03)	467.5 (±18.0)	120	280.5 (±50.0)
60	4.963 (±0.27)	115 (±6.85)	102	69.07 (±14.3)
110	1.19 (±0.14)	102.4 (±3.94)	11.9	61.43 (±3.6)
160	1.612 (±0.47)	90.32 (±1.94)	16.1	54.19 (±4.2)
240	-	-	-	-

Table S4 Archaeal and bacterial 16S rRNA gene clone library results of the high pressure reactor inoculated with Eckernförde bay sediment (HP-1). Sample was taken at 240 days of incubation.

Phylogenetic group	16S rRNA Phylotypes (#)	16S rRNA phylotypes (%)
Bacteria		
Deltaproteobacteria	**29**	**35**
SEEP-SRB2	11	13
Desulfuromonadales	6	7
Eel-1 group	5	6
Desulfosarcina	2	2
SEEP-SRB1	2	2
Myxococcales	2	2
Desulfobacterales uncultured	1	1
Acidobacteria	**6**	**7**
Bacteriodetes	**6**	**7**
Planctomycetes	**6**	**7**
Chloroflexi	**5**	**6**
Actinobacteria	**4**	**5**
Firmicutes	**4**	**5**
Gammaproteobacteria	**4**	**5**
Alpha-proteobacteria	**3**	**4**
Spirochaetes	**3**	**4**
Candidate division OP3	**2**	**2**
Candidate division WS3	**2**	**2**
Deferribacteres	**2**	**2**
Hyd24-12	**1**	**1**
Chlorobi	**1**	**1**
Cyanobacteria	**1**	**1**
Epsilon-proteobacteria	**1**	**1**
Gemmatimonadetes	**1**	**1**
Nitrospirae	**1**	**1**
Total	82	
Archaea		
ANME-2a/b	**42**	**56**
ANME-2c	**14**	**19**
MCG-15	**7**	**9**
MBG-D	**6**	**8**
ANME-1b	**3**	**4**
Methanococcoides	**1**	**1**
Other MCG	**1**	**1**
Methanosarcinales	**1**	**1**
Total	75	

CHAPTER 3

ANAEROBIC OXIDATION OF METHANE ASSOCIATED WITH SULFATE REDUCTION IN A NATURAL FRESHWATER GAS SOURCE

Peer H. A. Timmers, Diego A. Suarez-Zuluaga, Minke van Rossem, Martijn Diender, Alfons J. M. Stams and Caroline M. Plugge

Abstract

The occurrence of anaerobic oxidation of methane (AOM) and trace methane oxidation (TMO) was investigated in a freshwater natural gas source. Sediment samples were taken and analyzed for potential electron acceptors coupled to AOM. Long term incubations with ^{13}C-labeled CH_4 ($^{13}CH_4$) and different electron acceptors showed that both AOM and TMO occurred. In most conditions ^{13}C-labeled CO_2 ($^{13}CO_2$) simultaneously increased with methane formation, which is typical for TMO. In the presence of nitrate, neither methane formation nor methane oxidation occurred. Net AOM was measured only with sulfate as electron acceptor. Here, sulfide production occurred simultaneously with $^{13}CO_2$ production and no methanogenesis occurred, excluding TMO as possible source for $^{13}CO_2$ production from $^{13}CH_4$. Archaeal 16S rRNA gene analysis showed highest presence of ANME-2a/b (ANaerobic MEthane oxidizing archaea) and AAA (AOM Associated Archaea) sequences in the incubations with methane and sulfate as compared to only methane addition. Higher abundance of ANME-2a/b in incubations with methane and sulfate as compared to only sulfate addition was shown by qPCR analysis. Bacterial 16S rRNA gene analysis showed presence of sulfate-reducing bacteria belonging to SEEP-SRB1. This is the first report that explicitly shows that AOM is associated with sulfate reduction in an enrichment culture of ANME-2a/b and AAA methanotrophs and SEEP-SRB1 sulfate reducers from a low-saline environment.

Introduction

Anaerobic methane oxidation (AOM) coupled to sulfate reduction (SR) was first discovered to occur in marine sediments (Martens and Berner 1974, Reeburgh 1976). The process was found to be catalyzed by communities of anaerobic methanotrophic archaea (ANME) and sulfate reducing bacteria (SRB) of the *Deltaproteobacteria* (Boetius et al 2000, Hinrichs et al 1999, Orphan et al 2001). More recently, AOM was also reported to be coupled to other electron acceptors besides sulfate. In freshwater environments, AOM was coupled to the reduction of nitrate and nitrite (Deutzmann and Schink 2011, Ettwig et al 2008, Ettwig et al 2009, Haroon et al 2013, Hu et al 2009, Raghoebarsing et al 2006). Microbial methane oxidation with iron and/or manganese reduction was described in marine sediments (Beal et al 2009, Riedinger et al 2014), brackish sediments (Egger et al 2015), a terrestrial mud volcano (Chang et al 2012), and also in freshwater environments (Amos et al 2012, Crowe et al 2011, Sivan et al 2011). Recently, humic acids (HAs) were also hypothesized to act as electron acceptor for AOM (Gupta et al 2013). AOM coupled to SR in freshwater is likely limited by the low sulfate concentrations, which are around 10 to 500 µM (Holmer and Storkholm 2001).

Sulfate-dependent AOM has been observed in freshwater systems, but the involvement of other electron acceptors could not be excluded. Moreover, the responsible microorganisms were either not analyzed nor conclusively identified (Grossman et al 2002, Schubert et al 2011, van Breukelen and Griffioen 2004, Eller et al 2005, Segarra et al 2015). ANME-1 related archaea have been found in a terrestrial subsurface (Takeuchi et al 2011), but ^{13}C-labeled carbon dioxide ([13]CO_2) formation from ^{13}C-labeled methane ([13]CH_4) also occurred in control incubation where no electron acceptor was added. This was also the case in other incubation studies (Beal et al 2009, Egger et al 2015, Sivan et al 2011). These observations make it difficult to link ongoing methane oxidation to a particular electron acceptor. Moreover, [13]CO_2 can also be produced during methanogenesis in a process called trace methane oxidation (TMO) (Zehnder and Brock 1979). TMO was demonstrated to occur in pure cultures of different methanogens (Harder 1997, Moran et al 2005, Moran et al 2007, Zehnder and Brock 1979), in granular sludge (Harder 1997, Meulepas et al 2010, Zehnder and Brock 1980) and in freshwater and terrestrial environments (Blazewicz et al 2012, Zehnder and Brock 1980). Differentiation between AOM and TMO is difficult for several reasons: a) both processes can produce [13]CO_2 at comparable rates; b) at elevated methane partial pressure, TMO rates increase (Smemo and Yavitt 2007, Zehnder and Brock 1980) while methanogenesis is repressed, which favors sulfate reduction (Meulepas et al 2010); and c) ferrous sulfate addition may result in enhanced trace methane oxidation rates (Zehnder and Brock 1980). This means that with elevated [13]CH_4 partial pressure and presence of sulfate, an increase in [13]CO_2 and sulfide production cannot be taken as evidence for sulfate-dependent AOM unless net methane consumption is demonstrated. Moreover, although there is convincing evidence that anaerobic methane oxidizing archaea (ANME) archaea are capable of net AOM, detecting ANME sequences or cells in mixed communities that perform methanogenesis does not prove

that AOM takes place, since ANME could perform methanogenesis as well (Bertram et al 2013, Lloyd et al 2011) and as a consequence could perform TMO.

In this study we used long-term incubations (>168 days) with samples taken from a freshwater natural gas source with added $^{13}CH_4$ to investigate the occurrence of both TMO during net methanogenesis and AOM. AOM was distinguished from TMO by simultaneous detection of $^{13}CH_4$, $^{12}CH_4$ (produced during methanogenesis) and $^{13}CO_2$. We investigated the effect of different electron acceptors that possibly might be involved in AOM. Control incubations without addition of methane were done to accurately distinguish between net methane oxidation and net methanogenesis. Archaeal community analysis of long term incubations with methane and sulfate ($CH_4+SO_4^{2-}$), sulfate only (SO_4^{2-}-only), and methane only (CH_4-only) was performed at 323 days of incubation. Incubations with sulfate and with and without methane were monitored for an extended period of 728 days.

Materials and methods

Sampling

Samples were taken in spring of 2011 from two natural gas sources in Berkhout, Noord Holland, The Netherlands (52° 38'31'' N, 4° 59'49'' E). These gas sources were used for domestic purposes by capturing natural gas from groundwater pockets, using a 30 m long pipe (Fig 1). Different locations were sampled: the effluent of an active gas source ('tank') and the sediment of the ditch where the effluent is collected ('ditch 1'), the sediment of the ditch where the effluent of the storage tank is collected ('ditch 2'), and from the sediment inside a gas source that was no longer in use ('tank 2', not in Fig 1). Sediment samples were collected in nitrogen flushed bottles with an inversed pump. In the laboratory, the gas phase of the bottles was flushed with 100% 5.5 grade methane (99.999%) and stored at 4°C for ±21 months. All samples were pooled 1:1:1 (v/v/v) in an anaerobic chamber prior to inoculation.

Media composition

Media were prepared as described previously (Stams et al 1993) using 1 ml/L of the vitamin stock solution (for composition, see Table S1).

Experimental set-up

15 ml aliquots of the pooled sediments (0.07 g_{vss}) were incubated in triplicate in bicarbonate buffered medium (1:1 v/v) with sulfate (20 mM), iron (as ferrihydrite, 10 mM), humic acids (20 g l^{-1}), iron combined with humic acids (iron as ferrihydrite, 10 mM and humic acids, 2 g l^{-1}), and nitrate (20 mM). Iron was combined with humic acids to facilitate electron transfer from insoluble iron to soluble humic acids that can act as an electron shuttle (Kappler et al 2004). A control without electron acceptor was included. All triplicate conditions were tested with and without $^{13}CH_4$ in the headspace. All experiments were done in 60 ml serum bottles
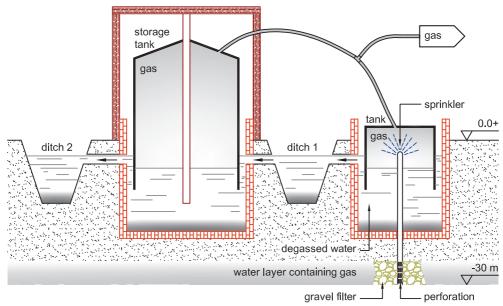
Figure 1 Schematic presentation of the system that is used for capturing natural gas at Berkhout, Noord-Holland, The Netherlands (adapted from Bartstra, 2003). A 30 m deep pipe reaches the pressurized groundwater pockets containing natural gas. Degasification occurs at lower pressure inside the gas source tank where the sprinkler facilitates the process. Gas can be transported to the house or to a storage tank floating on the water ditch. Sampling locations were inside an inactive tank (tank 2, not on picture), from the effluent of the active gas source (tank) and the sediment of the ditch where the effluent is collected (ditch 1) and from the sediment of a ditch where the effluent of the storage tank was collected (ditch 2).

closed with butyl rubber stoppers and aluminium caps. After 10 cycles of exchanging the headspace gas with N_2, it was changed to N_2/CO_2 (1:1) to a pressure of 1.5 bar. When $^{13}CH_4$ was added, N_2/CO_2 was added to a pressure of 1.3 bar and 99.99% $^{13}CH_4$ gas (Campro Scientific, Veenendaal, The Netherlands) was added to a final pressure of 1.8 bar. The serum bottles were incubated at 15°C in the dark.

Preparation of ferrihydrite

Ferrihydrite (simplified as $Fe(OH)_3$) was produced as described for obtaining nanoparticle size (<10 nm) minerals (Schwertmann and Cornell 1991). After preparing, the mineral was repeatedly washed and centrifuged for 3 times and subsequently dialyzed to remove electrolytes. The precipitate was then freeze-dried to remove access water and immediately added to the incubations.

Analytical measurements

Nitrate and sulfate were analysed by an Ion Chromatography system equipped with an Ionpac AS9-SC column and an ED 40 electrochemical detector (Dionex, Sunnyvale, CA). The system was operated at a column temperature of 35°C, and a flow rate of 1.2 ml min^{-1}. Eluent consisted of a carbonate/bicarbonate solution (1.8 and 1.7 mM respectively) in deionized water.

Headspace gas composition was measured on a gas chromatograph-mass spectrometer (GC-MS) composed of a Trace GC Ultra (Thermo Fisher Scientific, Waltham, MA) equipped with a Rt-QPLOT column (Restek, Bellefonte, PA), and a DSQ MS (Thermo Fisher Scientific). Helium was used as a carrier gas with a flow rate of 120 ml min^{-1} and a split ratio of 60. The inlet temperature was 80°C, the column temperature was set at 40°C and the ion source temperature at 200°C. CH_4 and CO_2 in the headspace were quantified from the peak areas in the gas chromatographs. The fractions of $^{13}CO_2$, $^{13}CH_4$ and $^{12}CH_4$ were derived from the mass spectrum based on a previous method (Shigematsu et al 2004), but the ratio of m/z 15 over m/z 17 was used as a proxy for $^{12}CH_4$. Validation of the method was done using standards with known mixture of $^{13}CO_2$, $^{12}CO_2$, $^{13}CH_4$ and $^{12}CH_4$. The concentrations of total CO_2, total CH_4, $^{13}CO_2$, and $^{12}CH_4$ (produced during methanogenesis in incubations with $^{13}CH_4$) were calculated as described in chapter 2. Headspace CO_2 and CH_4 after 168 days of incubation was quantified from the peak areas recorded with a CompactGC gas chromatograph (Global Analyser Solutions, Breda, The Netherlands) containing a Carboxen 1010 pre-column, followed by two lines: a Molsieve 5A column (pressure: 200 kPa, split flow: 20 ml min^{-1}, oven temperature: 80°C, and a PDD detector at 110°C) and a RT-Q-bond column (pressure: 150 kPa, split flow: 10 ml min^{-1}, oven temperature: 80°C with a TCD detector at 110°C) with a carrier gas flow of 10 ml min^{-1}.

The concentrations of iron(II) and iron(III) were measured with the ferrozine colorimetric method (Stookey 1970). Prior to analysis, samples were acidified with 2 M HCl (1:1 v/v) and centrifuged for 5 min at 15,700 rcf to precipitate humic acids. Absorbance at 562 nm was measured in a U-1500 spectrophotometer (Hitachi, Chiyoda, Tokyo, Japan).

Sulfide concentration was measured with the methylene-blue colorimetric method. Samples were directly diluted 1:1 (v/v) in a 5% (w/v) zinc acetate solution to bind all sulfide. Deionised water was added to a volume of 4.45 ml and 500 µl of reagent A (2 g l^{-1} dimethylparaphenylenediamine and 200 ml l^{-1} H_2SO_4) and 50 µl of reagent B (1 g l^{-1} Fe((NH$_4$)(SO$_4$))$_2$· 12 H_2O and 0.2 ml l^{-1} H_2SO_4) were added concurrently and mixed immediately. After 10 minutes, samples were measured with a Spectroquant Multy colorimeter (Merck Millipore, Darmstadt, Germany) at 660 nm.

Inductively Coupled Plasma-Optical Emission Spectroscopy (ICP-OES) using a Vista-MPX CCD simultaneous (Varian Inc., Palo Alto, CA) was used to quantify the elemental composition of all samples, as previously done (Hageman et al 2013). The standard deviation in all measurements was ≤1.8%.

The pressure of the serum vials was determined using a portable membrane pressure unit GMH 3150 (Greisinger electronic GmbH, Regenstauf, Germany). The pH was checked by pH paper. Conductivity was measured using a standard electrode. The VSS contents were analyzed according to standard methods (American Public Health Association, 1995).

DNA extraction

Genomic DNA was extracted from samples after 323 days of incubation from the triplicate incubations with methane and sulfate ($CH_4+SO_4^{2-}$), sulfate only (SO_4^{2-}-only), and methane only (CH_4-only) and from the original sediment (BHori). DNA was extracted in triplicate for every separate incubation using the Fast DNA Kit for Soil (MP Biomedicals, Santa Ana, CA) according to the manufacturer's protocol with two 45-second beat beating steps using a Fastprep Instrument (MP Biomedicals). Triplicate extracted DNA for every separate incubation was pooled and DNA concentrations were determined with the Qubit 2.0 fluorometer (Thermo Fisher Scientific).

Bacterial community profiling

Extracted DNA was subjected to barcoded amplification of the V1-V2 region of the 16S rRNA gene. A PCR amplification replicate of BHori (BHoriA and BHoriB) was done to correct for technical biases. Barcoded amplification was done using forward primer 27F-DegS (van den Bogert et al 2011) that was extended with the titanium adapter A and an eight-base sample specific barcode (Hamady et al 2008) at the 5'-end, and an equimolar mix of reverse primers 338R-I and 338R-II (Daims et al 1999) that were appended with the titanium adapter B at the 5'-end. All primers are given in Table S2. PCR amplification was performed in a thermocycler GS0001 (Gene Technologies, Braintree, UK) in a total volume of 100 µl containing 2 µl DNA (20 ng/ul), 500 nM of barcoded forward primer and reverse primermix (Biolegio BV, Nijmegen, The Netherlands), 2 U of Phusion Hot start II High-Fidelity DNA polymerase (Finnzymes, Vantaa, Finland), 20 µl of 5x HF buffer, 2 µl PCR grade nucleotide mix (Roche Diagnostics GmbH, Mannheim, Germany), and 65 µl nuclease free sterile water (Promega Corporation, Madison, WI). PCR amplification conditions were a pre-denaturing step of 3 min at 98ºC followed by 30 cycles of 98ºC for 10 s, 56ºC for 20 s and 72ºC for 20 s. Lastly, a post-elongation step of 10 min at 72ºC was done. PCR products were purified using a GeneJet PCR purification kit (Thermo Fisher Scientific) and the concentration was determined using the Qubit 2.0 fluorometer (Thermo Fisher Scientific). All samples for pyrosequencing were mixed in equimolar amounts. Pooled samples were loaded on a 1% (v/v) agarose gel containing 1x SYBR Safe (Invitrogen, Thermo Fisher Scientific) and bands of approximately 340 bp were excised and purified with the GeneJet Gel Extraction Kit (Thermo Fisher Scientific) using 25 µl elution buffer for collecting the amplified DNA. Mixed samples were quantified using the Qubit 2.0 fluorometer (Thermo Fisher Scientific) and submitted for pyrosequencing on the 454 Life Sciences GS-FLX platform using Titanium sequencing chemistry (GATC Biotech AG, Konstanz, Germany).

Archaea community profiling

Extracted DNA was subjected to barcoded amplification of the 16S rRNA gene. A PCR amplification replicate of BHori (BHoriA and BHoriB) was done to correct for technical biases.

A method adapted from Jaeggi *et al* (2014) was used. Barcoded amplification of 16S rRNA genes was done by using forward primer 340F (Gantner et al 2011) that was extended with the titanium adapter A and a ten-base sample specific barcode at the 5'-end, and reverse primer 1000R (Gantner et al 2011) that was appended with the titanium adapter B at the 5'-end. All primers are given in Table S2. PCR amplification was performed in a total volume of 50 µl containing 1 µl DNA, 200 nM of each forward and reverse primer (Biolegio BV), 1 U of KOD Hot Start DNA Polymerase (Merck Millipore), 5 µl of 10x KOD-buffer, 3 µl $MgSO_4$ (25 mM), 5 µl dNTP mix (2 mM each), and 33 µl nuclease free sterile water. PCR amplification conditions were a pre-denaturing step at 95°C for 2 minutes followed by 35 cycles of 95°C for 20 s, 5°C for 10 s, and 70°C for 15 s. The approximately 660 bp PCR amplicon was subsequently purified using the MSB Spin PCR apace kit (STRATEC Biomedical AG, Birkenfeld, Germany) and the concentration was checked with a Nanodrop 1000 spectrophotometer (Thermo Fisher Scientific). Purified PCR products were mixed in equimolar amounts. The mixed sample was further purified using the Purelink PCR Purification kit (Thermo Fisher Scientific), with high-cutoff binding buffer B3, and submitted for pyrosequencing on the 454 Life Sciences GS-FLX platform using Titanium sequencing chemistry (GATC Biotech AG).

Pyrosequencing analysis

The pyrosequencing data was analysed with a workflow based on Quantitative Insights Into Microbial Ecology (QIIME) v1.2 (Caporaso et al 2010), and reads were filtered for chimeric sequences using the usearch algorithm. OTU clustering was performed with settings as recommended in the QIIME newsletter of December 17th 2010 (http://qiime.wordpress. com/2010/12/17/new-default-parameters-for-uclust-otu-pickers/) using an identity threshold of 97%. The SILVA reference database was used for taxonomic classification (Quast et al 2013). After picking representative OTUs, the relative amount of reads of every OTU to the total amount of reads per sample was quantified. Afterwards, the average relative amount of reads per condition from the biological triplicate samples were calculated. For analysis of the original sample BHori, the average of the PCR duplicates (BHoriA and BHoriB) was calculated. Then, the significant differences of every representative OTU between the conditions $CH_4+SO_4^{2-}$ and CH_4-only and between $CH_4+SO_4^{2-}$ and SO_4^{2-}-only were calculated separately, using the Kruskal-Wallis test ($p<0.05$). For archaea, we then selected only representative OTUs that were significantly higher in conditions with $CH_4+SO_4^{2-}$ as separately compared to CH_4-only and SO_4^{2-}-only. For bacteria, we selected only representative OTUs that were significantly higher in conditions with $CH_4+SO_4^{2-}$ as compared to both CH_4-only and SO_4^{2-}-only.

Quantitative real-time PCR

Extracted genomic DNA was used for qPCR analysis. The DNA was purified with the DNA clean and concentrator-5 kit (Zymo Research, Irvine, CA) and the concentration was determined with the Qubit 2.0 fluorometer (Thermo Fisher Scientific). Amplifications with specific primers for ANME-2a/b were done as described in chapter 5. Quantification was expressed as the

total number of 16S rRNA gene copies per g_{vss} extracted from the incubations.

Nucleotide sequences

Nucleotide sequence data reported are available in the DDBJ/EMBL/GenBank databases under the accession numbers LN795911-LN796465 for archaeal sequences and LN796466-LN808676 for bacterial sequences.

Results and discussion

Trace methane oxidation

Methane production was observed in most conditions, but was negligible in the presence of sulfate and did not occur in the presence of nitrate (Fig 2). Methane production in conditions with and without added methane showed a similar pattern, but the amount of methane produced was lower in incubations where methane was added (Fig S1A). This was probably caused by the increase of TMO due to a higher methane concentration (Smemo and Yavitt 2007, Zehnder and Brock 1980). Production of $^{13}CO_2$ was apparent in all incubations with $^{13}CH_4$ in the headspace, except in the conditions with nitrate and HAs (Fig 2 and Fig S1B). Typical for TMO, $^{13}CO_2$ simultaneously increased with methane formation in the conditions with ferrihydrite, ferrihydrite + HAs and the control without electron acceptor (Fig 2). The $^{13}CO_2$ production was not substantially different between ferrihydrite, ferrihydrite + HAs and the control conditions (Table 1), indicating that TMO was not influenced by the electron acceptors added. When ferrihydrite was added, the $^{13}CO_2$ production continued when all iron was reduced to Fe(II) after 300 days without addition of HAs (Fig S2). Iron reduction did occur faster in incubations with ferrihydrite + HAs than in the incubations with only ferrihydrite. The incubations with 20 g l^{-1} HAs contained an average of 28.8 (±1.0) mM acid soluble Fe(II) after 300 days of incubation and did not show any detectable $^{13}CO_2$ increase (Fig 2, Fig S1B and Table 1). The HAs batch used contained calcium which could scavenge produced CO_2 to form calcium carbonate. After acidification of the samples, an increase in total CO_2 was observed but the percentage of $^{13}CO_2$ did not increase. It was reported that reduced methane emission after addition of HAs to peat ecosystems could be caused by increased methane oxidation (Blodau and Deppe 2012). In contrast, here we observed higher methane production after addition of HAs but no methane oxidation.

Anaerobic methane oxidation

Only in the incubations with sulfate, an increase in $^{13}CO_2$ with no increase in $^{12}CH_4$ was observed (Fig 2). The ratio of methane oxidized per methane produced was only >1 for conditions with sulfate, which is indicative for AOM (Table 1). In previous studies, sulfate addition inhibited methane formation and thus $^{13}CO_2$ production from TMO in freshwater sludge (Meulepas et al 2010, Zehnder and Brock 1980) and in freshwater slurries (Segarra et al 2013) and only

stimulated methane oxidation in brackish water slurries (Segarra et al 2013). In our study, the pooled inoculum contained an average of around 2 mM sulfate (Table S3). All sulfate was reduced after 41 days of incubation and methanogenesis continued in most conditions, which was accompanied by continued $^{13}CO_2$ production during TMO (Fig 2). Only where sulfate was added, sulfate addition stimulated methane oxidation and repressed methane production, indicating AOM coupled to sulfate reduction at low salinity. AOM could not be coupled to any other electron acceptor than sulfate. ICP measurements of all samples prior to mixing showed that only the elements sulfur and iron were present, which in oxidized form could be possible electron acceptors for AOM, whereas the amount of selenium and manganese was not significant (Table S4). In incubations with nitrate and humic acids, no $^{13}CO_2$ was produced.

Table 1 CH_4 oxidized per CH_4 formed after 168 days of incubation as calculated from the amount of $^{12}CH_4$ formed and the amount of $^{13}CO_2$ formed in incubations with a headspace of 100% $^{13}CH_4$ and with different electron acceptors.

Condition	Bottle #	Total CO_2 formed (µmol)	$^{13}CO_2$ formed (µmol)	$^{12}CH_4$ formed (µmol)	CH_4 oxidized/CH_4 formed
SO_4^{2-}	1A-1	432.3	6.2	1.8	>1
	1A-2	108.9	20.3	1.5	>1
	1A-3	532.7	10.4	0.9	>1
$Fe(OH)_3$	2A-1	0	2.2	14.8	0.15
	2A-2	209.4	4.8	34.5	0.14
	2A-3	433.3	8.1	41.7	0.19
$Fe(OH)_3$+HAs	3A-1	0	1.5	13.8	0.11
	3A-2	23.0	2.5	19.6	0.13
	3A-3	0	0	5.8	n/a
HAs	4A-1	0	0	51.4	n/a
	4A-2	0	0	56.0	n/a
	4A-3	0	0	47.4	n/a
NO_3^-	5A-1	0	0	0.0	n/a
	5A-2	0	0.2	0.0	n/a
	5A-3	0	0	0.0	n/a
None	6A-1	283.0	6.8	33.0	0.21
	6A-2	159.3	6.1	34.9	0.18
	6A-3	36.2	4.3	37.5	0.11

n/a means not applicable.

Reduction of the electron acceptors sulfate, ferrihydrite and nitrate occurred in all conditions with and without addition of methane (Table 2). The reduction rates of sulfate with and without added methane in the first 168 days were similar (2-tailed t-test with unequal variance, $p<0.05$), which was probably due to endogenous SR masking sulfate-dependent AOM. After 343 days of incubation, the SR rate in incubations with only sulfate had substantially decreased due to

endogenous substrate depletion whereas in conditions with methane and sulfate, there was no difference in SR rates. However, in this time period AOM could not be linked to SR and sulfide production as the abundant green sulfur bacteria (GSB) *Chlorobiaceae* (Fig S3) could have caused the fluctuations in sulfide levels. Growth and activity of *Chlorobiaceae* explained the green coloration occuring specifically in incubations amended with sulfate, which derived from the bacteriochlorophyll of GSB (Gorlenko 1970). GSB are strictly anaerobic autotrophic sulfide oxidizers and have been found to be active when exposed to very little light (Beatty et al 2005, Manske et al 2005), which could explain activity even in the dark with limited exposure to light during sampling of our incubations. Their activity probably kept the sulfide concentration low. After maintaining complete darkness in the slurries, the $^{13}CO_2$ production continued throughout incubation time and free sulfide was eventually measured. In bottle 1A-2 that showed the highest $^{13}CO_2$ production after 168 days of incubation (Table 1), sulfide production increased simultaneously with $^{13}CO_2$ production during the last period between 343 and 728 days (Fig S4). This shows that at long-term, net methane oxidation accompanied sulfide production.

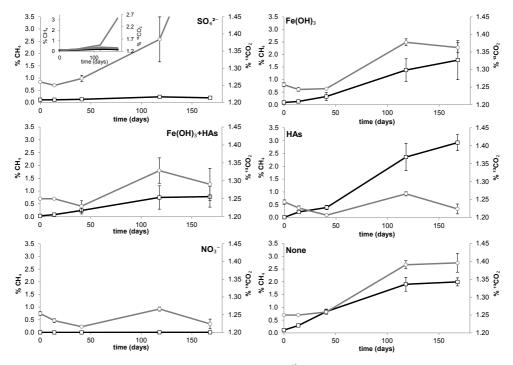**Figure 2** Percentage of methane (black lines) and percentage of $^{13}CO_2$ of total CO_2 (grey lines) during 168 days of incubation in bottles with 100% $^{13}CH_4$ in the headspace and with different electron acceptors. Standard deviations represent triplicate incubations. Note the different scale in the condition with sulfate where one of the triplicates '1A-2' highly increased in $^{13}CO_2$.

Table 2 Reduction rates of the electron acceptors sulfate, iron in the form of ferrihydrite with and without humic acids (HAs), and nitrate in each incubation with and without methane in the headspace during the first 168 days of incubation and sulfate reduction rates in incubations with sulfate between 343 and 728 days of incubation (in μmol g_{vss}^{-1} d^{-1}). Standard deviations represent biological triplicates.

Condition	Reduction rates (μmol g_{VSS}^{-1} d^{-1})
0-168 days	**Sulfate**
$CH_4+SO_4^{2-ac}$	5.14 (±3.04)
SO_4^{2-a}	7.58 (±0.50)
CH_4^b	0
343-728 days	
$CH_4+SO_4^{2-ac}$	5.94 (±0.83)
SO_4^{2-c}	5.02 (±0.16)
0-168 days	**Iron**
$CH_4+Ferrihydrite^a$	0.12 (±0.01)
$Ferrihydrite^a$	0.15 (±0.02)
$CH_4+Ferrihydrite+HAs^b$	10.58 (±1.95)
$Ferrihydrite+HAs^b$	4.29 (±7.10)
	Nitrate
$CH_4+NO_3^{-a}$	28.02 (±1.38)
NO_3^{-a}	25.32 (±1.02)

Means with different letters in superscript are significant (independent 2-tailed t-test with unequal variance, $p<0.05$).

Microbial community profiling

Microbial community profiling was only done on triplicates of the conditions $CH_4+SO_4^{2-}$, CH_4-only, SO_4^{2-}-only, and the original sediment after 323 days of incubation. For all samples that were analyzed, the highest average percentage of 16S rRNA reads for Archaea clustered within the *Methanosarcinaceae, Methanoregulaceae, Methanosaetaceae*, *Methanobacteriaceae*, and the Miscellaneous Crenarchaeota Group (MCG) (Fig S5). Archaeal OTUs that showed a significantly higher percentage of reads (Kruskal Wallis, $p<0.05$) in condition $CH_4+SO_4^{2-}$, as compared to CH_4-only (Fig 3A) and SO_4^{2-}-only (Fig 3B) make up less than 8% of all reads. In condition $CH_4+SO_4^{2-}$, ANME-2a/b sequences represented 0.16% of all reads and were much more abundant than in the condition CH_4-only. Higher abundance of ANME-2a/b in conditions $CH_4+SO_4^{2-}$ compared to SO_4^{2-}-only was shown by qPCR analysis (Fig S6). This indicates the involvement of ANME-2a/b in AOM coupled to SR, as shown before in marine environments (Orphan et al 2001a). The ANME-2a/b OTU showed 98% identity with ANME-2a/b from both marine and terrestrial environments and do not form a monophyletic cluster with ANME-2a/b found in other low-sulfate environments (Fig 4). A marine enrichment of ANME-2a/b species that share 98% identity was previously shown to be completely inhibited in AOM activity at a salinity of 5‰ (Meulepas et al 2009), indicating that the ANME-2a/b detected in this study are adapted to low salinity.
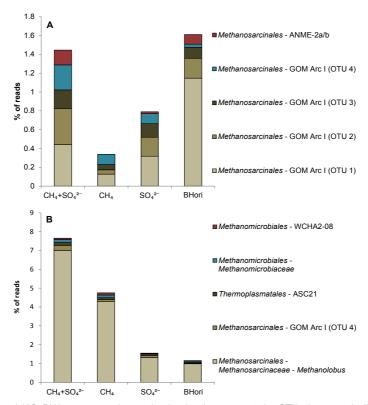
Figure 3 Archaeal 16S rDNA pyrosequencing results showing the representative OTUs that were significantly higher in the conditions $CH_4+SO_4^{2-}$ as compared to CH_4-only (A) and SO_4^{2-}-only (B) (Kruskall-Wallis, $p<0.05$). Also displayed is the original pooled sample (BHori). Displayed is the average percentage of reads per representative OTU of the three biological triplicates per condition.

A higher percentage of reads was also found for 1 OTU of Methanosarcinales GOM Arc I (OTU 4) in conditions $CH_4+SO_4^{2-}$ compared to both CH_4-only and SO_4^{2-}-only (Fig 3). This GOM Arc I group was previously named 'ANME-2d' (Mills et al 2003) but was renamed to 'GOM Arc I' since it was not monophyletic with other ANME-2 subtypes and no AOM activity or aggregation with sulfate reducers had been shown (Lloyd et al 2006). Recently, the name ANME-2d was re-adopted for a cluster that harbors "*Ca.* Methanoperedens nitroreducens", which performed AOM coupled to nitrate reduction (Haroon et al 2013). This cluster was previously identified in a nitrate-dependent AOM enrichment (Raghoebarsing et al 2006) and was named 'AOM associated archaea'(AAA) (Knittel and Boetius 2009). The GOM Arc I related OTU 4 found in this study was 97% identical to "*Ca.* M. nitroreducens" and was 99% identical to other AAA members that were proposed to be responsible for freshwater AOM coupled to SR in Lago di Cadagno sediments (Schubert et al 2011) (Fig 4). The AAA were also found to be abundant in an aquifer where methane and sulfate were present (Flynn et al 2013). It was already shown that "*Ca.* M. nitroreducens" uses the complete reverse methanogenesis pathway and it was suggested that the genes for nitrate reduction were obtained from a bacterial donor (Haroon

et al 2013). We did not find nitrate-dependent AOM activity, which leaves open the possibility that the AAA in this study could perform AOM coupled to SR. Sulfate addition in presence of methane also had a positive effect on other GOM Arc I related OTUs (Fig 3A, Fig 4), which makes a contribution of GoM Arc I to AOM activity likely. The higher percentage of reads of *Methanolobus* in conditions $CH_4+SO_4^{2-}$ compared to SO_4^{2-}-only (Fig 3B) implied that methane addition had an effect on *Methanolobus* abundance. The reason for this effect is unclear, since this genus is known to be able to utilize methylated compounds (Zhang et al 2008), but not methane. However, *Methanolobus* was also found in a marine methane-oxidizing bioreactor (Girguis et al 2003).
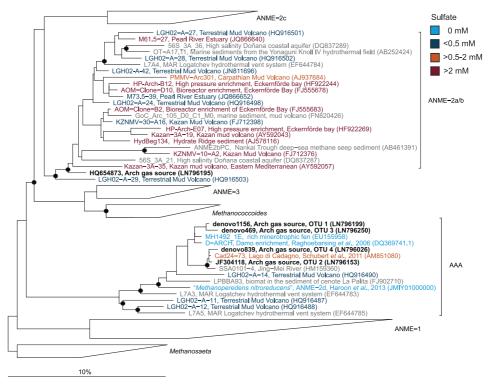

Figure 4 Phylogenetic tree of archaeal 16S rRNA gene sequences derived from the SILVA SSU Ref database (release 111). The tree was constructed using the ARB neighbor-joining method with terminal filtering and the Jukes-Cantor correction using almost full length 16S rRNA sequences. Closed circles represent bootstrap values >70% (1000 replicates). The scale bar represents the percentage of changes per nucleotide position. Short length 16S rRNA sequences (<1000 bp) were afterwards added to the tree using the ARB parsimony method. Colour-coding represents different sulfate concentrations (mM) of the environment where the sequences were found. Sequences in grey had no clearly reported sulfate data. Sequences found in this study are depicted in black and bold.

Bacterial diversity was high in all samples, with the highest relative number of reads for all samples clustering with the *Deltaproteobacteria* (*Syntrophobacteriacaea* and *Desulfobacteraceae*) and *Gammaproteobacteria* (*Methylococcaceae*), *Bacteroidetes*, *Chloroflexi, Firmicutes and Chlorobi* (family *Chlorobiaceae*) (Fig S3). Bacterial OTUs that showed a substantially

higher percentage of reads (Kruskal Wallis, $p<0.05$) in condition $CH_4+SO_4^{2-}$ as compared to both CH_4-only and SO_4^{2-}-only make up less than 0.5% of all reads (Fig 5). These OTUs clustered with the *Desulfobacteraceae, Clostridiales* and *Planctomycetaceae.* The OTUs of *Desulfobacteraceae* belonged to the Sva0081 sediment group, *Desulfobacterium* and the SEEP-SRB1 cluster. The latter OTU of SEEP-SRB1 (AB630772) was only found in condition $CH_4+SO_4^{2-}$. However, other SEEP-SRB1 OTUs that were detected did not show a difference in read abundance between the conditions $CH_4+SO_4^{2-}$,CH_4-only and SO_4^{2-}-only. The SEEP-SRB1 clade has been detected in several marine AOM mediating environments (Harrison et al 2009, Knittel et al 2003, Lösekann et al 2007, Orphan et al 2001b, Pernthaler et al 2008, Vigneron et al 2013, Yanagawa et al 2011) and enrichments (Jagersma et al 2009, Zhang et al 2011). The SEEP-SRB1 OTUs found in this study clustered in undefined subgroups outside the marine SEEP-SRB1 subgroups that were described previously (Fig 6), of which SEEP-SRB1a was identified as the dominant bacterial partner of ANME-2a/b in marine AOM mediating enrichments (Schreiber et al 2010). From the other OTUs that showed a higher percentage of reads in condition $CH_4+SO_4^{2-}$, little is known about their role in AOM coupled to SR. It has been shown before that different SRB besides SEEP-SRB1 belonging to *Desulfobacteraceae* form consortia with different ANMEs (Orphan et al 2002, Vigneron et al 2013) and even non-SRB were found to aggregate with ANMEs (Pernthaler et al 2008). We did not find any sequences related to the NC10 phylum of bacteria, harboring the nitrate-dependent methanotrophic bacterium "*Ca.* Methylomirabilis oxyfera" (Ettwig et al 2010), and we also did not obtain any PCR product using specific primers for this clade (data not shown), which is in line with the lack of AOM coupled to denitrification.

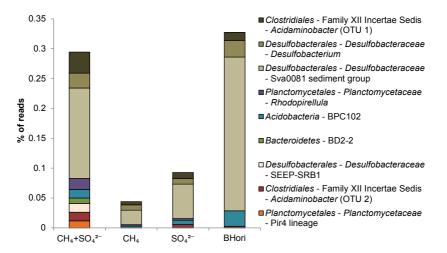**Figure 5** Bacterial 16S rDNA pyrosequencing results showing the representative OTUs that were significantly higher in the conditions $CH_4+SO_4^{2-}$ as compared to both CH_4-only and SO_4^{2-}-only (Kruskall-Wallis, $p<0.05$). Also displayed is the original pooled sample (BHori). Displayed is the average percentage of reads per representative OTU of the three biological triplicates per condition.
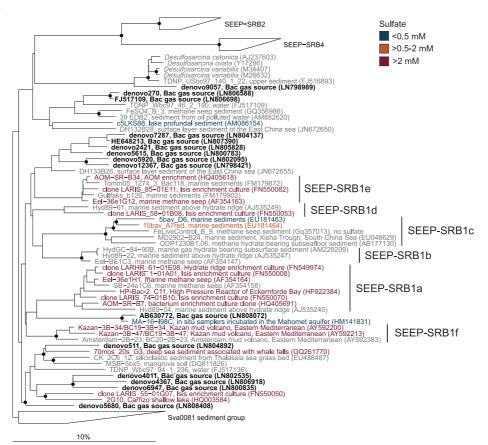
Figure 6 Phylogenetic tree of bacterial 16S rRNA gene sequences derived from the SILVA SSU Ref database (release 111). The tree was constructed using the ARB neighbor-joining method with terminal filtering and the Jukes-Cantor correction using almost full length 16S rRNA sequences. Closed circles represent bootstrap values >70% (1000 replicates). The scale bar represents the percentage of changes per nucleotide position. Short length 16S rRNA sequences (<1000 bp) were afterwards added to the tree using the ARB parsimony method. Colour-coding represents different sulfate concentrations (mM) of the environment where the sequences were found. Sequences in grey had no clearly reported sulfate data. Sequences found in this study are depicted in black and bold.

AOM at low sulfate concentrations

The sulfate concentration was 0.07 mM in the gas source effluent and about 2 mM in the pooled inoculum (Table S3). The measured conductivity and chloride concentration of the gas source effluent and pooled inoculum samples (Table S3) indicate a somewhat higher salinity than typical freshwater, but a much lower salinity than typical brackish environments. This could correspond to the historical marine influence of the adjacent lake (Markermeer) that was formed due to dike construction, as described for proximal sites (van Diggelen et al 2014). In marine environments, the sulfate:chloride ratio is around 1:19. The sulfate:chloride ratio of the lake surface water was around 1:2.6, with 1.7 mM sulfate and 4.4 mM chloride (Table S3). Therefore, marine influences cannot explain the relatively high sulfate concentrations. The

sulfate concentration in deeper layers of the gas source could be even higher than measured in the gas source effluent before AOM took place. In marine systems, AOM rates started to be affected below 2-3 mM sulfate (Meulepas et al 2009, Wegener and Boetius 2009) but occurred even below 0.5 mM of sulfate (Yoshinaga et al 2014, Beal et al 2011). In typical freshwater environments, the sulfate concentration is generally lower than 0.5 mM, making AOM-SR feasible but at low rates. AOM in freshwater was recently shown to be a strong methane sink at sulfate concentrations as low as 1.2-0.1 mM (Segarra et al 2015). Our finding of AOM activity only in conditions with methane and sulfate, and the enrichment of ANME-2a/b and SEEP-SRB1 suggests that these syntrophic clades are ubiquitously distributed in marine and in low-salinity environments and perform AOM at low sulfate concentrations.

3

Acknowledgements

Supplementary information

Figure S1 Methane production (µmol) after 168 days of incubation in conditions with 100% $^{13}CH_4$ in the headspace ($^{12}CH_4$ measured) and without methane (CH_4 measured), and with different electron acceptors added (A). $^{13}CO_2$ production (µmol) after 168 days of incubation in conditions with 100% $^{13}CH_4$ in the headspace with different electron acceptors added (B). Standard deviations represent biological triplicates. Means with different letters are significant (independent 2-tailed t-test with unequal variance, $p<0.05$).
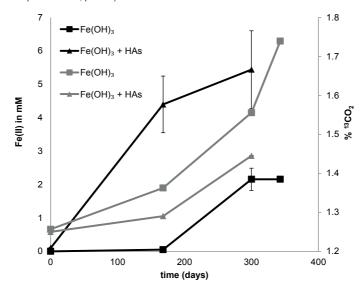
Figure S2 Iron (II) in mM (black lines) and % $^{13}CO_2$ of total CO_2 (grey lines) during time in incubations with ferrihydrite (squares) and ferrihydrite with humic acids (triangles).
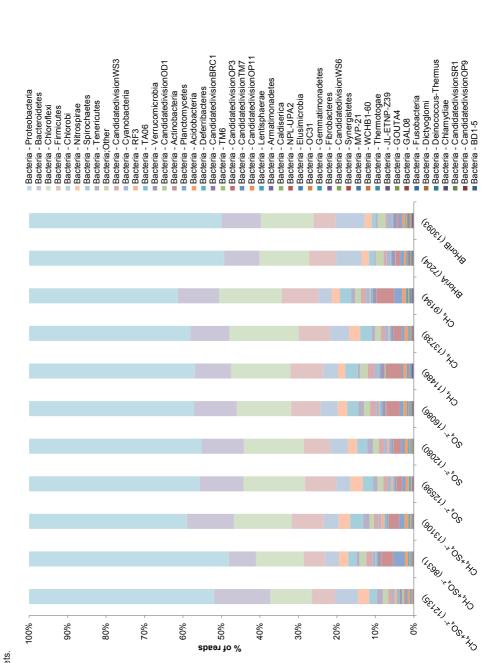
Figure S3 Bacterial pyrosequencing results showing the percentage of reads of every representative OTU within every sample. The number of reads of every sample is given between brackets.
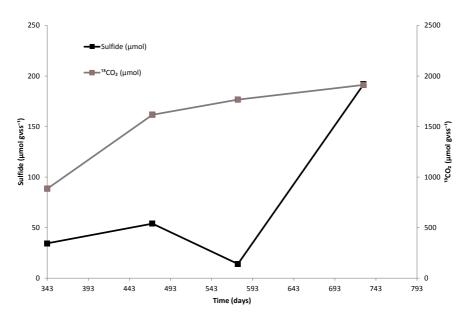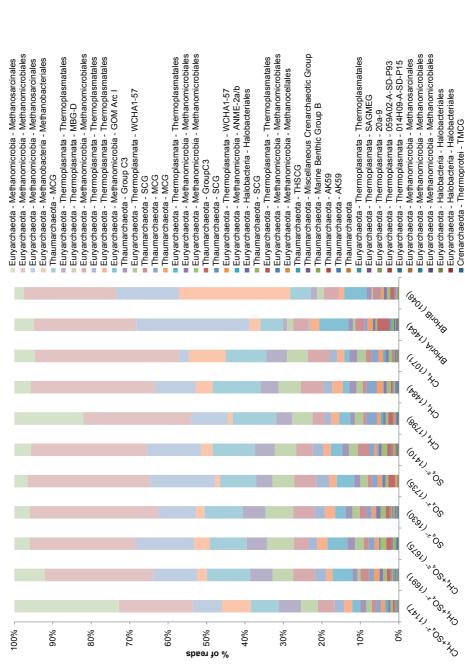
Figure S4 Amount of sulfide (µmol g_{vss}^{-1}) and $^{13}CO_2$ (µmol g_{vss}^{-1}) in one of the triplicates '1A-2' with sulfate and 100% $^{13}CH_4$ in the headspace after 343 days of incubation. Technical standard deviations of measurements between time points were on average 7.7% for $^{13}CO_2$ and 4.3% for sulfide as determined from replicate measurements of standards with known composition.

Figure S5: Archaeal pyrosequencing results showing the percentage of reads of every representative OTU within every sample. The number of reads of every sample is given between brackets.

3
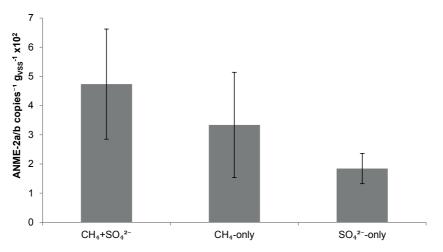
Figure S6 16S rRNA gene abundance of ANME-2a/b (copies g_{VSS}^{-1}) with standard deviations representing biological triplicates of conditions $CH_4+SO_4^{2-}$, CH_4-only, and SO_4^{2-}-only after 323 days of incubation.

Table S1 Composition of concentrated anaerobic media stocks before 1:1 mixing (v/v) with sample.

Compound	Concentration (g l^{-1})
$Na_2HPO_4 \cdot 2H_2O$	0.53
KH_2PO_4	0.41
NH_4Cl	0.3
$CaCl_2 \cdot 2H_2O$	0.11
$MgCl_2 \cdot 6H_2O$	0.1
NaCl	0.3
$NaHCO_3$	4.0
$Na_2S \cdot 9H_2O$	0.48
Acid trace element solution	1ml l^{-1} (Composition in mM: $FeCl_2$, 7.5; H_3BO_4, 1; $ZnCl_2$, 0.5; $CuCl_2$, 0.1; $MnCl_2$, 0.5; $CoCl_2$, 0.5; $NiCl_2$ 0.1; HCl, 50)
Alkaline trace element solution	1 ml l^{-1} (Composition in mM: Na_2SeO_3, 0.1; Na_2Wo_4, 0.1;Na_2MoO_4, 0.1; NaOH, 10)
Vitamin solution	0.2 ml l^{-1} (Composition in g l^{-1}: biotin, 0.02; niacin, 0.2; pyridoxine, 0.5; riboflavin, 0.1; thiamine, 0.2; cyanocobalamin, 0.1; p-aminobenzoic acid, 0.1; pantothenic acid, 0.1)

According to Stams *et al* (1993).

Table S2 Adapters and primers used in this study for pyrosequencing analysis

Primer	Primer sequence (5'-3')	Reference
Adapter A	CCATCTCATCCCTGCGTGTCTCCGACTCAG	Provided by GATC Biotech
Adapter B	CCTATCCCCTGTGTGCCTTGGCAGTCTCAG	Provided by GATC Biotech
27F-DegS	GTTYGATYMTGGCTCAG	(van den Bogert et al 2011)
338R-I	GCWGCCTCCCGTAGGAGT	(Daims et al 1999)
338R-II	GCWGCCACCCGTAGGTGT	(Daims et al 1999)
340F	CCCTAYGGGGYGCASCAG	(Gantner et al 2011)
1000R	GGCCATGCACYWCYTCTC	(Gantner et al 2011)

Table S3 Physico-chemical analysis *in situ* and from the pooled inoculum sample

	Surface water	Ditch 1	Gas source effluent	Pooled inoculum
NO_3-N (mg l^{-1})	N/A	0.77	0.45	0
SO_4 (mg l^{-1})	160	25.7	6.3	192
PO_4-P (mg l^{-1})	N/A	3.5	2.7	N/A
Chloride (mg l^{-1})	158	N/A	N/A	294
pH	8.1	7.5	7.5	7.5
Conductivity (mS cm^{-1})	N/A	2.2	2.6	2.0

N/A: not measured. Surface-water measurements were done by Hoogheemraadschap Hollands Noorderkwartier on 11 August, 1995.

Table S4 Physico-chemical analysis using ICP of all original samples before pooling 1:1:1 (v/v/v).

Liquid	Fe (µM)	Mn (µM)	S (µM)	Se (µM)
Ditch 1	5.0	2.0	25	0
Ditch 2	97	1.0	77	0
Tank 2	15	7.7	47	0
Solid	**Fe (µmol g^{-1})**	**Mn (µmol g^{-1})**	**S (µmol g^{-1})**	**Se (µmol g^{-1})**
Ditch 1	163	1.1	44	0
Ditch 2	312	2.5	123	0
Tank 2	227	2.2	146	0

Chapter 4

Enrichment and cultivation of sulfate-reducing bacteria from a bioreactor performing anaerobic oxidation of methane coupled to sulfate reduction

Peer H. A. Timmers, Daan van Vliet, Hauke F. Treppke, Ahmad F. Khadem, Caroline M. Plugge and Alfons J. M. Stams

Abstract

Anaerobic methane oxidizing archaea (ANME) are able to perform reverse methanogenesis. It is presumed that the ANME transfer electrons released from methane oxidation to sulfate-reducing bacteria (SRB), but little is known about the mechanisms of electron transfer and the interspecies electron carrier (IEC) involved. In different environments, phylogenetically divergent SRB associate with ANME, most of which belong to the *Desulfococcus/Desulfosarcina* (DSS) clade. Since growth on methane is slow, physiological studies on both the ANME and the associated SRB are hampered. In this study, a variety of electron donors were used to enrich for SRB from a highly diluted sediment-free enrichment culture that performed sulfate-dependent AOM. Incubations harboured different SRB mostly falling within the DSS clade and with high similarity to clones found in AOM mediating enrichments. With acetate, a slow growing enrichment (1.3-3.1 mM sulfide production in 762 days) of *Desulfosarcina* spp. was obtained. This type of SRB was also found in the propionate, H_2/CO_2 and formate fed cultures. No activity or growth was found with methanethiol nor did polysulfide addition result in sulfide disproportionation. These results indicate that polysulfide and methanethiol are not acting as IEC, while acetate and possibly H_2/CO_2 and formate are important for the AOM enrichment used in this study. All enrichment cultures except for the ones with acetate were tested separately to stimulate AOM when added to an AOM performing enrichment, but none resulted in increased AOM activity.

Introduction

Anaerobic oxidation of methane (AOM) coupled to sulfate reduction (SR) is a process found in anoxic methane-rich environments where sulfate is the dominant electron acceptor. It was first uncovered in marine environments and the process is presumably performed by anaerobic methanotrophic archaea (ANME) in consortia with sulfate-reducing bacteria (SRB) (Boetius et al 2000, Hinrichs et al 1999, Orphan et al 2001a). The microorganisms mediating AOM coupled to SR grow extremely slow with estimated doubling times between 1.5 and 7 months (Girguis et al 2005, Krüger et al 2008, Meulepas et al 2009a, Nauhaus et al 2007, Orphan et al 2009). This makes it difficult to study the physiology of ANME and the associated SRB. As a result, the postulated syntrophic interaction between ANME and SRB is not yet understood. It was suggested that the methanotrophic archaea oxidize methane and transfer electrons to the sulfate-reducing partner, either through direct electron transfer or indirectly using interspecies electron carriers (IEC) such as acetate, formate, hydrogen, or methanol. Most research has excluded these methanogenic intermediates as IEC (Meulepas et al 2010b, Nauhaus et al 2002, Nauhaus et al 2005, Orcutt et al 2008, Treude et al 2007), and other carriers such as methanethiol (Moran et al 2008) and polysulfides (Milucka et al 2012) were proposed as alternatives. The widespread occurrence of AOM coupled to SR in marine habitats, ranging from methane seeps to diffusive sediments, could mean that different strategies of electron transfer exist in different environments (Alperin and Hoehler 2010). The substantial phylogenetic diversity of the associated SRB found in different AOM mediating environments supports this. In seep sediments, associated bacteria mainly belonged to the *Desulfococcus/Desulfosarcina* (DSS) cluster of the *Deltaproteobacteria* (Boetius et al 2000, Orphan et al 2001a). In most studies, the bacterial partner was mainly detected by fluorescence *in situ* hybridisation microscopy using probe DSS658 (Manz et al 1998), which targets many bacteria within this DSS cluster. Using more specific probes, a subclass of the DSS called SEEP-SRB1a was found to be the predominant partner of ANME-2 in two enrichment cultures (Schreiber et al 2010). However, ANME-2 have also been reported to occur in consortia with SRB outside the DSS cluster, such as SEEP-SRB2 (Kleindienst et al 2012, Chapter 2), *Desulfobulbus* related spp. (Lösekann et al 2007, Pernthaler et al 2008, Vigneron et al 2013b), *Desulfurella* related spp. (Holler et al 2011b), and even with non SRB, such as *Alphaproteobacteria* and *Betaproteobacteria* (Pernthaler et al 2008). This indicates that the syntrophic interaction depends on several factors and is not fixed to a certain phylogenetic cluster of SRB.

Versatility in metabolic properties could exist between AOM associated SRB. Research suggested that members of SEEP SRB2 are capable of performing other processes unrelated to AOM coupled to SR (Kleindienst et al 2012, Orcutt et al 2005, Vigneron et al 2013b). The DSS clade includes a multitude of SRB which are able to degrade non-methane alkanes (Aeckersberg et al 1991, Higashioka et al 2009, Jaekel et al 2013, Jaekel et al 2015, Kleindienst et al 2014, Kniemeyer et al 2007). It is therefore plausible that both ANME and SRB use different substrates apart from methane and sulfate for growth. Alternative substrates could

fuel ANME and/or associated SRB with the energy to attain faster growth. This would enable enrichment or even isolation and further physiological studies, which could give insights into the IECs that are used in AOM.

In this study, an enrichment culture from an AOM performing bioreactor, reactor R4 (Meulepas et al 2009a), was subjected to multiple dilution series for more than 4 years (Fig 1, step 1-3). The highest dilution that still showed sulfide production activity was used as inoculum to test the growth of SRB on a variety of canonical sulfate-reducing substrates (Fig 1, step 4). These substrates included H_2/CO_2, formate, methanol, acetate, butyrate, pyruvate, propionate and lactate. Methanethiol and polysulfide as possible IECs in AOM were also tested as substrates. Sulfide production was monitored and community analysis was done using 16S rRNA gene cloning and sequencing. To assess if the enriched SRB could stimulate AOM coupled to SR, the enriched SRB (except the enrichment on acetate) were subsequently added separately to an AOM reactor enrichment (10^{-1} dilution of the first dilution series from October 2008, Fig 1, step 1) together with $^{13}CH_4$ and sulfate.
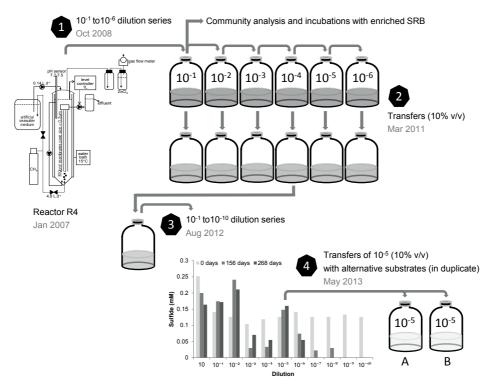
Figure 1 History of the biomass used as inoculum in presented studies. The reactor R4 enrichment (Meulepas et al 2009a) was subjected to a dilution series and transfers (step 1-3) done prior to specific SR enrichment, in articifical sea water medium with only methane and sulfate and without bicarbonate. The 10^{-5} dilution from the second dilution series of August 2012 was transferred in duplicate (A and B) to medium with SR substrates (step 4). The first dilution of the reactor enrichment (10^{-1}) from October 2008 was used for community analysis through 16S rRNA pyrosequencing and for incubations with enriched SRB (see materials and methods section 'addition of enrichments to AOM culture').

Materials and methods

Source of inoculum

The inoculum was derived from an enrichment culture performing AOM coupled to SR in a submerged membrane bioreactor R4 (Meulepas et al 2009a). The sediment used in this enrichment was taken from station B, Eckernförde Bay, Baltic Sea (water depth 28 m; 54º31'15N, 10º01'28E during a cruise of the German research vessel *Littorina* in June 2005 as described by Meulepas *et al* (2009a). The sampling site has been described by Treude *et al* (2005b). Reactor R4 was operated from January 2007 for 355 days with methane and sulfate as sole electron donor and acceptor, respectively. A sample from the reactor was used as inoculum for a 10-fold dilution series in serum vials containing only methane (1.8 bar) and sulfate (20 mM) in October 2008 (Fig 1, step 1). These incubations were transferred after 944 days of incubation with only methane and sulfate (10% v/v) in March 2011 (Fig 1, step 2). After one year of incubation, the most diluted culture that still showed sulfide production activity (10^{-4} dilution) was transferred to a new dilution series in August 2012 (Fig 1, step 3). One year later in March 2013, the highest dilution that still showed sulfide production activity (10^{-5} dilution), was used for selective enrichment of SRB in new artificial sea water medium (Fig 1, step 4).

Medium composition and cultivation

The reactor R4 dilution series (Fig 1, step 1-3) were done in phosphate buffered artificial sea water medium as used in the reactor studies (Meulepas et al 2009a). Enrichments on canonical sulfate-reducing substrates (Fig 1, step 4) were done in carbonate buffered artificial sea water medium consisting of: 20.78 g l^{-1} NaCl, 5.1 g l^{-1} MgSO$_4$*7H$_2$O, 4.25 g l^{-1} MgCl$_2$*6H$_2$O, 0.68 g l^{-1} K$_2$HPO$_4$*3H$_2$O, 0.45 g l^{-1} KCl, 0.27 g l^{-1} KH$_2$PO$_4$, 0.19 g l^{-1} NH$_4$Cl, 0.11 g l^{-1} CaCl$_2$*2H$_2$O and 0.07 g l^{-1} KBr, all dissolved in demineralized water and amended with 1 ml l^{-1} trace solution, 1 ml l^{-1} vitamin solution, 0.5 mg l^{-1} resazurin, 3.92 g l^{-1} NaHCO$_3$ bicarbonate buffer and 1.5 mM Na$_2$S as reducing agent, with a final pH of 7. When sulfate was omitted, MgSO$_4$*7H$_2$O was replaced by 5.1 g l^{-1} MgCl$_2$*6H$_2$O. The vitamin solution and trace solution (adapted from the non-chelated trace solution) were both adapted from Widdel and Bak (1992).

For solid cultivation in serum bottles, 0.8% of BD Difco noble agar (Thermo Fisher Scientific, Waltham, MA) was added to 120 ml serum vials containing 50 ml of artificial sea water medium prior to autoclaving. For plating on media containing 0.8% noble agar, PIPES buffer (20 mM, pH 7) and cysteine as reducing agent (0.5 g l^{-1}) were used. Plates were poured in an anoxic chamber and were placed in anoxic jars after cooling and immediately the headspace gas was exchanged to N$_2$/CO$_2$ (80:20 v/v).

Experimental set-up

Enrichment cultures were done in duplicate in serum vials of 120 ml with 50 ml of anoxic carbonate-buffered artificial sea water medium and sealed with butyl-rubber stoppers and aluminium caps. Prior to autoclaving, bottles were gas exchanged with N$_2$/CO$_2$ for 8 cycles

with an end pressure of 1.5 bar N_2/CO_2 (80:20 v/v) or H_2/CO_2 (80:20 v/v) when hydrogen was used as electron donor. Canonical sulfate-reducing substrates were added after autoclaving from sterile stock solutions to a concentration of 20 mM for formate, acetate, butyrate, lactate, propionate, pyruvate and methanol. Methanethiol was added from a liquid stock in NaOH to an end concentration of 0.75 mM and the pH was adjusted to 7. Polysulfide was produced as described (Milucka et al 2012, Steudel et al 1988) and added to a concentration of 1 mM after pH correction to 7.7. Control cultures contained only methane (1.8 bar) and sulfate (20 mM). As inoculum, the biomass of the 10^{-5} dilution of reactor R4 (Fig 1, step 4) was added (10% v/v).

For solid cultivation in serum vials, serum vials were cooled down to 50°C after autoclaving before inoculation with liquid inoculum (10% v/v). For plating, 100 µl liquid inoculum was streaked on the plates and incubated in anoxic jars with either N_2/CO_2 (80:20 v/v) or H_2/CO_2 (80:20 v/v) when H_2 was used as electron donor. After growth, colonies were picked in the anoxic tent and were transferred to new anoxic artificial sea water medium with sulfate and the appropriate substrate and sealed with butyl-rubber stoppers and aluminium caps. Colonies were incubated with and without addition of yeast extract (0.2 g 1^{-1}). Bottles were gas exchanged immediately after removal from the anoxic chamber. All incubations were done in duplicate at 15°C in the dark.

Addition of SRB enrichments to AOM culture

After primary enrichment and subsequent serial dilutions, most enrichment cultures (except for acetate enrichments) were added to an active AOM culture to test if the cultures could stimulate AOM. Empty 10 ml-bottles were sealed with butyl-rubber stoppers and aluminium caps and were gas exchanged with N_2 for 8 cycles with an end pressure of 1.3 bar N_2. Afterwards, 100% $^{13}CH_4$ was added to an end pressure of 1.8 bar and 3 ml of the 10^{-1} dilution of the first dilution series from reactor R4 enrichment (Fig 1, step 1) was added to the bottles. For every substrate except acetate, 10 ml sample of grown enrichment cultures was filtered over a 0.2 µm filter to concentrate the cells on the filter. Then, 2 ml of fresh marine media containing 20 mM sulfate was drawn onto the filter to resuspend the cells. The resuspended cells with media were subsequently added to the aliquots of the AOM enrichment culture, resulting in a total volume of 5 ml. Control incubations contained only the AOM enrichment culture, with either $^{13}CH_4$ and sulfate or only sulfate addition.

Pyrosequencing analysis

DNA was extracted from the 10^{-1} dilution culture of the first dilution series made with R4 sediment as inoculum (Fig 1, step 1) and was subjected to community analysis by bacterial 16S rRNA pyrosequencing, as described in chapter 3.

Analytical methods

The pressure in anaerobic vials was checked using a Greisinger GMH3150 (GHM Messtechnik, Erolzheim, Germany) portable pressure meter. The pH was measured with a ProLine B210

pH meter from ProSense (Oosterhout, The Netherlands).

Sulfate and sulfide were analysed as described in chapter 3.

Acetate, pyruvate, propionate, butyrate, lactate, and formate were measured by HPLC equipped with a Varian Metacarb column operated at 30°C and a flow of 0.8 to 1.0 ml min^{-1} with an RI and UV detector.

Isotopic composition of CH_4 and CO_2 was measured using a gas chromatograph coupled to a mass spectrometer (GC-MS), as described in chapter 3.

Headspace H_2 quantification was done by comparing the peak areas to known standard peak areas recorded with a Compact GC gas chromatograph (Global Analyser Solutions, Breda, The Netherlands), containing a Carboxen 1010 pre-column, followed by two lines: a Molsieve 5A column (pressure: 200 kPa, split flow: 20 ml min^{-1}, oven temperature: 80°C, and a PDD detector at 110°C) and a RT-Q-bond column (pressure: 150 kPa, split flow: 10 ml min^{-1}, oven temperature: 80°C with a TCD detector at 110°C) with a carrier gas flow of 10 ml min^{-1}.

Microscopy

Phase-contrast microscopy was done with a Leica DM2000 (Leica Microsystems, Wetzlar, Germany) and an AX10 microscope (Carl Zeiss Microscopy GmbH, Jena, Germany).

Scanning electron microscopy (SEM) was done after samples were fixed on 0.2 μm filters (Millipore, Billerica, MA) with 2.5% (v/v) glutaraldehyde (Sigma Aldrich, St Louis, MO) for 2 hours at room temperature and rinsed 3 times with 1xPBS for 5 min. Dehydration was done with subsequently 30, 50, 70, 90 and 100% ethanol for 20 min each and 2 x 30 min at 100%. Samples were air dried for a maximum of 60 min at 40°C and were stored in a desiccator before microscopic examination. Samples were analysed using the JSM-6480LV scanning electron microscope (JEOL USA inc., Peabody, MA).

Clone library construction and analysis

DNA extraction and clone library construction for both bacterial and archaeal 16S rRNA gene sequences was done as described in chapter 2. The forward and reverse reads were trimmed for vector sequences and bad quality ends, and assembled into contiguous sequences with the DNAbaser software package version 4.12 (Heracle BioSoft SRL, Pitesti, Romania). Only sequences longer than 1000 bp were used for further analysis and were checked for artificial chimera products using the 'Find Chimeras' DECIPHER web tool (Wright et al 2012). A vector screening was done with the *blastn* tool from the BLAST+ 2.2.29 tools suite (Camacho et al 2009). Sequences were aligned with the SINA online alignment tool version 1.2.11 (Pruesse et al 2012) and merged with the SILVA SSU Ref NR99 database (version 115) and additional relevant sequences provided by SILVA (Quast et al 2013), using ARB version 5.5-org-9167 (Ludwig et al 2004). With the ARB FastAligner, vectors were removed and the alignment was manually optimized. Sequence similarities were calculated with the ARB distance matrix

methods, using similarity correction. Phylogenetic trees were calculated using the ARB neigbor joining algorithm.

Results

Community analysis of the R4 inoculum

Since the reactor dilutions contained very little biomass for DNA extraction, bacterial community analysis was only done on the first dilution (10^{-1}), obtained from the first dilution series of October 2008 (Fig 1, step 1). Archaeal 16S rRNA cloning showed that ANME-2a/b archaea were present (Fig 2B). Bacterial 16S rRNA pyrosequencing gave a total of 15112 sequences of which most belonged to *Chlorobiaceae* (>90% of all reads). Fig S1 shows the pyrosequencing results where GSB sequences and OTUs with less than 5 representing sequences were omitted. It shows a large bacterial diversity of which most belong to *Desulfobacter latus* (1.1% of reads), *Desulfuromusa succinoxidans* (0.7%), *Desulfuromusa bakii* (0.7%), *Desulfuromonadales* (0.7%), *Desulfocapsa sulfoexigens* (0.3%), SEEP-SRB1e (0.3%) and two OTUs related to *Desulfotignum* spp. (0.1% and 0.04%). The OTU with 0.1% of reads was most related to *D. toluenicum* (99%). The OTU with 0.04% of reads was highly related (99% similarity) to clone AOM-B-c9 (Jagersma et al 2009) from another AOM performing reactor enrichment (reactor R3) of the same Eckernförde bay inoculum (Meulepas et al 2009a).
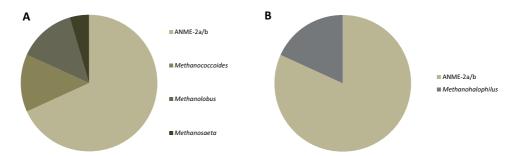
Figure 2 Archaeal 16S rRNA gene sequencing results of 22 clones of control culture A (A) and 11 clones of the first dilution (10^{-1}) from the first dilution series of October 2008 (B).

Canonical sulfate-reducing substrates

In most cultures, sulfide production activity commenced within 60 days. The pyruvate and lactate grown cultures showed the shortest lag phase, accompanying with fastest sulfide production rates. In contrast, propionate and acetate grown cultures showed the longest lag phase with slowest sulfide production rates (Fig 3). Cultures incubated with methanol and sulfate showed no sulfide production and only methane was produced (Fig 3). Cloning results showed presence of only *Methanolobus profundi* related sequences (2 OTUs; 97-99% similarity). Community analysis of all other cultures showed that with most canonical sulfate-reducing substrates, enrichments contained little diversity with mainly SRB belonging to the

Deltaproteobacteria and non-SRB (related to *Bacteroidetes* and *Synergistetes*) (Fig 4)*.* Many of the dominant sulfate-reducing bacterial sequences clustered within the *Desulfosarcina/ Desulfococcus* (DSS) clade, which included SRB that are thought to be involved in AOM. Many of the enriched SRB were related to sequences which were previously detected in AOM mediating enrichments (Fig 5, Table 1).
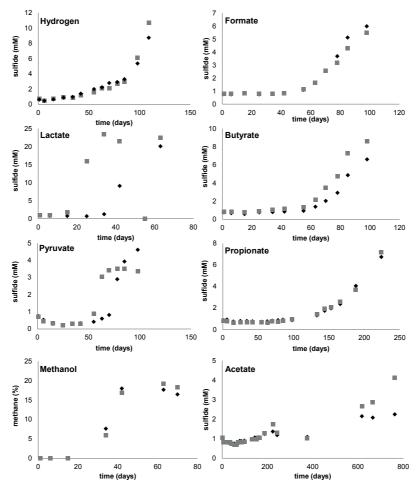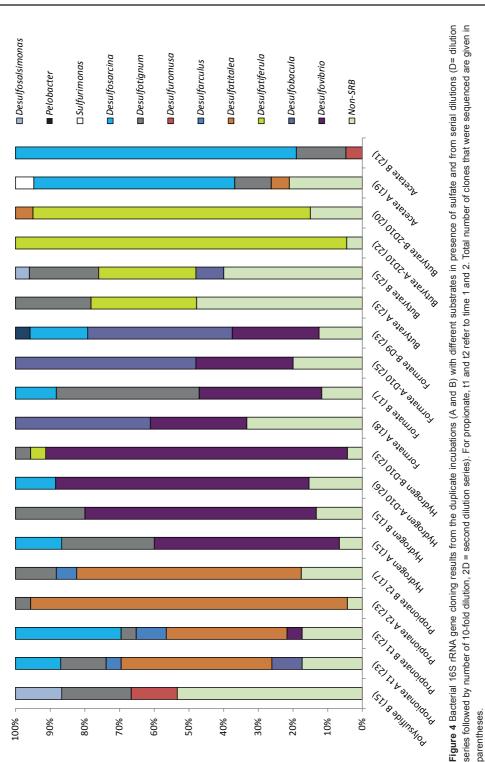
Figure 3 Sulfide (mM) and methane (%) accumulation with different SR substrates together with sulfate. Incubations with acetate also contained $^{13}CH_4$ after 160 days of incubation. Note that both the x- and y-axis are different for all incubations. All incubations were performed in duplicate (grey and black data points).

Table 1 Most abundant sulfate-reducing and non-sulfate-reducing bacterial taxa that were present in the enrichment cultures with different electron donors and with sulfate as electron acceptor.

Closest cultured representative (% similarity)	Substrate	Closest AOM enrichment representative (% similarity)	Stoichiometry
Desulfovibrio dechloracetivorans (96.6%)	Lactate, Pyruvate, H_2/CO_2, Formate	-	ND
Desulfovibrio sulfuricans (98%)	Pyruvate	-	ND
Desulfatitalea tepidiphila (98.4%)	Propionate	HP-Bac-G11 (92.5%)	$4\ CH_3CH_2COO^- + 3\ SO_4^{2-} \rightarrow 4\ CH_3COO^- + 4\ HCO_3^- + 3\ HS^- + H^+$ (1)
Desulfatiferula olefinivorans (97.1%)	Butyrate	HP-Bac-G11 (91.6%)	$2\ CH_3(CH_2)_2COO^- + SO_4^{2-} \rightarrow 4\ CH_3COO^- + HS^- + H^+$ (2)
Desulfosarcina sp. (97.4-97.8%)	H_2/CO_2, Formate, Acetate	HP-Bac-E11(98.3%), LARIS 32-01H04 (99%), LARHR 86-01F11 (99%)	ND
Desulfotignum balticum (98.4-99.2%)	H_2/CO_2	AOM-B-c9 (96.7-98%)	ND
Desulfotignum toluenicum (97%)	Formate	AOM-B-c9 (99.9%)	$4\ HCOO^- + SO_4^{2-} + H^+ \rightarrow 4\ HCO_3^- + HS^-$ (3)
Desulfobacula toluolica (95.8%)	Formate	AOM-SR-B24 (94.9%)	$4\ HCOO^- + SO_4^{2-} + H^+ \rightarrow 4\ HCO_3^- + HS^-$ (3)
Desulfotignum toluenicum (98.2%)	H_2/CO_2, Polysulfide	AOM-B-c9 (97.7%)	ND
Desulfuromusa bakii (99.7%)	Polysulfide	HP-Bac-B03 (92.1%)	ND
Desulfosalsimonas (91%)	Polysulfide	AOM-SR-B8 (96%)	ND
Aminobacterium colombiense (87.6%)	Formate/methanol +YE	-	ND
Sunxiuqinia elliptica (95.7%)	Methanol+YE	AOM-SR-B32 (98%)	ND

Similarity was determined using the ARB neighbour joining distance matrix method with similarity correction. ND: Not determined, YE: yeast extract (0.2 g l⁻¹).

The *Desulfotignum* related sequences found only in the formate culture B, were mostly related to *D. toluenicum* (Fig 5, Table 1). One of these sequences was highly similar to the uncultured clone AOM-B-c9 (99.9%), which was abundant in an AOM performing bioreactor (Jagersma et al 2009). The *Desulfotignum* related sequences in the H_2/CO_2 cultures were mostly related to *D. balticum* (2 OTUs), and were 97% to 98% identical to clone AOM-B-c9 (Fig 5, Table 1). Serial dilution of formate culture A shows the same distribution as from the original enrichment culture. Serial dilution of formate culture B (Formate-B-D9) resulted in a composition change to *Desulfobacula toluolica* (96%)*, Desulfosarcina* (97-98%) and *Desulfovibrio* related sequences as mostly abundant, making it similar to culture A (Fig 4, Table 1).

With propionate, clone libraries were constructed twice for the primary enrichments; firstly on day 195 during acetate production ("t1"), secondly on day 297 when all acetate was consumed ("t2"). In both samples *Desulfatitalea tepidiphila* related sequences (98%) were dominant (Fig 4 and Table 1) and were 92.5% similar to clone HP-Bac-G11 found in a high pressure AOM performing bioreactor inoculated with the same sediment as reactor R4 (Chapter 2). Cultures fed with butyrate showed SRB sequences mostly related to different *Desulfatiferula* spp. and a minor fraction to *Desulfotignum toluenicum* (98% similarity) (Fig 4). Serial dilutions showed aggregating microorganisms mainly related to *Desulfatiferula olefinovorans* (97%) (Table 1) and which were 91.6% similar to the same AOM performing bioreactor clone HP-Bac-G11 as mentioned for the propionate cultures. Both propionate and butyrate cultures showed incomplete oxidation; 1.93 moles of acetate were produced per mole butyrate consumed and 0.76 moles of sulfide were produced per mole of propionate consumed (Table 1, reaction 1 and 2). Both *D. olefinovorans* (Cravo-Laureau et al 2007) and *D. tepidiphila* (Higashioka et al 2013) are known to be incomplete oxidizers.

In the acetate fed incubations, sulfide production activity gradually increased and cultures produced about 2.3 to 4.1 mM of sulfide in 762 days (Fig 3). Trace amounts of methane derived from the inoculum (0.1-0.2% v/v) were present in the acetate cultures. After 160 days, labelled $^{13}CH_4$ was added to a pressure of around 2.4 bar and the sulfide production coincided with the addition of $^{13}CH_4$ to these cultures. However, no $^{13}CO_2$ production was observed in all cultures during incubation. DNA was extracted at 617 days of incubation and both acetate fed cultures showed dominance of *Desulfosarcina* spp. related sequences (97-98% similarity). These were also found in the initial H_2/CO_2, formate and propionate ("t1") fed cultures (Table 1, Fig 4). Most of these sequences were 98-99% similar to uncultured clones HP-Bac-G11 and HP-Bac-E11 found in a high pressure AOM performing bioreactor (Chapter 2), and to clones from Isis (LARIS 32-01H04), and Hydrate Ridge (LARHR 86-01F11) AOM enrichment cultures (Schreiber et al 2010) (Fig 5 and Table 1). Cells were small, oval rod shaped with size between 0.5 to 0.8 µm and were forming aggregates that contained iron sulfide minerals (Fig 6, Fig S2). No PCR product was obtained from the acetate-fed cultures using archaea specific primers.

Figure 4 Bacterial 16S rRNA gene cloning results from the duplicate incubations (A and B) with different substrates in presence of sulfate and from serial dilutions (D= dilution series followed by number of 10-fold dilution, 2D = second dilution series). For propionate, t1 and t2 refer to time 1 and 2. Total number of clones that were sequenced are given in parentheses.
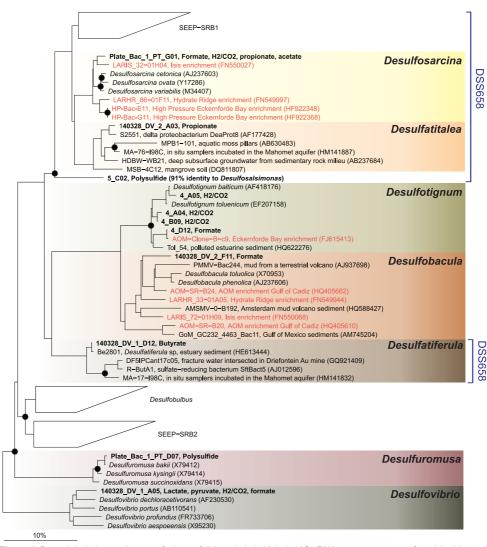
Figure 5 Bacterial phylogenetic tree of almost full-length (±1400 bp) 16S rRNA gene sequences found in this study belonging to the *Deltaproteobacteria*. The tree was constructed using the ARB neighbor-joining algorithm and jukes-cantor correction. Closed circles represent nodes with bootstrap values >70%. Taxonomic clusters were based on the SILVA taxonomy. The *Chloroflexi* functioned as outgroup and was removed from the tree after reconstruction. Sequences in bold are clones found in this study, sequences in red are clones found in sulfate-dependent AOM enrichment cultures. The targets for probe DSS658 are shown.
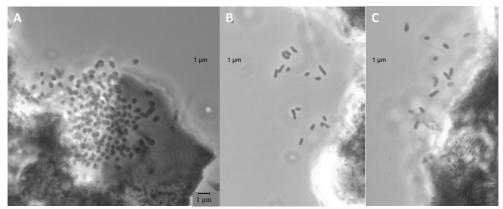
Figure 6 Phase-contrast microscopic image of acetate culture B showing aggregates of cells (A) and close association with iron sulfide minerals (B and C).

Possible intermediate electron carriers

Cultures incubated with methanethiol showed no increase in sulfide during 525 days of incubation. The control cultures with methane and sulfate produced 0.6 mM of sulfide during 670 days of incubation (Fig 7). After 525 days, archaeal community analysis was done on the control cultures and showed dominance of ANME-2a/b in control culture A (Fig 2A). No DNA could be extracted from control culture B. Bacterial 16S rRNA gene amplification was unsuccessful in both control cultures. These results show that the highly diluted, sediment-free reactor sample still performed AOM coupled to SR, mediated by ANME-2a/b archaea.

Cultures incubated with polysulfide were devoid of sulfate and the pH was corrected to 7.7 before inoculation to favour the chemical balance of both colloidal sulfur and sulfide to polysulfide. However, sulfate was present on day 0, which indicates that chemical disproportionation had already taken place. At day 63, 1 mM additional polysulfide was added, amounting to a total of 2 mM. A steep increase in sulfide concentration was immediately apparent (Fig 7) after which a decrease followed. Sulfate concentrations did however not increase, indicating that not polysulfide disproportionation but sulfur reduction and sulfide oxidation were the dominant processes. Dilution series and plating did not yield any growth. However, the original incubation showed microbes aggregating around sulfur particles in the media (Fig 8) and 16S rRNA cloning results after 200 days of incubation showed presence of *Desulfuromusa bakii* (99% identity), *Desulfotignum toluenicum* (98%), *Desulfosalsimonas* spp. (91%), and *Sulfurimonas denitrificans* (96%) related bacteria (Fig 4). *D. bakii* was described to mediate sulfur reduction while *Sulfurimonas* species are known to grow chemolithoautotrophically with sulfide, elemental sulfur, thiosulfate and hydrogen as electron donor and oxygen, nitrate or nitrite as electron acceptor (Labrenz et al 2013).
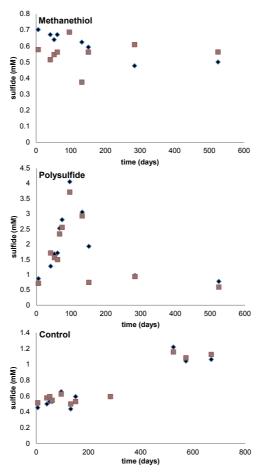
Figure 7 Sulfide (mM) accumulation in incubations with different SR substrates together with sulfate. The control incubation is fed with only methane and sulfate. Note that both the x- and y-axis are different for all incubations. All incubations were performed in duplicate (grey and black lines).

Heterotrophic growth

When formate-fed cultures were incubated in media with agar in serum vials, colonies developed. Colonies were picked and transferred to liquid media with yeast extract. Community analysis showed dominance of sequences with highest similarity (96.3%) to uncultured clone SBYC_5692 found in a hypersaline microbial mat (Harris et al 2013) and 87.6% similarity to *Aminobacterium colombiense*.

From the methanogenic cultures that were fed with methanol, a dilution series up to 10^{-10} was made with addition of BES and with and without sulfate addition. No growth was observed during 173 days of incubation in both cultures with and without sulfate addition. After that period, yeast extract (0.2 g l^{-1}) was added and growth was observed after 13 days of incubation. After 27 days, a clone library was constructed and revealed dominance of

sequences related to *Aminobacterium colombiense,* identical to the formate cultures, but also presence of *Bacteroidetes* related sequences. The *Bacteroidetes* were 98% similar to clone AOM-SR-B32 from an AOM-SR mediating enrichment (Zhang et al 2011) and 99.8% similar to the sequences found in a subseafloor organics- and methane-rich sediment (Kobayashi et al 2008). The closest cultivated bacterium was the aerobic bacterium *Sunxiuginia elliptica* strain DQHS4 with 95.7% similarity (Qu et al 2011).
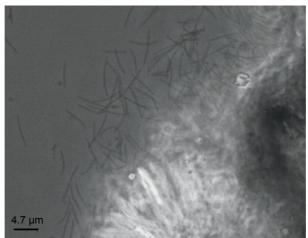
Figure 8 Phase-microscopic image of the polysulfide culture showing cells surrounding a sulfur crystal.

Discussion

Community analysis of R4 inoculum

The abundant *Chlorobiaceae* are phototrophic green sulfur bacteria (GSB) that fix CO_2 while oxidizing sulfide to sulfur and eventually sulfate, using light as energy source (Gorlenko 1970). The presence of these organisms was apparent by the green colour of the culture. No other dilutions showed this green coloration. GSB are known to be able to grow with minimum quantities of light (Beatty et al 2005, Manske et al 2005) which explains their growth in our incubations that were kept in dark conditions and were only exposed to light during sampling. *Desufocapsa* spp*., Desulfotignum* spp. and SEEP-SRB1 related sequences were also abundant in the AOM performing enrichment of reactor R3 (Jagersma et al 2009, Meulepas et al 2009a). The 0.3% of SEEP-SRB1 sequences were highly related (99% identity) to sequences found in another AOM mediating reactor enrichment with a different inoculum (Zhang et al 2011). SEEP-SRB1a were previously recognised as the dominant partner in seep-derived AOM enrichments (Schreiber et al 2010). *Desulfovibrio* species were highly present in most of the initial enrichment cultures (Fig 4), but no *Desulfovibrionales* related sequences were detected in the inoculum. This was also the case for the *Desulfarculus* related species that were enriched in propionate enrichment cultures and for the *Synergistetes* related species enriched on yeast extract. According to the pyrosequencing data, these must therefore have

formed very minor fractions of the population in the R4 reactor. This shows that even with high sequencing depth, the detection limit of 16S rRNA gene sequencing does not match cultivation efforts, which can be used to detect organisms in very low abundance (Lagier et al 2012). This proves that culturing methods thus provide a high resolution for qualitative community analysis but, dependent on the substrates used, do not always enrich for the most abundant organisms.

Possible interspecies electron carriers

Methanethiol

Sulfide levels in the methanethiol cultures suggest no SR activity (Fig 7). Since control incubations amended with methane and sulfate showed sulfide accumulation and presence of ANME-2a/b, methanethiol can therefore be most likely excluded as intermediate in AOM coupled to SR in these cultures. It was shown before with the same Eckernförde bay sediment inoculum and a higher methanethiol concentration (1 mM), that AOM coupled to SR was inhibited after methanethiol addition (Meulepas et al 2010b). Moran *et al* (2008) also showed inhibition of AOM by 1 mM methanethiol addition and postulated that it could function as IEC. Toxicity effects could not be excluded in all previous studies, as well as in this study, although the used concentration was low (0.75 mM). It was shown before that *Desulfosarcina variablis* (97%) related bacteria could oxidize methanethiol up to concentrations of 5 mM (Lyimo et al 2009).

Polysulfide

The initial sulfide increase in the polysulfide cultures (Fig 7) was probably attributed to the reduction of sulfur coupled to oxidation of endogenous organic compounds by *D. bakii*, and not to sulfide disproportion. Even if sulfate was produced, it could have been reduced by other SRB such as *Desulfotignum* and *Desulfosarcina* related species, coupling it to oxidation of organic compounds. The following decrease in sulfide concentration could be attributed to *Sulfurimonas* related species that use sulfide as electron donor (Labrenz et al 2013). However, no oxygen, nitrate or nitrite was present in the medium, nor was any electron acceptor for ammonium oxidation. The detected sequences were only 96% related to *S. denitrificans.* Therefore, the metabolism can be different. Moreover, aerobic microorganisms have been detected in subsurface sediments as well, which suggests that even well-studied microorganisms can express unknown metabolic pathways when exposed to energy-limiting anoxic conditions (Lever et al 2015). Since we could not detect any sulfate production, it remains unclear whether microbial polysulfide disproportion is an important process in AOM coupled to SR, as stated in a previous study on an AOM mediating enrichment (Milucka et al 2012). In their study, the measured sulfide and sulfate production ratio was 7:1. The authors used a highly enriched and highly active, almost axenic culture (95% ANME-SRB consortia) originating from a seep-sediment (Schreiber et al 2010). We used an AOM

performing enrichment originating from a shallow gassy diffusion-based marine sediment from Eckernförde bay (Treude et al 2005b). This different environment with a diverse bacterial community (Fig S1) can harbour methanotrophic communities that exhibit diverse metabolic pathways and thus yield different IECs (Alperin and Hoehler 2010). Also, after this strong dilution it showed very low AOM activity as deduced from the control culture fed with methane and sulfate (Fig 7). Therefore, activity of the SRB possibly involved in polysulfide disproportionation was probably not detectable from sulfate production alone.

Acetate, H_2/CO_2 and formate

The increase in sulfide production in both acetate cultures was slow and relatively small, with sulfide production rates of 0.002 and 0.013 mmol l^{-1} day^{-1} within the last 97 days of incubation (Fig 3). The control cultures fed with methane and sulfate showed a similar trend, but produced less sulfide (Fig 7). No methane oxidation activity was detected upon $^{13}CH_4$ addition, leaving acetate as only possible donor for sulfate reduction. *Desulfosarcina* spp. related sequences dominated in both cultures which indicates that no other SRB competed with *Desulfosarcina* for this substrate, despite this very slow growth (Fig 4). No archaea were detected in these incubations since no amplification of the 16S rRNA gene could be achieved. For H_2/CO_2 and formate, the *Desulfosarcina* spp. related sequences were present in lower numbers and the SRB probably competed with the other SRB that were present. Only *Desulfosarcina* was adapted to use acetate, which would explain the production and consumption of acetate in the propionate enrichments at "t1" (Fig 4). The *Desulfotignum* sequences found in the formate and H_2/CO_2 cultures (Table 1) were abundant in the inoculum sample, of which the OTU with 0.04% of reads (Fig S1) was highly related to sequences found in the AOM performing reactor R3 (Jagersma et al 2009). Hydrogen or acetate, or a combination of both were proposed as IEC in AOM coupled to SR (DeLong 2000). Valentine and Reeburgh (2000) speculated that the ANME archaea produce acetate and hydrogen from two molecules of methane. *Desulfosarcinales* related species were shown to be able to consume acetate and hydrogen, which would explain the isotopically depleted carbon in lipids of associated SRB (Orphan et al 2001b). Model predictions showed that acetate as IEC would give highest bulk AOM rates (Orcutt and Meile 2008). Stams and Plugge (2009) also speculated on multiple intermediates such as hydrogen and acetate. Here, methane will be converted to methyl coenzyme M, but the subsequent steps to form acetate and CO_2 will go through the acetate pathway (CO_2 reduction) and hydrogen pathway (CO_2 formation), respectively. Genome and transcriptome studies on ANME-1 (Meyerdierks et al 2010, Hallam et al 2004) and genome studies on ANME-2a/b (Wang et al 2014), as well as *in situ* carbon isotopic data from acetate (Heuer et al 2006) confirmed that acetate could function as IEC. The multiple intermediate theory might explain why *in vitro* experiments with AOM performing sediments with solely acetate or hydrogen excluded these as sole IEC for at least ANME-2a/b archaea (Nauhaus et al 2005, Orcutt and Meile 2008, Meulepas et al 2010b). In our AOM enrichments, acetate was apparently not a competitive substrate since growth of *Desulfosarcina* was extremely slow. This was an

unexpected result since in marine sediments, acetate is a main substrate for SRB since it is a major end-product of fermentation, with porewater acetate concentrations above 10 µM (Ozuolmez et al 2015). The slow growth of *Desulfosarcina* on acetate could indicate that they share a similar metabolism with the related AOM partner. If acetate is used as IEC, growth of ANME-associated SRB is likely to be slow as in situ concentrations would be very low to make AOM thermodynamically feasible. It could therefore be that *in situ* acetate concentrations at AOM 'hot spots' are locally low enough to act as IEC in AOM. Since the enrichments on acetate were not fully grown, addition of these SRB to AOM performing enrichments was not possible to assess their effect on AOM.
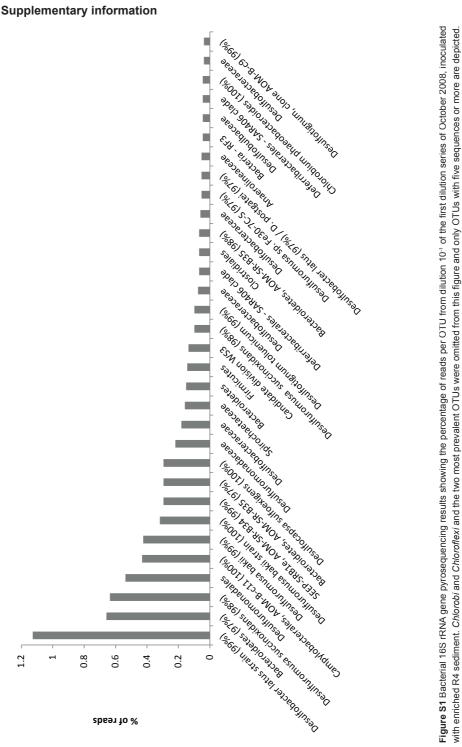
Non-sulfate reducers

Different AOM enrichments from different marine sediments show presence of similar *Bacteroidetes* spp. Moreover, in the R4 inoculum, other *Bacteroidetes* were identical to clone AOM-SRB-B35 from an AOM-SR mediating enrichment derived from the Gulf of Cádiz (Zhang et al 2011) (Fig S1). It can therefore not be excluded that these microorganisms are indirectly involved in AOM. In this study, these grew on yeast extract, but not on any other substrate added to the incubations. This indicated that the *Bacteroidetes* degraded amino-acids and/or dead cell material. Very little is known about the diversity and role of other prokaryotes in AOM mediating environments and reactors. At the sulfate-methane transition zone of marine sediments, prokaryotes apart from ANME and DSS form the majority and populations of ANME and SRB are quite low (Webster et al 2011). Understanding the role of these organisms through isolation and characterization could therefore be helpful.

Conclusion

All reported attempts to grow the ANME associated SRB in the absence of the methanotrophic archeon failed so far. However, many studies on AOM coupled to SR have been done with probes and primers targeting the DSS group (such as DSS658, Fig 5) and thus differentiation between the recently described SEEP-SRB and other SRB possibly involved in AOM could not be done. Moreover, it seems that the bacterial partners of ANME are not the same in different environments. In our study, several SRB were enriched using canonical SR substrates. Most enrichments belonged to the DSS clade and were related to SRB previously found in AOM performing enrichments. Methane oxidation of the first R4 dilution (Oct 2008, Fig 1) was not stimulated by addition of any of the enriched SRB. Still, as many yet unknown factors may effect AOM coupled to sulfate reduction, it is not possible to exclude the enriched SRB as involved in AOM. Methanethiol and polysulfide could not be confirmed as IEC for AOM, whereas acetate and/or hydrogen could be important in AOM environments.

Acknowledgements

Supplementary information

Figure S1 Bacterial 16S rRNA gene pyrosequencing results showing the percentage of reads per OTU from dilution 10^{-1} of the first dilution series of October 2008, inoculated with enriched R4 sediment. *Chlorobi* and *Chloroflexi* and the two most prevalent OTUs were omitted from this figure and only OTUs with five sequences or more are depicted. The total number of sequences was 15112. The percentage of identity with given species or environmental sequences are indicates between brackets.

4

Figure S2 Phase-contrast microscopy image of rod- and oval-shaped microbes from formate culture A-D10 (A) and SEM imaging of rods and cocci-shaped microorganisms in a sample from formate culture B-D9 (B).

CHAPTER 5

EVALUATION AND OPTIMIZATION OF PCR PRIMERS FOR SELECTIVE AND QUANTITATIVE DETECTION OF ANME ARCHAEA IN GASEOUS AND DIFFUSIVE MARINE SEDIMENTS

Peer H. A. Timmers, H. C. Aura Widjaja-Greefkes, Caroline M. Plugge and Alfons J. M. Stams

Abstract

Since the discovery that anaerobic methanotrophic archaea (ANME) were responsible for anaerobic methane oxidation coupled to sulfate reduction in marine sediments, different primers and probes specifically targeting these archaea have been developed. Microbial investigation of the ANME clades and subclusters (ANME-1, ANME-2a/b, ANME-2c and ANME-3) was mainly done in sediments where the amount of methanotrophic archaea is high and methanogenic cell numbers are low. In different sediments with higher archaeal diversity including methanogens, it is important that primers and probes targeting ANME are very specific and do not detect closely related methanogens that could be present. In this study, developed primers and probes that were regularly used in AOM studies were tested *in silico* on coverage and specificity. Most of the previously developed primers and probes were not specific for the ANME subclusters, thereby not reflecting the actual ANME population. Selected primers for the clades and subclusters ANME-1, ANME-2a/b and ANME-2c with good coverage and high specificity were thoroughly validated using quantitative PCR (qPCR). From these qPCR tests, only some combinations seemed suitable for selective amplification. After optimization of these primer sets, we obtained valid primer combinations for the selective detection and quantification of ANME-1, ANME-2a/b and ANME-2c in samples where both methanogens and ANME archaea could be present. We propose a standard workflow to facilitate selection of suitable primers for qPCR experiments on novel environmental samples.

Introduction

Anaerobic Oxidation of Methane (AOM) was first discovered in marine sediments at the zone where methane and sulfate come in contact, the sulfate-methane transition zone (SMTZ) (Martens and Berner 1974, Reeburgh 1976). Previous molecular studies showed that most archaeal 16S rRNA sequences that were retrieved from methane-oxidizing environments belonged to new clades in the *Euryarchaeota* and were named ANaerobic MEthanotrophic archaea (ANME) (Boetius et al 2000, Hinrichs et al 1999, Orphan et al 2001a). The sequences derived from clone libraries in these studies were used to develop probes for FISH and primers for PCR analysis. These probes and primers were mainly used in studies of samples directly derived from seep systems and/or from microbial mats where methanogens are low in abundance and the archaeal community *in situ* was known. Therefore, the majority of the previously developed and widely used probes such as EelMS932 (Boetius et al 2000), ANME-1-350 (Boetius et al 2000), ANME2a-647, ANME-2c-622 and ANME-2c-760 (Knittel et al 2005) were indeed suitable for these environments. In different sediments and enrichment studies that have a more diverse community and contain methanogens, it is important that primers and probes targeting ANME are very specific and do not detect closely related methanogens that could be present. In these environments, published primer pairs and probes were less suited, especially for quantitative PCR (qPCR). Therefore, new primers specific for the different methanotrophic communities emerged, but the design, validation and optimization of primers is difficult for the ANME clades. This is mainly because phylogenetically the distance between ANME clades is large (rRNA gene sequence similarity of 75-92%), as well as within the subclusters (Knittel and Boetius 2009). With more 16S rRNA sequences emerging in the database, primers and probes are continuously developed when published ones were deemed not specific or not covering novel ANME sequences.

In this study, we performed *in silico* validation of published primers and probes, focussing on the coverage and the specificity of the target ANME clades and subclusters. When primers and probes seemed suitable, validation and optimization was done for specific amplification of ANME-1, ANME-2a/b and ANME-2c, using quantitative PCR. Validation of primers was done using cloned full length 16S rRNA archaeal gene inserts of ANME-1, ANME-2a/b and ANME-2c archaea, as well as with genomic DNA from the highly related *Methanosarcina mazei* strain MC3 and *Desulfovibrio* G11. We also included environmental samples from Eckernförde bay (Baltic Sea, Denmark) which is a gassy diffusive sediment containing ANME-1, ANME-2a/b and ANME-2c. These sediments are very different from seeps and hydrothermal vents since methane is produced from *in situ* organic matter degradation (Treude et al 2005b), and therefore harbour both methanotrophic archaea and methanogens of which the latter are most abundant. For these types of environments, it is important that primers and probes are highly specific for the different ANME subclusters, to enable studies on biodiversity and activity.

Materials and Methods

In silico testing of probes and primers

Reported probes and primers used in AOM studies were tested for coverage and specificity, using the SILVA Probe Match and Evaluation Tool - TestProbe 3.0 and Testprime 1.0 services (Klindworth et al 2013) from the SILVA SSU 16S rRNA database version r122 Ref NR (Quast et al 2013). Only results with 100% specificity (0 mismatches) were used for both probes and primers. Primer pairs from the literature that were a mixture of multiple forward or reverse primers were made degenerate prior to submitting these to Testprime 1.0. For instance, primer ANME1-395F consists of a mixture of three different primers and ANME1-1417R consisted of a mixture of two different primers for increasing coverage of the target ANME-1 group (Miyashita et al 2009). We therefore combined two primers in each Testprime submission by producing one degeneracy; in this case we submitted ANME1-395F (1+2) / ANME1-1417R (1+2) and ANME1-395F (3) / ANME1-1417R (1+2) to Testprime, which thus gives a different coverage than when combining all three with *in vitro* PCR (Table 1). Probe coverage of target and non-target groups is given in Table 2.

Environmental samples and pure cultures

Samples were taken at Eckernförde Bay (Baltic Sea) at station B (water depth 28 m; position 54°31'15N, 10°01'28E) during a cruise of the German research vessel *Littorina* in June 2005. This sampling site has been described by Treude *et al* (2005b). Sediment samples were taken as described in chapter 2. *Methanosarcina mazei* strain MC3 (DSM-2907) and *Desulfovibrio* G11 (DSM-7057) were obtained from the culture collection (DSMZ, Braunschweig, Germany).

DNA isolation

Genomic DNA was extracted using the Fast DNA Kit for Soil (MP Biomedicals, Santa Ana, CA) according to the manufacturer's protocol with two 45-second beat beating steps using a Fastprep Instrument (MP Biomedicals). Afterwards, DNA was purified and concentrated using the DNA Clean & Concentrator kit (Zymo Research Corporation, Irvine, CA). The DNA concentrations were either determined with the NanoDrop® ND-2000 (Thermo Sientific, Wilmington, DE) or the Qubit 2.0 fluorometer (Thermo Fisher Scientific, Waltham, MA).

Quantitative real-time PCR

PCR amplifications were done in triplicate in a BioRad CFX96 system (Bio-Rad Laboratories, Hercules, CA) in a final volume of 25 µl using iTaq Universal SYBR Green Supermix (Bio-Rad Laboratories), 5 µl of template DNA and 1 µl of forward and reverse primer (concentration of 10 µM), all according to the manufacturer's recommendations. Triplicate standard curves were obtained with 10-fold serial dilutions ranged from $2x10^5$ (corresponding to 1 ng µl^{-1} DNA) to $2x10^{-2}$ copies per µl of plasmids containing 16S rRNA archaeal inserts of ANME-1 (HP-Arch-D10, Genbank ID: HF922261.1), ANME-2a/b (HP-Arch-B12, Genbank ID: HF922244.1)

and ANME-2c (HP-Arch-F07, Genbank ID: HF922279.1). All used primers were extensively tested for specificity with the same cloned archaeal inserts of ANME-1, ANME-2a/b, ANME-2c, and genomic DNA of *Methanosarcina mazei* strain MC3 (DSM-2907) and *Desulfovibrio* G11 (DSM-7057), as well as with a complex environmental sample from Eckernförde bay (EB0). For most primer sets, the first strategy was to reproduce PCR conditions as described in the original literature. When not satisfactory, annealing temperatures were optimized by performing a gradient PCR using all the above listed test samples. Primers specific for amplification of ANME-1, ANME-2a/b and ANME-2c archaea were validated. After amplification, specificity was checked by a melting curve analysis (72-95°C) and loading of 3 µl PCR products on a 1.5% agarose gel stained with SYBR Safe DNA Gel Stain (Life Technologies Ltd, Paisley, UK) and illuminated with UV light.

Results

In silico testing of primers

In silico PCR with described primers was done to obtain coverage and specificity of target groups (ANME clades) and non-target groups, allowing 0 mismatches (100% specificity). In Table 1, results are shown for all primer pairs used in previous studies. Most primer pairs showed a good coverage of the target group with little amplification of non-target groups. Only primer pair ANME-2aF/ANME-2aR gave no specific target product and primer pair ANMEF/907R amplified only a small fraction of ANME-3. Primer pairs with highest target group coverage and least non-target group coverage were tested *in vitro* using quantitative PCR (qPCR) and are given in bold in Table 1.

5

Table 1 Primers described in the literature that were used for ANME detection.

Primer combination	Target	Coverage (%)	Non-target	Coverage (%)	Product size (bp)	Reference
*ANME1-395F (1+2) / ANME1-1417R (1+2)	ANME-1	53	Methanomicrobia	3	1039	Miyashita et al 2009
			Archaea	≤0.8		
*ANME1-395F (3) / ANME1-1417R (1+2)	ANME-1	1.5	Methanomicrobia	0.1	1039	Miyashita et al 2009
ANME-1-337F / ANME-1-724R	ANME-1	56.6	Methanomicrobia	2.6	358	Girguis et al 2005
			Archaea	≤0.6		
ANME1-628f / ANME1-830r	ANME-1	31.3	Methanomicrobia	1.4	219	Lloyd et al 2011
			Archaea	≤0.3		
*ANME2a -426F (1+2) /ANME2a-1242R	ANME-2a/b	30.9	Methanosarcinales	2.7	833	Miyashita et al 2009
			Methanomicrobia	1.5		
			Archaea	≤0.3		
*ANME-2a-426F (3) / ANME2a-1242R	ANME-2a/b	7.4	Methanosarcinales	0.6	833	Miyashita et al 2009
			Methanomicrobia	0.4		
			Archaea	≤0.1		
ANME-2aF / ANME-2aR	-		Archaea	0	-	Vigneron et al 2013a
			Ancient Archaeal Group(AAG)	0		
ANME2b-402F / ANME2b-1251R	ANME-2b	12.5	Methanomicrobia	0.1	866	Miyashita et al 2009
			Methanosarcinales	0.1		

All primer combinations were tested using the online Testprime database of SILVA, using 100% specificity (0 mismatches). Non-targets that are highly unwanted are given in red. Primers tested *in vitro* in this study are displayed in bold. *: These primers are a mixture of separately designed primers (indicated by number in brackets) as described by Miyashita et al (2009), see materials and methods for explanation.

Table 1 continued

Primer combination	Target	Coverage (%)	Non-target	Coverage (%)	Product size (bp)	Reference
*ANME2c-AR468F (1+2) / ANME2c-AR-1411R	ANME-2c	30.8	Methanosarcinales	1.3	960	Miyashita et al 2009
			Methanomicrobia	0.7		
			Archaea	≤0.2		
*ANME2c-AR468F (3) / ANME2c-AR-1411R	ANME-2c	19.2	Methanosarcinales	0.8	960	Miyashita et al 2009
			Methanomicrobia	0.4		
			Archaea	≤0.1		
ANME2c-F / ANME-2c-R	ANME-2c	51.7	Methanosarcinales	2.1	221	Vigneron et al 2013a
			Methanomicrobia	1.2		
			ANME-2a/b	1		
			Archaea	≤0.3		
Ar-468F / AR736R	ANME-2c	46.7	Methanosarcinales	1.9	268	Girguis et al 2003
			Methanomicrobia	1.1		
			Archaea	≤0.3		
ANMEF / 907R	ANME-3	2.1	Thaumarchaeota	0.2-25	816	Thomsen et al 2001
			Methanobacteriales	0.1-1.1		
			Desulfuromonadaleas	0.1-0.3		
			Methanosarcinales	0.1-0.2		
			Thermoplasmatales	0.1-0.2		

All primer combinations were tested using the online Testprime database of SILVA, using 100% specificity (0 mismatches). Non-targets that are highly unwanted are given in red. Primers tested *in vitro* in this study are displayed in bold. *: These primers are a mixture of separately designed primers (indicated by number in brackets) as described by Miyashita *et al* (2009), see materials and methods for explanation.

5

In vitro testing of primers

ANME-1

ANME-1-337F and ANME-1-724R (Girguis et al 2005) showed highest coverage of the target group, with lowest coverage of non-target groups. This primer pair was described to be specific for ANME-1, had strong 3'-mismatches to closely related out-groups, and was tested for amplification with *Desulfobulbus* spp., *Beggiatoa* spp, and 28 archaeal and bacterial phylotypes commonly found in seep sediments (Girguis et al 2005). Here, specificity was tested using qPCR with genomic DNA of *Methanosarcina mazei* and cloned full length 16S rRNA inserts of ANME-1 and ANME-2c sequences. This revealed that the ANME-1 primer pairs were not specific under described reaction conditions. The ANME-1 primer pair amplified genomic DNA of *Methanosarcina mazei,* which resulted in the same melting curve as the positive control (cloned ANME-1 insert), as well as two bands with one having the correct fragment size of 358 bp. The primer pair also amplified cloned ANME-2c inserts but did not give the correct amplicon size and resulted in multiple bands (Fig S1).

Another primer pair was described to be specific for ANME-1 (ANME1-395F and ANME1-1417R) (Miyashita et al 2009). With the newly designed primers for ANME-1, Miyashita *et al* (2009) tested the specificity using genomic DNA from *Methanogenium organophilum* and *Methanomicrobium mobile*. Detection of ANME in methanogenic environments such as methanogenic sludge, rice field soils, lotus field sediment and natural gas fields has also been performed (Miyashita et al 2009). However, under the reported conditions that were applied to our Eckernförde bay samples, the PCR efficiency with the ANME-1 primers was only 61.8% with an R^2 of 0.973 and melting curves for ANME-1 clones inserts gave small peaks (Fig S2A). After optimization, mainly changing annealing temperatures, a higher efficiency (87%, R^2 =0.998) was obtained and melting curves gave larger peaks for both ANME-1 cloned inserts and Eckernförde bay environmental sample EB0 (Fig S2B). For the ANME-1 primer set, genomic DNA from *M. mazei* strain MC3 and *Desulfovibrio* G11 was not amplified after optimization. Only when using high copy concentrations of >2×10^2 copies μl^{-1}, cloned ANME-2a/b and ANME-2c inserts were amplified. Amplification of ANME-2a/b cloned inserts only occurred at concentrations of >2×10^2 copies μl^{-1} and showed a PCR product on agarose gel only from 2×10^4 copies μl^{-1} (Fig S3). Amplification of ANME-2c cloned inserts only occurred at concentrations of >2×10^2 copies μl^{-1} and melting curves were not the same as for the cloned ANME-1 insert and sample EB0 and did not show a visible PCR product on an agarose gel (Fig S4). Although the efficiency of the primer set is not high, probably due to the length of the PCR product (efficiency should be between 90-100% and product length is optimal between 150-250 bp), these primers seem to be specific and appropriate for quantification, but the low efficiency could result in low sensitivity when target concentrations are low. Moreover, these primers can only be used when the environmental samples contain less amount of copies of non-target groups than where amplification starts to occur.

ANME-2a/b

The subclusters ANME-2a and ANME-2b were firstly subdivided, but when more 16S rRNA gene sequences were recovered from the environment, this group appeared monophyletic and was therefore considered as one group under the name ANME-2a/b. Therefore, previous primer sets covering only ANME-2a or only ANME-2b were not tested in this work. For the ANME-2a/b primer set ANME-2a-426-F and ANME-2a-1242-R, amplification of cloned ANME-1 inserts only occurred at concentrations of >$2x10^1$ copies µl^{-1}, with different melting curves at lower concentrations and only products on an agarose gel at concentrations of >$2x10^2$ copies µl^{-1} (Fig S5). Cloned ANME-2c inserts with this ANME-2a/b primer pair were also only amplified at concentrations of >$2x10^2$ copies µl^{-1} as seen from melting curve analysis, but showed no visible product on an agarose gel (Fig S6). The Eckernförde bay sample showed a melting curve corresponding to the cloned ANME-2a/b insert. Since the environmental sample EB0 used in this study has low copy numbers of ANME-2c, this protocol can be applied for this specific sample (Fig 1). Although the coverage of this primer set is not optimal (±38%), other published ANME-2a/b primer sets were not sufficiently covering the target groups (Table 1).

ANME-2c

Primer pair AR468f and AR736r was described to be specific for ANME-2c and has been tested for specificity with *Methanosarcina acetivorans* and other representative archaeal groups commonly found in seep sediments (Girguis et al 2003). The primers showed a high coverage of target groups with low coverage of non-target groups (Table 1). However, when we performed qPCR, the primer pair was not specific under described reaction conditions. It showed amplification with *M. mazei* strain MC3*,* with a similar melting curve as the positive control, as well as a fragment of the correct size of 268 bp (Fig S7).

The forward primer AR468f was also used in a mixture of three separate forward primers to increase coverage, together with a new reverse primer ANME-2c-AR-1411R (Miyashita et al 2009). This primer pair indeed showed higher coverage of the target group with low coverage of non-target groups (Table 1). This primer pair has been tested for specificity using genomic DNA from *Methanogenium organophilum* and *Methanomicrobium mobile* (Miyashita et al 2009). Detection of ANME in methanogenic environments such as methanogenic sludge, rice field soils, lotus field sediment and natural gas fields has also been performed, as was done for the ANME-1 primers (Miyashita et al 2009). In our study, the primer set showed amplification of genomic DNA from *M. mazei* strain MC3 and *Desulfovibrio* G11 and with all cloned ANME-1 and ANME-2a/b inserts. The melting curves did not correspond to cloned inserts from ANME-2c and multiple products emerged on an agarose gel, with none having the expected product size (Fig S8). The authors claimed that it was indeed difficult to design primers perfectly specific for ANME-2c sequences (Miyashita et al 2009).

Primers for ANME-2c were designed by others as well, such as ANME-2c-F and ANME-2c-R

5

that showed highest coverage of the target group (Table 1) (Vigneron et al 2013a). Under described PCR conditions, ANME-1, ANME-2a/b and all negative controls were amplified, with melting curves corresponding to the positive control (Fig S9). However, after optimization, no amplification of ANME-2a/b was observed, although ANME-2a/b were targeted with 0 mismatches (Table 1). Amplification of cloned ANME-1 inserts only occurred with inserts at concentrations >2x10^2 copies µl^{-1} (Fig S10). The Eckernförde bay sample showed a good melting curve corresponding to the cloned ANME-2c insert. Eckernförde bay samples have low copy numbers of the ANME-1 clade, and therefore this protocol can be used in these types of sediments. However, *M. mazei* strain MC3 and *Desulfovibrio* G11 did show a melting curve not corresponding to the melting curve of the cloned ANME-2c insert, which is reflected in the different product size shown on the agarose gel. Therefore, when using these primers for environmental samples, quantification of ANME-2c cannot be done when melting temperatures are identical to those of *M mazei* strain MC3. The optimized protocol for the ANME-2c specific primers is given in Figure 1.
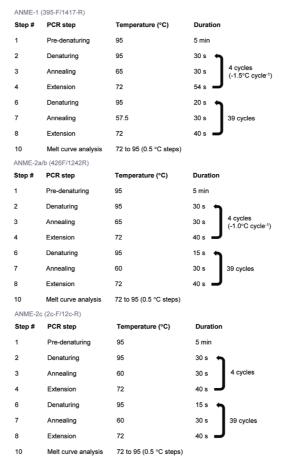
ANME-1 (395-F/1417-R)

Step #	PCR step	Temperature (°C)	Duration	
1	Pre-denaturing	95	5 min	
2	Denaturing	95	30 s	
3	Annealing	65	30 s	4 cycles (-1.5°C cycle^{-1})
4	Extension	72	54 s	
6	Denaturing	95	20 s	
7	Annealing	57.5	30 s	39 cycles
8	Extension	72	40 s	
10	Melt curve analysis	72 to 95 (0.5 °C steps)		

ANME-2a/b (426F/1242R)

Step #	PCR step	Temperature (°C)	Duration	
1	Pre-denaturing	95	5 min	
2	Denaturing	95	30 s	
3	Annealing	65	30 s	4 cycles (-1.0°C cycle^{-1})
4	Extension	72	40 s	
6	Denaturing	95	15 s	
7	Annealing	60	30 s	39 cycles
8	Extension	72	40 s	
10	Melt curve analysis	72 to 95 (0.5 °C steps)		

ANME-2c (2c-F/12c-R)

Step #	PCR step	Temperature (°C)	Duration	
1	Pre-denaturing	95	5 min	
2	Denaturing	95	30 s	
3	Annealing	60	30 s	4 cycles
4	Extension	72	40 s	
6	Denaturing	95	15 s	
7	Annealing	60	30 s	39 cycles
8	Extension	72	40 s	
10	Melt curve analysis	72 to 95 (0.5 °C steps)		

Figure 1 Optimized qPCR programs for all archaeal primer sets used in this study.

Probes

Probe coverage testing was done for all published probes and results are given in Table 2. Probe EelMS932 is widely used in AOM studies and together with a competitor probe, it is specific for ANME archaea (Boetius et al 2000). However, since this probe targets most ANME subclusters and other methanogenic clusters (Table 1), it is recommended to use more specific probes for ANME-2 such as ANME-2-538 (Treude et al 2005c). This probe shows good coverage for all ANME-2 but also for the GoM-Arc I cluster, for which growing evidence indicates that these also can oxidize methane (Flynn et al 2013, Raghoebarsing et al 2006, Schubert et al 2011, chapter 3), and form a separate ANME-2 subcluster (Haroon et al 2013). Therefore, this new subcluster should be considered in probe and primer design. The specific probes for ANME-2a/b and ANME-2c, ANME2a-647 and ANME-2c-622, respectively, target only few other ANME subclusters and have good coverage for the specific targets whereas ANME-2c-760 (Knittel et al 2005) is less specific (Table 2). For ANME-1, more specific probes have been designed and these target mostly ANME-1. The probe with highest coverage, ANME-1-350 (Boetius et al 2000), is widely used in AOM studies. However, when testing probe EelMS932 and ANME-1-350 in FISH experiments using *Methanosarcina mazei* strain MC3, we found hybridization of both probes with 40% formamide (Fig 2), and even up to 60% formamide. Probe ANME2a-647 (Knittel et al 2005) did not show any hybridization with *M. mazei* strain MC3 at 40% formamide (data not shown).
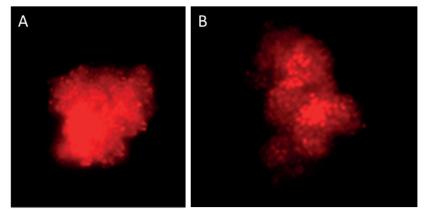
5

Figure 2 FISH hybridization of *Methanosarcina mazei* strain MC3 with probe ANME-1-350 (A) and probe EelMS932 (B) with 40% formamide in the hybridisation buffer.

Table 2 Probes described in the literature that were used for ANME detection.

Probe name	Sequence (5'-3')	Target site	Target	Coverage (%)	Non-target	Coverage (%)	Reference
ANME-1-305	AGT CCG GAG ATG GGT TCT	305-322	ANME-1	54.9	*Methanomicrobia*	1.4-100	Boetius et al 2000
					Thermoplasmatales	0.8-80	
					Thermoprotei	20	
					Methanosarcinales	≤0.2	
					Crenarchaeota	1.7	
					GOM Arc I	1	
					Euryarchaeota	0.1-0.9	
ANME-1-350	AGT TTT CGC GCC TGA TGC	350-367	ANME-1	78.8	*Thaumarchaeota*	29	Boetius et al 2000
					Methanomicrobia	3.6	
ANME1-632	TCA GGG AAT ACT GCT TGG	632-649	ANME-1	39.1	*Methanomicrobia*	1.7	Boetius et al 2000
					Archaea	0.2-0.4	
ANME-1-862	GGC GGG CTT AAC GGG CTT C	86-880	-		*Sulfolobales*	0.6-5.6	Orphan et al 2002
ANME1-830	TCG CAG TAA TGC CAA CAC	830-847	ANME-1	62.6	*Methanomicrobia*	2.7	Boetius et al 2000
					Archaea	0.4-0.6	
EelMS240	CCC ACT ACA ACC TGA TAG	240-257	ANME-2a/b	64.2	*Methanosarcinales*	0.4-85.7	Boetius et al 2000
			ANME-2c	38.5	*Thermoplasmatales*	0.2-55.6	
			ANME-3	22.4	*Methanomicrobiales*	0.4-25	
					Thermococcales	0.5-11.1	
					GOM Arc I	11	
EelMS538	CGG CTA CCA CTC GGG CCG C	538-556	ANME-2c	78.3	GOM Arc I	55	Boetius et al 2000
			ANME-2a/b	50.5	*Methanosarcinales*	0.2-21.1	
					Thermoplasmata	0.1-8.1	
					Methanomicrobia	6.1	
					Euryarchaeota	1.5	
EelMS932	AGC TCC ACC CGT TGT AGT	932-949	ANME-2b	10	*Methanosarcinales*	12	Boetius et al 2000
			ANME-2c	8.3	*Methanococcales*	10	
			ANME-1	5.2	*Archaeoglobales*	5.6	
			ANME-3	2			

All probes were tested using the online Testprobe database of SILVA, using 100% specificity (0 mismatches). Non-targets that are highly unwanted are given in red. Probes tested *in vitro* in this study are given in bold.

Table 2 Continued

Probe name	Sequence (5'-3')	Target site	Target	Coverage (%)	Non-target	Coverage (%)	Reference
ANME-2-538	GGC TAC CAC TCG GGC CGC	538–555	ANME-2c	78.3	GOM Arc I	56	Treude et al 2005c
			ANME-2a/b	52.4	Methanosarcinales	9.4-21.1	
					Methanococci	2.8-8.7	
					Thermoplasmata	8.1	
					Methanomicrobia	6.4	
ANME-2-712	TTC GCC ACA GAT GGT CCC	712-729	ANME-2a/b	71.8	Methanosarcinales	7.9-10.5	Knittel and Boetius 2009
			ANME-2c	71.7	Methanomicrobia	0.4-4.5	
			ANME-2b	50	Halobacteriales	0.1-1.7	
					Archaea	≤1.1	
ANME2a-647	TCT TCC GGT CCC AAG CCT	647-664	ANME-2a/b	49.5	Methanosarcinales	10.5	Knittel et al 2005
					ANME-2c	6.7	
					Methanomicrobia	≤3.8	
ANME2c-622	CCC TTG GCA GTC TGA TTG	622-639	ANME-2c	65	Methanosarcinales	2.7	Knittel et al 2005
					Methanomicrobia	1.5	
					ANME-2a/b	1	
ANME-2c-760	CGC CCC CAG CTT TCG TCC	760-777	ANME-2c	71.7	Archaeoglobales	3.2-3.6	Knittel et al 2005
					Methanosarcinales	3.2	
					ANME-2a/b	2.9	
					Methanomicrobia	1.9	
					ANME-1b	1.3	

All probes were tested using the online Testprobe database of SILVA, using 100% specificity (0 mismatches). Non-targets that are highly unwanted are given in red. Probes tested *in vitro* in this study are given in bold.

5

Discussion

Most reported primers and probes to target ANME groups were designed for seep systems where the archaeal community is not very diverse. Most of these primers and probes can therefore not be applied to other environments, especially when these harbour methanogenic and methanotrophic archaeal populations. Validation with sequences from the *in situ* archaeal community is therefore mandatory. When no data on the archaeal community are available, one needs to be sure that the primers and probes used do not target close relatives and are very specific. This especially applies to studies where growth of ANME clades on alternative substrates besides methane is investigated. For instance, it was investigated if ANME clades could grow on short-chain fatty acids (Jagersma et al 2012). In these experiments, even if the archaeal community *in situ* is known, it is unknown which methanogenic or methanotrophic archaea could proliferate under certain conditions that were undetectable in community analysis. Primer design for ANME clades and subclusters is deemed difficult since inter and intra-group diversity is high. Therefore, new sequences added to the database drastically change coverage and specificity of previously designed primers and probes and primer validation needs to be reconsidered constantly. Obviously, described PCR conditions cannot be applied to other complex samples and plasmid inserts and need to be optimized every time. Here, we describe the validation and optimization of described primer sets for specific quantitative detection of ANME-1, ANME-2a/b and ANME-2c subclusters in complex environments where methanogenic and methanotrophic clades are present.

For future qPCR determination, we propose a standard operating procedure when new samples with complex archaeal communities are obtained (Fig 3):

1. Consult the literature for developed primers or design new primers. Perform *in silico* PCR to check coverage of target and non-target groups or check binding specificity of both forward and reverse primers.

2. Perform gradient qPCR with a range around the obtained/described melting temperature (-5/+5 °C) using suitable positive and negative controls to obtain the optimal annealing temperature.

3. Analyse the melting curves and use the annealing temperature that shows as little amplification with negative controls as possible, especially close relatives and sequences know to be abundant in the samples.

4. When the melting curve is the same between target and non-target: Perform qPCR with DNA concentration gradient (10-fold dilutions) of positive (target) control and negative (non-target) control samples to determine at which concentrations the negative controls start to be amplified. When samples have quantities of non-target below the threshold concentration where non-target starts to be amplified, one can use the primer set for the target. Positive target DNA gradient PCR is used as a calibration curve to obtain if

positive target shows good efficiency (90-100%) and a R^2 >0.99%.

5. When the melting curve of the target is different than from the non-target, primers still can be used (obviously only with good efficiency and R^2), but results with a different melting curve than for target microorganisms cannot be used for quantification since non-target DNA may become amplified. Moreover, melting curves of non-target DNA could change with changing concentration of template and therefore a concentration gradient of DNA is also advisable (Fig 1, grey line).

6. When applying to environmental samples, sequencing of the amplified product is advisable to check if the right product is obtained.
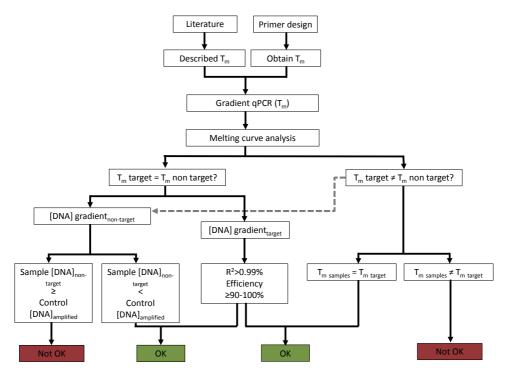
Figure 3 Flow chart of qPCR approach when existing or newly designed primers are used with a complex AOM sample.

Acknowledgements
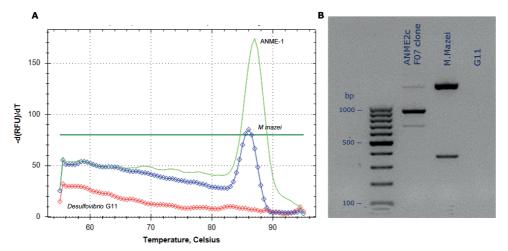
Supplementary data

Figure S1 A) Melting curve of the amplicon of ANME-1 primer pair ANME-1-337F and ANME-1-724R with *M. mazei* strain MC3 (purple diamonds, 1 ng µl^{-1} DNA), *Desulfovibrio* G11 (red diamonds, 1 ng µl^{-1} DNA) and cloned ANME-1 insert (yellow line, 2x10^3 copies µl^{-1}). **B)** Agarose gel showing PCR products (expected product size of 358 bp) of ANME-2c cloned insert (2x10^3 copies µl^{-1} in PCR) and products of *M. mazei* strain MC3 and *Desulfovibrio* G11(1 ng µl^{-1} DNA in PCR). The green line indicates the threshold line for quantification.
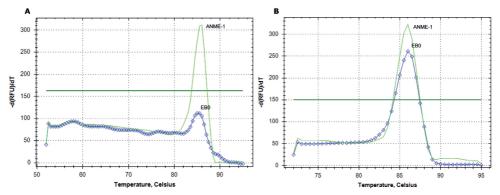

Figure S2 A) Melting curve of the amplicon of ANME-1 primer pair ANME-1-395f and ANME-1-1417r with the protocol as described in Miyashita *et al* (2009) and **B)** the optimized protocol for the Eckernförde bay sample (purple diamonds, 1 ng µl^{-1} DNA) and cloned ANME-1 insert (yellow line, 2x10^3 copies µl^{-1}). The green line indicates the threshold line for quantification.
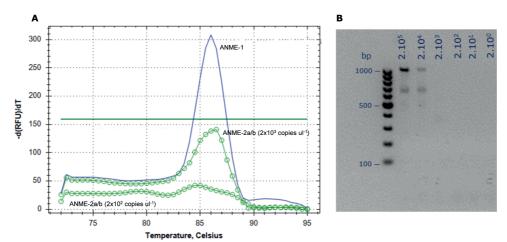
Figure S3 A) Melting curve of the amplicon of ANME-1 primer pair ANME-1-395f and ANME-1-1417r with cloned ANME-1 insert (purple line, $2x10^3$ copies μl^{-1}), cloned ANME-2a/b insert (green circles, $2x10^2$ copies μl^{-1} and $2x10^3$ copies μl^{-1}). **B)** Agarose gel showing products (expected product size of 1039 bp) of ANME-2a/b cloned inserts with different concentrations (copies μl^{-1}) in the reaction mix. The green line indicates the threshold line for quantification.
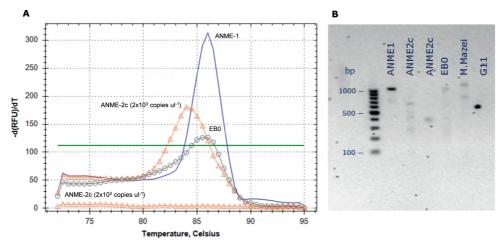
5

Figure S4 A) Melting curve of the amplicon of ANME-1 primer pair ANME-1-395f and ANME-1-1417r with cloned ANME-1 insert (purple line, $2x10^3$ copies μl^{-1}), cloned ANME-2c insert (triangles, $2x10^2$ copies μl^{-1} and $2x10^3$ copies μl^{-1}) and the Eckernförde bay sample (EB0, brown circles, 1 ng μl^{-1} DNA). **B)** Agarose gel showing products (expected product size of 1039 bp) of ANME-1 cloned insert, both ANME-2c cloned inserts, the Eckernförde bay sample (EB0), *M. mazei* strain MC3 and *Desulfovibrio* G11 (1 ng μl^{-1} DNA in PCR). The green line indicates the threshold line for quantification.
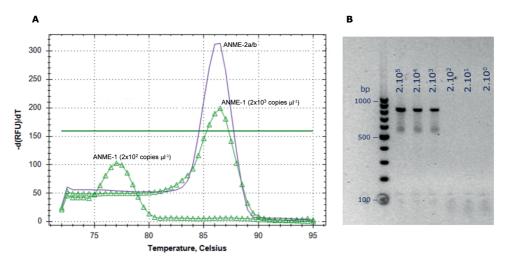
A

B

Figure S5 A) Melting curve of the amplicon of ANME-2a/b primer pair ANME-2a-426-F and ANME-2a-1242-R with cloned ANME-2a/b insert (purple line, 2×10^3 copies μl^{-1}) and cloned ANME-1 insert (triangles, 2×10^2 copies μl^{-1} and 2×10^3 copies μl^{-1}). **B)** Agarose gel showing products (expected product size of 833 bp) of ANME-1 cloned inserts with different concentrations (copies μl^{-1}) in the reaction mix. The green line indicates the threshold line for quantification.
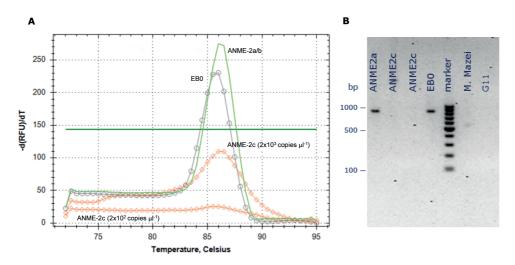
A

B

Figure S6 A) Melting curve of the amplicon of ANME-2a/b primer pair ANME-2a-426-F and ANME-2a-1242R with cloned ANME-2a/b insert (orange line, 2×10^3 copies μl^{-1}), cloned ANME-2c insert (diamonds, 2×10^2 copies μl^{-1} and 2×10^3 copies μl^{-1}) and the Eckernförde bay sample (EB0, brown cirlces, 1 ng μl^{-1} DNA). **B)** Agarose gel showing products with expected product size of 833 bp of ANME-2a/b cloned inserts, both ANME-2c cloned inserts, the Eckernförde bay sample (EB0), *M. mazei* strain MC3 and *Desulfovibrio* G11 (1 ng μl^{-1} DNA in PCR). The green line indicates the threshold line for quantification.
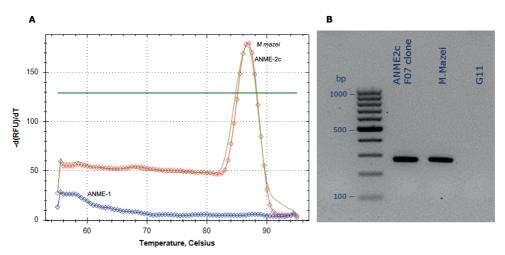
Figure S7 A) Melting curve of the amplicon of ANME-2c primer pair AR-468f/AR-736r with *M. mazei* strain MC3 (red diamonds, 1 ng µl⁻¹ DNA) and cloned ANME-1b insert (purple diamonds, (2x10³ copies µl⁻¹) and cloned ANME-2c insert (yellow line, 2x10³ copies µl⁻¹). **B)** Agarose gel showing products (expected product size of 268 bp) of ANME-2c cloned insert and products of *M. mazei* strain MC3 and *Desulfovibrio* G11 (1 ng µl⁻¹ DNA in PCR). The green line indicates the threshold line for quantification.
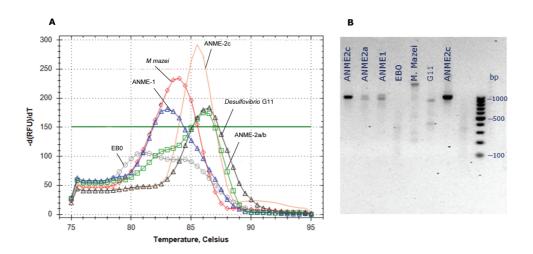
5

Figure S8 A) Melting curve of the amplicon of ANME-2c primer pair AR468f and ANME-2c-1411R with cloned ANME-2c insert (yellow line, 2x10³ copies µl⁻¹), cloned ANME-1 insert (purple triangles, 2x10³ copies µl⁻¹), cloned ANME-2a/b insert (orange squares, 2x10² copies µl⁻¹), the Eckernförde bay sample (grey circles, EB0, 1 ng µl⁻¹ DNA), *Desulfovibrio* G11 (brown triangles, 1 ng µl⁻¹ DNA) and *M. mazei* strain MC3 (orange diamonds, 1 ng µl⁻¹ DNA). **B)** Agarose gel showing no products (expected product size of 960 bp) of ANME-2c, ANME-2a/b and ANME-1 cloned insert, the Eckernförde bay sample (EB0), *M. mazei* strain MC3 and *Desulfovibrio* G11. The green line indicates the threshold line for quantification.
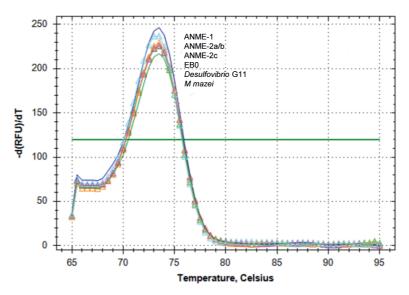
Figure S9 Melting curve of the amplicon of ANME-2c primer pair ANME-2c-F and ANME-2c-R with cloned ANME-2a/b, ANME-1, and ANME-2c insert (2×10^3 copies μl^{-1}), the Eckernförde bay sample (EB0), *Desulfovibrio* G11 and *M. mazei* strain MC3 (1 ng μl^{-1} DNA). The green line indicates the threshold line for quantification.
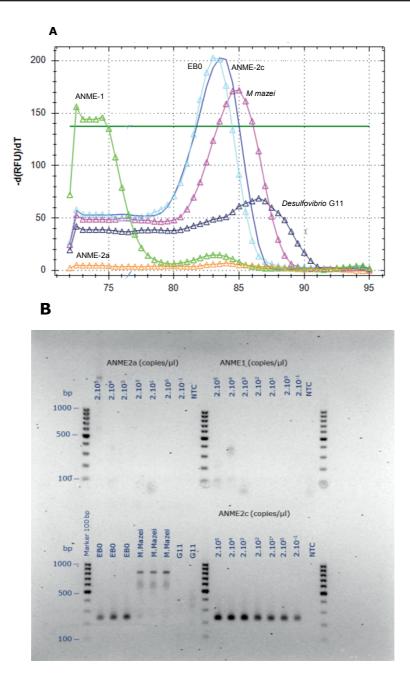
Figure S10 A) Melting curve of the amplicon of ANME-2c primer pair 2c-F and 2c-R with cloned ANME-2c (purple line) and ANME-1 insert (orange traingles, $2x10^3$ copies μl^{-1}), the Eckernförde bay sample (EB0, blue triangles), *Desulfovibrio* G11(purple triangles) and *M. mazei* strain MC3 (purple triangles) (1 ng μl^{-1} DNA). **B)** Agarose gel showing products (expected product size of 221 bp) of ANME-2a/b, ANME-1 and ANME-2c cloned insert with different concentrations (copies μl^{-1}), the Eckernförde bay sample (EB0), *M. mazei* strain MC3 and *Desulfovibrio* G11. The green line indicates the threshold line for quantification.

Chapter 6

Growth and activity of anme clades with different sulfate and sulfide concentrations in the presence of methane

Peer H. A. Timmers, H.C. Aura Widjaja-Greefkes, Javier Ramiro-Garcia, Caroline M. Plugge and Alfons J. M. Stams

Abstract

Extensive geochemical data showed that significant methane oxidation activity exists in marine sediments. The organisms responsible for this activity are anaerobic methane-oxidizing archaea (ANME) that occur in consortia with sulfate-reducing bacteria. A distinct zonation of different clades of ANME (ANME-1, ANME-2a/b and ANME-2c) exists in marine sediments, which could be related to the localized concentrations of methane, sulfate and sulfide. In order to test this hypothesis we performed long-term incubation of marine sediments under defined conditions with methane as a headspace gas: low or high sulfate (± 4 and ± 21 mM, respectively) in combination with low or high sulfide (± 0.1 and ± 4 mM, respectively) concentrations. Control incubations were also performed, with only methane, high sulfate or high sulfide. Methane oxidation was monitored and growth of subtypes ANME-1, ANME-2a/b, and ANME-2c assessed using qPCR analysis. A preliminary archaeal community analysis was performed to gain insight into the ecological and taxonomic diversity. Almost all of the incubations with methane had methane oxidation activity, with the exception of the incubations with combined low sulfate and high sulfide concentrations. Sulfide inhibition occurred only with low sulfate concentrations, which could be due to the lower Gibbs free energy available as well as sulfide toxicity. ANME-2a/b appear to mainly grow in incubations which had high sulfate levels and methane oxidation activity, whereas ANME-1 did not show this distinction. ANME-2c only grew in incubations with only sulfate addition. These findings are consistent with previously published *in situ* profiling analysis of ANME subclusters in different marine sediments. Interestingly, since all ANME subtypes also grew in incubations with only methane or sulfate addition, ANME may also be able to perform anaerobic methane oxidation under substrate limited conditions or alternatively perform additional metabolic processes.

Introduction

Anaerobic oxidation of methane (AOM) coupled to sulfate reduction (SR) has been found to occur in a wide range of marine sediments. The process is presumably performed by anaerobic methanotrophic archaea (ANME) in association with sulfate-reducing bacteria (SRB) belonging to the *Deltaproteobacteria* (Boetius et al 2000). Recently, evidence has emerged that suggests ANME archaea can perform both AOM and SR to elemental sulfur (Milucka et al 2012). The marine ANME clades presumed to be involved in AOM that have been described to date include ANME-1, ANME-2 and ANME-3. The ANME-2 clade has been further refined into subclusters a/b (previously considered to be two separate groupings) and subcluster c. The ANME-2 clade is closely related to cultivated members of the *Methanosarcinales*, the ANME-1 clade is related to *Methanomicrobiales* and *Methanosarcinales* (Hinrichs et al 1999) and the ANME-3 clade is most related to *Methanococcoides* spp. (Knittel et al 2005). Due to this divergent taxonomy, it is expected that distinct ecological and physiological niches exist between the different ANME clades. The ANME clades 1 and 2 have been found in many different environments, whereas ANME-3 has been mainly found in mud volcanoes and some seep sediments (Knittel and Boetius 2009, Lösekann et al 2007, Niemann et al 2006). Different ANME types do occur in the same marine environment, but show distinct zone formation in microbial mats or sediment cores. For instance, ANME-2 dominated surface layers of Hydrate Ridge sediments whereas ANME-1 was detected in deeper sediment layers with decreased sulfate and increased sulfide concentrations (Knittel et al 2005). In another study, the ANME-2a/b was shown to be more predominant at low methane and low sulfide levels, with ANME-2c dominance occurring in deeper sediment layers closer to gas hydrates where the methane flux and sulfide concentration were relatively high (Roalkvam et al 2011). Others have also observed an ecological transition of ANME-2a/b to ANME-2c and/or ANME-1 with increasing sediment depth (Nunoura et al 2006, Orcutt et al 2005, Orphan et al 2004, Pachiadaki et al 2011, Roalkvam et al 2012, Yanagawa et al 2011). As deduced from the data of Roalkvam *et al* (2012), it is likely that a concentration below 5 mM sulfate has resulted in a shift from ANME-2a/b to ANME-1 and ANME-2c. These observations imply that there are distinct parameters that determine the distinctive ecological niches of different ANME subtypes. Direct characterization of the impact of these parameters on ANME subtypes would generate a deeper systematic understanding of the microbial ecology and physiology of AOM in marine sediments. Since many other uncontrolled factors are prevalent *in situ*, however, it is difficult to directly determine which factors actually influence ANME subtype presence, activity and growth.

We report here on the use of batch incubations to directly investigate AOM activity and growth of ANME subtypes under defined and controlled sulfate and sulfide concentrations in presence of methane. The experimental approach used slurries for inoculating the batch incubations. The slurries were prepared from Eckernförde bay sediment, which is an AOM mediating sediment known to contain ANME-1, ANME-2a/b and ANME-2c subtypes. Incubation of the

slurries was then performed using methane-oxidizing conditions with low sulfate (± 4 mM) or high sulfate (± 21 mM) concentrations in combination with low sulfide (± 0.1-0.4 mM) or high sulfide (± 3-4 mM) concentrations. Control incubations were also performed where only methane, high sulfate or high sulfide was added. Growth of ANME subtypes after 344 days was assessed by qPCR and compared to baseline values at the start of the incubations. In incubations which contained methane as headspace, after 540 days of incubation ^{13}C-labelled CH_4 was added to enable measurement of methane oxidation activity to be made until 947 days of incubation. Archaeal community analysis was done on selected samples to observe differences in the ecological and taxonomic diversity of the different incubations.

Materials and methods

Origin of the inoculum

Samples were taken at Eckernförde Bay (Baltic Sea) at station B (water depth 28 m; position 54º31'15N, 10º01'28E) during a cruise of the German research vessel *Littorina* in June 2005. This sampling site has been described by Treude *et al* (2005b). Sediment samples were taken as described in chapter 2.

Media composition

The basal artificial marine medium used was prepared as described previously (Meulepas et al 2009a). The mineral media did not contain any carbon source and no possible electron acceptors. The media were boiled, cooled down under a nitrogen (N_2) flow and transferred into stock bottles. The headspace gas was exchanged 10 cycles with N_2, with an end pressure of 1.5 bar N_2 until use. The final pH of the media was 7.2. The phosphate provided buffering capacity to maintain a neutral pH value.

Experimental set-up

For every condition, 30 ml Eckernförde bay sediment was incubated in triplicates with 90 ml of artificial marine medium in 244 ml serum bottles closed with butyl rubber stoppers and aluminum caps. Before inoculation, the headspace gas was exchanged 10 cycles with N_2, with an end pressure of 1.8 bar N_2 when no methane was added. When methane was added, the headspace gas was exchanged 10 cycles with 99.999% CH_4 (Linde AG, Munich, Germany), with an end pressure of 1.8 bar CH_4. Sulfide was then added to the artificial medium before inoculation to avoid toxicity effect of the concentrated sulfide stock solution. After sulfide addition, the pH was adjusted to 7.5 and then the bottles were inoculated. Serum bottles were horizontally incubated in the dark at 15°C without shaking. During incubation, sulfide, sulfate and methane concentrations were monitored. Sulfide and sulfate concentrations for low and high conditions were kept at a constant concentration (Table 1). When sulfide concentrations were too high, a calculated amount of $FeCl_2$ was added to precipitate excess sulfide. When sulfate concentrations were too low, Na_2SO_4 was added to obtain the desired concentration again. When sulfide concentrations were too high and sulfate concentrations were too low,

$FeSO_4$ was added to precipitate sulfide and to replenish sulfate (Fig 1 and 2). After 540 days of incubation of the bottles where methane was added to the headspace, 99.999% CH_4 was added to an end pressure of 1.6 bar. Then, 99.99% $^{13}CH_4$ (Campro Scientific, Veenendaal, The Netherlands) was added to a final pressure of 1.8 bar. Sulfide and sulfate concentrations were determined and adjusted afterwards when necessary.

Table 1 Experimental set-up and calculated Gibbs free energy changes.

	Condition	Sulfate (mM)	Sulfide (mM)	CH_4 (mM)	Total CO_2 (mM)	$\Delta_r G'$
Methane-oxidizing	1: $CH_4 \uparrow SO_4^{2-}$	21.6	0.4	1.31	3.8	-28.1
	2: $CH_4 \uparrow SO_4^{2-} \uparrow S^{2-}$	21.1	3.8	1.31	6.9	-21.1
	3: $CH_4 \downarrow SO_4^{2-}$	3.6	0.4	1.31	4.4	-23.4
	4: $CH_4 \downarrow SO_4^{2-} \uparrow S^{2-}$	4.0	3.6	1.31	6.4	-17.4
Non-methane-oxidizing	5: $\uparrow SO_4^{2-}$	21.6	0.2	-	3.2	-
	6: CH_4	0.1	0.1	1.31	2.7	-19.2
	7: $\uparrow S^{2-}$	0.4	3.0	-	4.4	-

All conditions were performed in triplicate slurry incubations. Sulfate, sulfide and CO_2 concentrations represent average concentrations of triplicates during 942 days of incubation (see Fig 1 and 2 for detailed concentrations over time). Methane concentrations are theoretical maximum dissolved seawater concentrations (Yamamoto et al 1976).

Analytical measurements

The pressure of the serum vials was determined using a portable membrane pressure unit GMH 3150 (Greisinger Electronic GmbH, Regenstauf, Germany). The pH was measured using a solid gel epoxy electrode (Qis, Oosterhout, The Netherlands). Sulfate and sulfide were analysed as described in chapter 3. Headspace gas composition was measured as described in chapter 3.

DNA extraction

Genomic DNA was extracted from all triplicate incubations at the beginning of the experiment and after 344 days. Samples of 2 ml were taken every time point and DNA was extracted using the Fast DNA Kit for Soil (MP Biomedicals, Solon, OH) according to the manufacturer's protocol with two 45-second beat beating steps using a Fastprep Instrument (MP Biomedicals, Solon, OH). Afterwards, DNA was purified and concentrated using the DNA Clean & Concentrator kit (Zymo Research Corporation, Irvine, CA). DNA concentrations were determined with the Qubit 2.0 fluorometer (Thermo Fisher Scientific, Waltham, MA).

6

Quantitative real-time PCR

Extracted DNA from the incubations at two time points (0 days and 344 days of incubation) was used for qPCR analysis as described in chapter 5. Quantification of specific archaeal groups was expressed as total 16S rRNA gene copies $g_{wet\ weight}^{-1}$.

Archaeal community analysis

Extracted DNA from selected samples (1C: $CH_4 \uparrow SO_4^{2-}$, 5A: $\uparrow SO_4^{2-}$, 6B: CH_4, 7A: $\uparrow S^{2-}$) at 344 days of incubation was used for archaeal community analysis. Firstly, amplification of archaeal 16S rRNA gene fragments was done using primers 518F (5'-CAGCMGCCGCGGTAA-3') (Wang and Qian 2009) and 905R (5'-CCCGCCAATTCCTTTAAGTTTC-3') (Kvist et al 2007). PCR amplification was performed in a total volume of 50 µl containing 500 nM of each forward and reverse primer (Biolegio BV), 1 unit of Phusion DNA polymerase (Thermo Scientific), 10 µl of HF-buffer, 200 µM dNTP mix, made to a total volume of 50 µl with nuclease free sterile water. The PCR program was as follows: denaturing at 98 °C for 30 s, followed by 25 cycles of denaturing at 98 °C for 10 s, annealing at 60 °C for 20 s, extension at 72 °C for 20 s, followed by a final extension step at 72 °C for 10 min. Secondly, an additional PCR was performed to extend 8nt barcodes to the generated amplicons, as used previously (Hamady et al 2008). Barcoded amplification was performed in a total volume of 100 µl containing 5 µl of the first PCR product, 500 nM of each forward and reverse primer (Biolegio BV), 2 units of Phusion DNA polymerase (Thermo Scientific), 20 µl of HF-buffer, 200 µM dNTP mix, made to a total volume of 100 µl with nuclease free sterile water. The PCR program was as follows: denaturing at 98 °C for 30 s, followed by 5 cycles of denaturing at 98 °C for 10 s, annealing at 52 °C for 20 s, extension at 72 °C for 20 s, followed by a final extension at 72 °C for 10 min. Barcoded PCR products were cleaned using the HighPrep PCR clean-up system (MagBio Genomics Inc., Gaithersburg, MD). DNA concentrations were quantified using Qubit (Invitrogen, Bleiswijk, The Netherlands). Afterwards, barcoded samples were pooled in equimolar quantities, purified using the MagBio HighPrep PCR- 96 well protocol and then quantified using Qubit. Samples were submitted for MiSeq sequencing on the Illumina platform using sequencing by synthesis chemistry.

Sequencing data analysis

For analysis of the 16S RNA gene sequencing data, an in-house pipeline was used (Ramiro-Garcia et al unpublished). Shortly, paired-end libraries were filtered to contain only read pairs with perfectly matching primer and barcodes. Resulting reads were separated by sample using the barcode and operational taxonomic units (OTUs) were assigned using an open reference approach and a customized reference SILVA 16S rRNA database (Quast et al 2013). Microbial composition plots were generated using a workflow based on Quantitative Insights Into Microbial Ecology (QIIME) v1.2 (Caporaso et al 2010).

Results

qPCR and archaeal community analysis

The Eckernförde bay sediment inoculum contained mostly ANME-2a/b, few ANME-1 and even less ANME-2c copies. The fold increase of ANME-1, ANME-2a/b and ANME-2c therefore gives more information on which subtype increased most in copy numbers during incubation. Figure 3 shows that at almost all methane-oxidizing conditions, the ANME-2a/b subtype had a higher fold increase than ANME-1 and ANME-2c, except where sulfate is low and sulfide is high. ANME2a/b archaea apparently grew best when sulfate was supplied in high concentrations in presence of methane, with or without high levels of sulfide (Fig 3). The ANME-1 subtype also seemed to proliferate under methane-oxidizing conditions, but showed similar growth in all other conditions. ANME-2c seemed to grow only when sulfate but no methane was added. These results were confirmed by archaeal community analysis that showed higher abundance of ANME-2a/b in condition with methane as compared to conditions without methane (Fig S4). ANME-1 seemed to be equally abundant in every condition sequenced, except for the condition with only sulfide where it showed a slightly higher relative abundance (Fig S4).

AOM activity

During the whole incubation period of 947 days, sulfate and sulfide concentrations were monitored and controlled at the desired level. In high sulfide incubations, sulfide concentrations were decreasing over time and sodium sulfide had to be added at some time points, where the condition with only sulfide showed highest sulfide decrease (Fig 1). In incubations with low sulfide concentrations, sulfide was produced only in presence of methane, and no sulfide production occurred in the absence of methane (Fig 1). Conditions with methane and high sulfate concentrations showed highest sulfate reduction and sulfide had to be precipitated with ferrous sulfate regularly, whereas with methane and low sulfate, sulfate reduction was lower with the exception of one of the triplicates (Fig 2). Although sulfate reduction was highest in condition with high sulfate concentrations, sulfate reduction did take place in all conditions, even where no sulfate was added; the endogenous sulfate of less than 0.4 mM was completely reduced (Fig 2). When ^{13}C- labeled methane was added to the headspace at day 540 of methane-containing conditions, $^{13}CO_2$ production was also monitored. Production of $^{13}CO_2$ was apparent in all conditions, except where no $^{13}CH_4$ was added (Fig 4). Only the combined addition of high sulfate with low sulfide showed substantially higher AOM rates relative to the non-methane-oxidizing conditions (t-test unequal variance, $p<0.05$). When sulfate was high, there was no substantial difference between low sulfide and high sulfide addition. When sulfide was low, there was no substantial difference between high sulfate and low sulfate addition. However, there was a substantial difference when sulfate was high together with low sulfide and when sulfate was low together with high sulfide (t-test unequal variance, $p<0.05$). Methane oxidation was associated with sulfide production in conditions with methane and sulfate when sulfide levels were low (Fig S5).
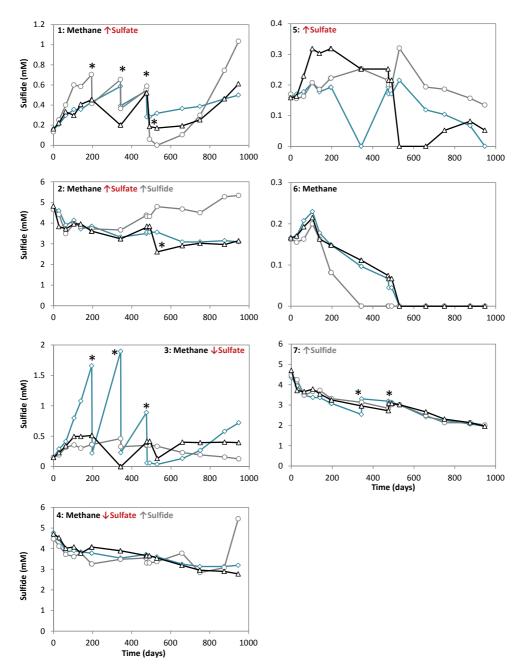
Figure 1 Sulfide concentrations (y-axis, mM) during 947 days of incubation (x-axis, days) in all conditions. Arrows indicate either high (↑) or low (↓) sulfate and sulfide concentrations. The time points where either ferrous sulfate or sodium sulfide was added are indicated by an asterisk. Different lines represent triplicate incubations (A: blue diamonds, B: grey circles, C: black triangles).

Figure 2 Sulfate concentrations (y-axis, mM) during 947 days of incubation (x-axis, days) in all conditions. Arrows indicate either high (↑) or low (↓) sulfate and sulfide concentrations. The time points where either ferrous sulfate or sodium sulfate was added are indicated by an asterisk. Different lines represent triplicate incubations (A: blue diamonds, B: grey circles, C: black triangles).
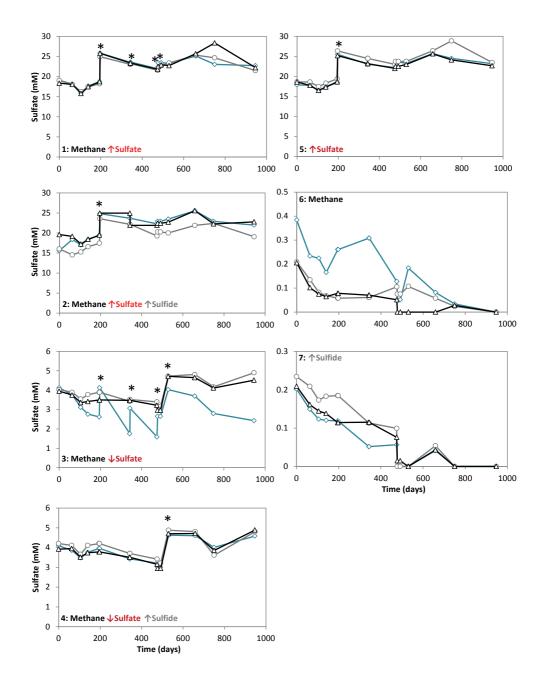
133

Almost no methane production was observed in conditions with 'sulfate only' addition; 0.2 mM methane at 659 days of incubation in all triplicates and 0.9 mM in one of the triplicates at 947 days of incubation. Both methane peaks were not detectable upon further incubation. Triplicate incubations of the condition with 'sulfide only' addition did show methane accumulation up to 3.7, 1.4, and 1.0 mM after 947 days.
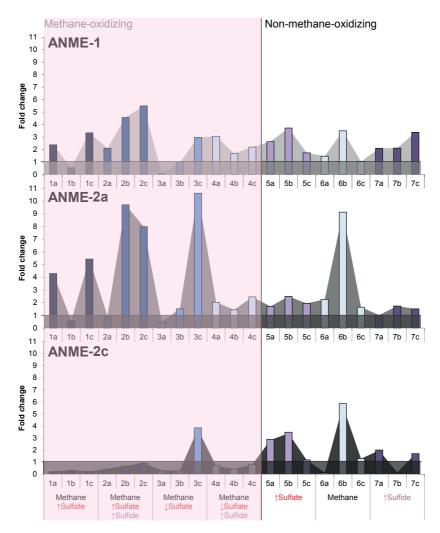

Figure 3 The fold change of ANME-1, ANME-2a/b and ANME-2c total 16S rRNA gene copies $g_{wet\ weight}^{-1}$ after 344 days of incubation in all conditions. Arrows indicate either high (↑) or low (↓) sulfate and sulfide concentrations. The horizontal lines at a fold change of 1 show fold changes that indicate growth.

For each experimental condition, $\Delta_r G'$ values were calculated (Table 1) according to the $\Delta_r G^{\circ}$'of -21 kJ mol^{-1}, assuming methane as a gas molecule and products to be in the form of CO_2 and HS^- (Thauer 2011). For the calculation, we used the maximum dissolved methane concentration of 1.31 mM at a salinity of 30 ‰ and 20°C (Yamamoto et al 1976), assuming the effect of 0.5-1 bar overpressure is negligible to increase solubility. The CO_2, sulfide and sulfate concentrations used for the calculations are also given in Table 1. These concentrations were the average concentration during 947 days of incubation in triplicate incubations. Detailed concentrations over time are given in Fig 1 for sulfide and Fig 2 for sulfate. According to the calculations, the lowest Gibbs free energies (most negative) were associated with high sulfate and low sulfide concentrations, and the Gibbs free energy changes were smallest with low sulfate and high sulfide concentrations.
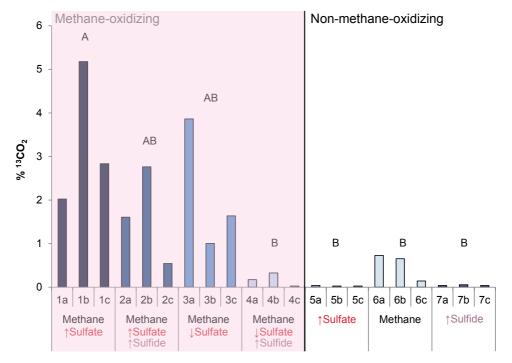

Figure 4 The produced $^{13}CO_2$ (%) after $^{13}CH_4$ addition between 540 days and 947 days of incubation in all conditions. Arrows indicate either high (↑) or low (↓) sulfate and sulfide concentrations. Different letters represent significant difference (t-test with unequal variance, p<0.05).

Discussion

Methane-oxidizing conditions

Growth of ANME-2a/b was apparent when methane was added and was highest with high sulfate concentrations, independent of the sulfide concentration. Only when sulfate was low together with high sulfide, was growth substantially less. This was confirmed by archaeal 16S rRNA gene sequencing. Methane oxidation was also substantially lower with low sulfate and high sulfide concentrations, compared to high sulfate and low sulfide concentrations. Moreover, no substantial difference in AOM rates between high and low sulfate addition in the presence of methane was observed. It was shown before with the same Eckernförde bay sediment enriched in ANME-2a/b that AOM rates only became affected when sulfate concentrations were below 2 mM. This indicates that the Km for sulfate is lower than 2 mM (Meulepas et al 2009b) and thus 5 mM sulfate should not result in lower rates of AOM. Therefore, the sulfate and sulfide concentrations seemed to have a combined effect in terms of determining growth and activity of ANME-2a/b.

The $\Delta_r G'$ of methane-oxidizing conditions are similar to reported $\Delta G'$ values for non-seep environments with low methane concentrations (Caldwell et al 2008, Thauer 2011). These values were previously argued to be close to the minimum energy required to sustain life. The translocation of one proton over the membrane, the minimum biological energy quantum, was calculated to have a $\Delta G'$ of around -19 kJ mol sulfate^{-1} for sulfate-reducing bacteria and -10.6 kJ mol methane^{-1} for methanogenic archaea (Hoehler et al 2001). This corresponded to estimates of critical energy yields for ANME/SRB aggregates of -10 kJ mol methane^{-1} (Alperin and Hoehler 2009), and activity at the calculated value of -10.6 kJ mol^{-1} methane was confirmed *in situ* (Nauhaus et al 2002). Until now, it has been unclear if AOM activity under the least favorable conditions could still be associated with microbial growth. Conditions which were above the threshold of -19 kJ mol methane^{-1} in this study did show AOM activity and associated growth of ANME-2a/b, while other conditions showed substantially less activity and growth. This implies that below this threshold ANME-2a/b growth was probably inhibited in our incubations. Since growth and activity of ANME-2a/b seems to be directly related to the theoretical available energy, this explains the sulfide dependency only at low sulfate concentrations. The $\Delta G'$ values of AOM in non-seep sediments are quite low (-18 to -25 kJ mol methane^{-1}) as compared to seep sediments (-35 kJ mol methane^{-1}) (Alperin and Hoehler 2009, Caldwell et al 2008, Thauer 2011, Valentine and Reeburgh 2000, Wang et al 2010), mainly due to the differences in the dissolved methane concentrations. Sulfate and sulfide concentrations can therefore have a larger effect on AOM rates in non-seep systems relative to seep systems as with similar sulfate and sulfide concentrations, the $\Delta G'$ of the reaction can still stay low enough for the reaction to occur in seep systems. This could explain the lack of sulfide inhibition in seep sediments that showed AOM activity under conditions where 10-15 mM sulfide was produced (Valentine 2002, Joye et al 2004, Nauhaus et al 2002). However,

sensitivity to sulfide toxicity may also differ between ANME species, as an AOM performing enrichment has also been reported to have complete inhibition at 2.5 mM of sulfide, despite AOM still being thermodynamically feasible (Meulepas et al 2009a, Meulepas et al 2009b).

ANME-1 seemed to grow in almost every condition, and did not show the differential growth characteristics that ANME-2a/b did. On this basis, under methane-oxidizing conditions, it could be predicted that the ANME-2a/b subtype would outcompete ANME-1 in the presence of high amounts of sulfate (with either high or low amounts of sulfide) but not in the combined presence of low amounts of sulfate and high amounts of sulfide. This is generally consistent with the *in situ* observations of ANME-1 thriving in low-methane (Blumenberg et al 2004, Elvert et al 2005), methane-free (Bertram et al 2013), sulfate-depleted environments (Vigneron et al 2013, Yanagawa et al 2011) and in environments with elevated sulfide levels (Biddle et al 2012, Knittel et al 2005, Krüger et al 2008). ANME-2a/b thrive at low sulfide levels (Biddle et al 2012, Knittel et al 2005, Roalkvam et al 2011), high sulfate concentrations (Yanagawa et al 2011, Rossel et al 2011) or both (Krüger et al 2008). Higher sulfate concentrations generally occur close to the surface of sediments where ANME-2a/b are generally found to be dominant (Nunoura et al 2006, Orcutt et al 2005, Orphan et al 2004, Pachiadaki et al 2011, Roalkvam et al 2012). Moreover, previous reactor studies with Eckernförde bay sediment where sulfate was kept high and sulfide was kept low were successful in obtaining high rates of AOM and enrichment of ANME-2a/b archaea (Meulepas et al 2009a and chapter 2).

Non-methane-oxidizing conditions

Under non-methane-oxidizing conditions where growth of ANME archaea was observed, it is possible that the ANME could still perform AOM or potentially another process. In the 'methane only' condition, growth of all ANME types and methane oxidation was apparent. Archaeal community analysis also showed a higher abundance of ANME-2a/b as relative to 'sulfate only' and 'sulfide only' conditions. With the 'methane only' condition, methane oxidation was probably partly coupled to sulfate reduction since the 0.2-0.4 mM sulfate that was present was completely reduced during incubation. It has been reported that AOM occurs even below 0.5 mM sulfate, but at lower rates than at higher sulfate concentrations (Beal et al 2011, Meulepas et al 2009b, Wegener et al 2009, Yoshinaga et al 2014). However, it has also been reported that when labelled methane is used in incubations, methanogenesis can also produce labeled CO_2 in a process called 'trace methane oxidation' (Zehnder and Brock 1979). Archaeal community analysis showed high abundance of *Methanococcoides* in the 'methane only' condition, indicating that methanogenesis (and thus trace methane oxidation) and AOM did indeed co-occur.

In the 'sulfate only' conditions, very little sulfide production was found, suggesting that endogenous substrates were an unimportant source for sulfate reduction. We did observe presence of methane at two time points (0.2 mM and 0.9 mM at day 659 and 947, respectively), indicating that methane was produced. In theory, this methane could have been oxidized since

the 0.2 mM could not be detected at day 750. At 0.2 mM methane, the ΔG' of the reaction already is -25.7 kJ mol^{-1}, which is sufficiently negative for growth of ANME. However, since methane was not measurable at other time points, it is not clear if 'sulfate only' conditions were favorable for AOM throughout the experiment.

In the condition with 'sulfide only', both sulfate reduction and methane production (3.7, 1.4, and 1.0 mM methane in biological triplicates after 947 days) took place, making AOM possible. However, at these conditions, the ΔG' was a maximum of -13.1 kJ mol^{-1}. Methane accumulated slowly throughout the experiment under this conditions, in contrast to the 'sulfate only' condition. It is likely that this was due to the energetic yield being too low to allow significant AOM activity. In both 'sulfate only' and 'sulfide only' conditions, we did not find an abundance of methanogens (<0.5% of reads belonging to *Methanococcoides* under both conditions, and <0.2% of reads of *Methanobacteriaceae* in 'sulfide only' condition) although methanogenesis did occur. In the 'sulfide only' condition, ANME-1 grew and appeared to be relatively more abundant than in the other conditions analyzed by 16S rRNA gene sequencing. ANME-1 cells have been frequently observed to occur without a bacterial partner (Blumenberg et al 2004, Knittel et al 2005, Orphan et al 2002, Orphan et al 2004) and it has been postulated that ANME-1 can either oxidize methane alone (Maignien et al 2013, Orphan et al 2002, Pachiadaki et al 2011). Indications also exist that ANME-1 can perform methanogenesis (Lloyd et al 2011) as was also found for ANME-2 (Bertram et al 2013).

Yoshinaga *et al* (2014) showed that when the ΔG' of AOM decreases (from -35 to -20 kJ mol^{-1}) due to sulfate depletion and sulfide accumulation, the AOM back flux becomes significant. As the AOM rates decrease, the AOM back flux increases, resulting in significant production of methane from CO_2 (Yoshinaga et al 2014). The observed ^{13}C depletion below the sulfate-methane transition zone (SMTZ) in marine sediments that was previously thought to come from methanogenesis, may thus come from the back flux of AOM. This corresponds to reports of high AOM activities below the SMTZ in the methanogenic zone (Knab et al 2009, Parkes et al 2007, Treude et al 2005, Yoshioka et al 2010). This back flux could have been occurring in 'methane only' and 'sulfate only' conditions, which could also explain growth of ANME subtypes.

Insight into the diversity of potential metabolic properties of ANME archaea also derived from metagenomic and metaproteomic studies of ANME-1 and ANME-2a/b methanotrophs (Hallam et al 2004, Meyerdierks et al 2005, Meyerdierks et al 2010, Stokke et al 2012, Wang et al 2014). For instance, ANME-2a/b seems to have the potential to metabolize acetate (Wang et al 2014) and although the canonical dissimilatory sulfate reduction pathway was not present, potential alternative pathways for sulfate reduction has been postulated to exist in ANME-1 (Meyerdierks et al 2005, Meyerdierks et al 2010, Stokke et al 2012). It was experimentally shown that ANME-2 archaea could reduce sulfate to elemental sulfur coupled to methane oxidation (Milucka et al 2012). This indeed implied that ANME could use alternative pathways

for sulfate reduction. Therefore, more research on the metabolic capabilities of ANME, especially sulfate reduction and methanogenesis, could also explain presence of ANME at unexpected sites where methane oxidation activity is not observed.

Acknowledgements

6

Supplementary information

Figure S1 qPCR results of specific primers for ANME-1 expressed as the absolute amount of ANME-1 (copies $g_{wet\,weight}^{-1}$) at 0 days and at 344 days of incubation. Arrows at conditions on the x-axis indicate either high (↑) or low (↓) sulfate and sulfide concentrations.
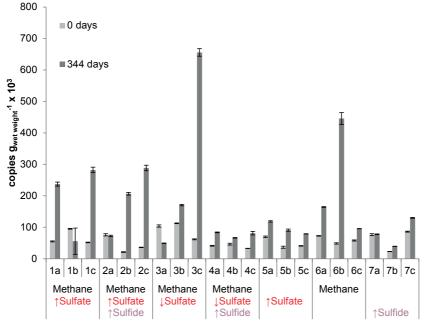
Figure S2 qPCR results of specific primers for ANME-2a/b expressed as the absolute amount of ANME-2a/b (copies $g_{wet\,weight}^{-1}$) at 0 days and at 344 days of incubation. Arrows at conditions on the x-axis indicate either high (↑) or low (↓) sulfate and sulfide concentrations.
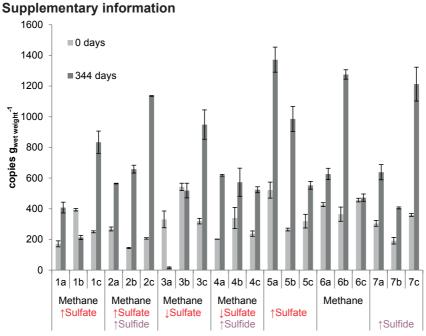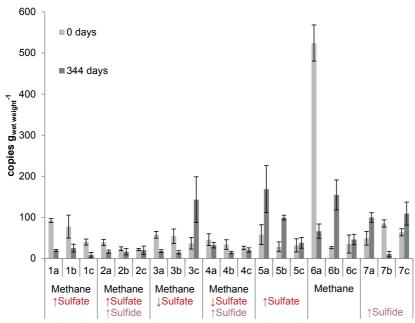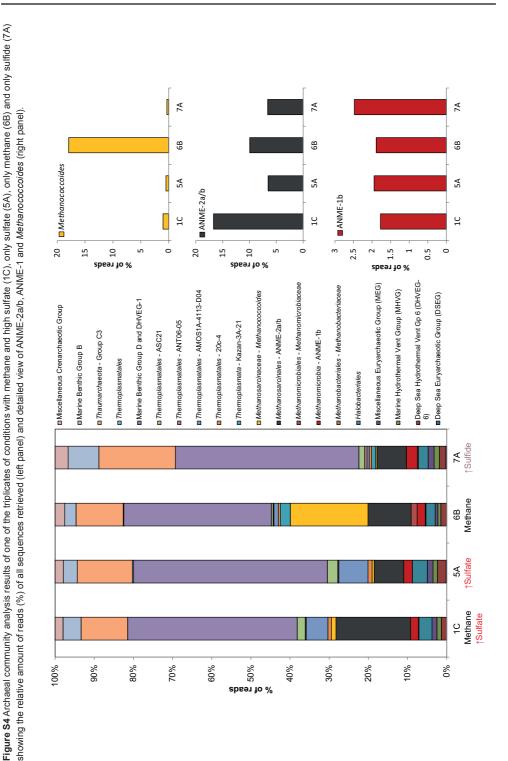
Figure S3 qPCR results of specific primers for ANME-2c expressed as the absolute amount of ANME-2c (copies $g_{wet\ weight}^{-1}$) at 0 days and at 344 days of incubation. Arrows at conditions on the x-axis indicate either high (↑) or low (↓) sulfate and sulfide concentrations.

Figure S4 Archaeal community analysis results of one of the triplicates of conditions with methane and high sulfate (1C), only sulfate (5A), only methane (6B) and only sulfide (7A) showing the relative amount of reads (%) of all sequences retrieved (left panel) and detailed view of ANME-2a/b, ANME-1 and *Methanococcoides* (right panel).

Figure S5 Sulfide (squares, black lines) and $^{13}CO_2$ concentration (diamonds, grey lines) in mM in methane-oxidizing conditions 1 and 3 (arrows indicate either high (↑) or low (↓) sulfate and sulfide concentrations) incubated with $^{13}CH_4$ after 530 days of incubation. Standard deviations represent triplicate incubations.
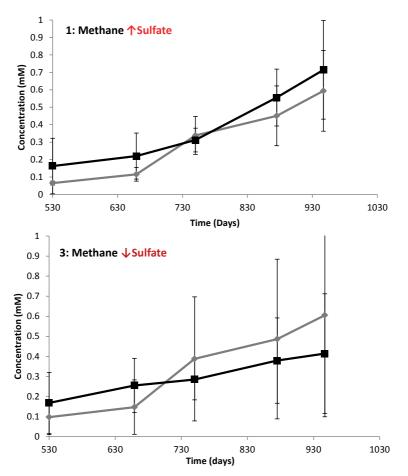
CHAPTER 7

GENERAL DISCUSSION

On the reversibility of methanogenesis

Methane oxidation was observed in many methanogens and was named 'trace methane oxidation' (TMO), since it only occurs during net methane production. Methane production was observed in anaerobic methane oxidizing archaea (ANME) and was attributed to the enzymatic back flux since it only occurs during net anaerobic methane oxidation (AOM). In chapter 1, the differences between these processes have been described. Since methane production and methane oxidation can co-occur in the same environment, TMO and AOM can co-occur, which makes it hard to study and differentiate both processes. It is not known if methanogens can perform net methane oxidation and if ANME can perform net methanogenesis.

AOM in diffusive sediments

At the pioneering stage of the discovery of anaerobic oxidation of methane coupled to sulfate reduction, the responsible microorganisms for the process were not described yet. As methane oxidation coupled to sulfate reduction is a reversal of methanogenesis coupled to sulfate reduction (discussed in chapter 1), either methanogens and/or sulfate reducers would be the most plausible responsible microorganisms. Sulfate reducers were not capable to oxidize methane when supplied as sole carbon source (Sorokin 1957) but later research indicated otherwise (Davis and Yarbroug 1965). However, in the latter study lactate medium was used and negligible oxidation of labelled methane was observed (Reeburgh 1976). Pure strains of methanogens were found to be able to oxidize methane, but only during net methane production, in a process called 'trace methane oxidation'(TMO)(discussed in chapter 1). Therefore, methanogenic archaea were thought to be responsible for both TMO and AOM (Harder 1997) and the electrons derived from AOM are presumably transferred to the sulfate-reducing partner via an unknown interspecies electron carrier (IEC).

Assuming that sulfate-dependent AOM in diffusive sediments is the reversal of hydrogenotrophic methanogenesis, Hoehler *et al* (1994) postulated that hydrogen must be efficiently removed and maintained at low concentrations by the sulfate-reducing partner. Sulfate-reducing bacteria outcompete methanogens for substrates such as H_2/CO_2 since SRB remove H_2 more efficiently. Therefore, hydrogen concentrations are generally lower during sulfate reduction than during methanogenesis (Lovley and Goodwin 1988), which creates conditions that thermodynamically favor methane oxidation (Valentine and Reeburgh 2000). Field and laboratory studies showed that pore water hydrogen concentrations in AOM mediating sediment incubations were indeed low enough to allow energy conservation via reverse methanogenesis (Hoehler et al 1994). Reversal of metabolic pathways with the H_2 concentration acting as switch had been shown before for some bacteria producing H_2/CO_2 from acetate under low H_2 pressure (Lee and Zinder 1988). Co-cultures grown on acetate or methanol showed sulfate-dependent H_2 transfer from *M. barkeri* (closely related to ANME) to *D. vulgaris*, resulting in less methane production and more CO_2 and sulfide production (Phelps et al 1985), as was also observed with complex communities (Achtnich et al 1995). The switch

from methanogenesis to hydrogen production does not need to occur due to competition with SRB. Marine sediments incubated with the non-competitive substrates ^{14}C-labeled methylamine and ^{14}C-labeled methanol showed increasing '% $^{14}CO_2$ (=[$^{14}CO_2/(^{14}CO_2+^{14}CH_4)$])' with increasing sulfate concentrations and decreasing hydrogen concentrations, up to 95% $^{14}CO_2$ (Finke et al 2007). The methanogens started to produce H_2/CO_2 instead of CH_4 upon sulfate addition and the sulfate-reducing partner scavenged the produced hydrogen efficiently to keep the concentration low enough for the methanogens to continue producing H_2/CO_2. This "hydrogen leakage" was also reported to occur in co-cultures of methanogens and sulfate reducers with acetate as electron donor (Ozuolmez et al 2015). It was also reported that pure cultures of methanogens under low hydrogen concentrations produced hydrogen (Valentine et al 2000). However, these cultures did not produce hydrogen in presence of methane and did not oxidize methane.

Considering acetate as IEC, concentrations need to be below 0.6 nM for acetoclastic methanogenesis to become endergonic (Finke et al 2007) and thus allow AOM to dominate when acetate would be the IEC. Porewater acetate concentrations of marine sediment cores are however higher than 10 µM (Ozuolmez et al 2015). In **chapter 4**, we describe enrichment of SRB related to *Desulfosarcina* on acetate with extremely slow growth, indicating that acetate was not a competitive substrate in this AOM enrichment. It could therefore be that *in situ* acetate concentrations at AOM 'hot spots' are locally low enough for it to act as IEC in AOM. Since both H_2 and acetate are plausible IECs for AOM in diffusive sediments (discussed in chapter 4), further enrichment studies with both substrates on AOM enrichments from diffusive sediments might allow to isolate SRB involved in AOM.

Trace methane oxidation and anaerobic oxidation of methane

TMO reached up to 98% of the methane produced when manganese dioxide and ferrous sulfate were added to digested sludge (Zehnder and Brock 1980). This made the authors speculate on the use of these added electron acceptors (manganese dioxide and sulfate) by consortia of methanogens and sulfate reducers to oxidize methane. The stimulating effect of iron was explained by efficient sulfide removal due to precipitation with iron. Multiple studies showed that sludge and other mixed communities showed much higher TMO rates as compared to pure cultures of methanogens (Meulepas et al 2010a, Zehnder and Brock 1980), which could be due to the removal of organic matter and sulfide, making the reverse of methanogenesis more favourable. This works the other way around as well; the reported AOM back flux (Holler et al 2011a) went up to 78% of net AOM when sulfate was depleted and the Gibbs free energy change decreased due to sulfate limitation (Yoshinaga et al 2014). It was also shown that the sulfur and oxygen isotopic fractionation of sulfate was highly dependent on the methane concentration (Antler et al 2015, Deusner et al 2014). The reversibility of this weakly exergonic process operating close to its thermodynamic equilibrium is thus highly dependent on substrate and product concentration.

7

Besides the effect on TMO, it was shown previously that a higher methane partial pressure led to increased AOM rates (Kallmeyer and Boetius 2004, Krüger et al 2005, Meulepas et al 2009b, Nauhaus et al 2002) and in **chapter 2** we show faster growth and activity of ANME under high methane partial pressure. In **chapter 6**, we showed higher AOM activity and growth under thermodynamically favourable combinations of sulfate and sulfide concentrations for AOM to occur. It is therefore likely that in an organic matter depleted system rich in sulfate and low in hydrogen, such as the sulfate-methane transition zone (SMTZ) of diffusion-based sediments, AOM will start to dominate over time (Fig 1). AOM probably becomes an active process (no enzyme equilibrium) directed by environmental parameters such as substrate availability (methane and sulfate) and product stripping (hydrogen and sulfide), making net methane oxidation feasible. Therefore, long-term incubations are crucial to differentiate AOM from TMO. In **chapter 2** and **chapter 3** we showed that during long-term incubation, endogenous substrates became depleted and methanogenesis (and thus TMO) and sulfate reduction rates decreased, while AOM coupled to sulfate reduction continued and even increased.

Methanogenic and methanotrophic archaea

Since ANME archaea perform reverse methanogenesis, one would speculate that ANME archaea could perform net methane production when environmental parameters are in favor of it. Several indications exist that ANME-1 could oxidize methane alone or perform other processes such as methanogenesis (discussed in chapter 1 and 6). However, since the AOM back flux can be significant under substrate limitation, especially below the SMTZ, these indications may well point to net AOM and not net methanogenesis (Yoshinaga et al 2014). In **chapter 6**, we indeed found that ANME archaea under substrate limited conditions either perform net AOM with high back flux or net methanogenesis. In some cases, researchers seemed to be able (Bertram et al 2013, Orcutt et al 2008) and others were unable (Treude et al 2007) to stimulate net methanogenesis through addition of methanogenic substrates. In **chapter 6**, we also found indications that ANME-2a/b were specialists and grew most under methane-oxidizing conditions, while ANME-1 could include generalists, being able to grow when circumstances are less favorable for AOM. In **chapter 2**, we showed growth of ANME-2c at high methane partial pressure, which did not occur in previous experiments at low methane partial pressure, implying ANME-2c proliferation under high methane pressure. More research should be done to obtain the ecological parameters that determine niche differentiation of all ANME clades and the differences in methanotrophic and methanogenic capabilities. If some ANME clades are incapable of methanogenesis, the question remains if they lost this capability or never exhibited it.

The same question remains for methanogenic archaea; could they switch from TMO to AOM under the right circumstances and adaptation time? Thus far, no known methanogen was found to oxidize methane under low hydrogen conditions (Valentine et al 2000) nor did methane oxidation rates ever exceed methanogenesis rates (discussed in chapter 1 and 3).

In **chapter 2**, we showed that anaerobic sludge was unable to perform AOM during long term incubation with methane and sulfate. However, organic matter was not as depleted as in the AOM performing reactor when the experiment was stopped (discussed in chapter 2). ANME subclusters are ubiquitously distributed in marine sediments all over the world and there are only a few reports of AOM activity without detection of ANME archaea. Many of these reports can however not discriminate between TMO and AOM (discussed in chapter 1 and 3). Additionally, the use of aspecific primers and probes for detection of ANME archaea (discussed in chapter 5) could therefore lead to many false positive findings. In **chapter 3**, we described the presence and activity of ANME-2a/b in a freshwater environment, expanding the dispersion of ANME archaea outside marine environments. We also found indications that GoM Arc I/ANME-2d archaea are able to perform reverse methanogenesis coupled to sulfate reduction in freshwater conditions, which confirmed previous findings (Flynn et al 2013, Schubert et al 2011). Recently, it was shown that AOM coupled to sulfate reduction in freshwater systems indeed forms a major sink for methane (Segarra et al 2015). This indicates that ANME are ubiquitously distributed and are specialized in AOM (see chapter 1, Fig 3). More ANME members and possibly new clades have yet to be discovered, but until now only specific clades related to the *Methanosarcinales*, *Methanomicrobiales* and *Methanococcoides* are found to be capable of performing net reverse methanogenesis.

AOM in non-diffusive sediments

It may well be that in diffusive sediments other IECs are transferred than in systems with higher flux. At the typical SMTZ, single cells of archaea or small mono-specific archaeal clusters exist without closely associated sulfate-reducing bacterial partners (Chapter 1, Fig 4). Model predictions suggested that in these environments, aggregates with considerable size cannot be formed due to energetic constraints (Alperin and Hoehler 2009). As cells are not closely connected, interspecies electron transport through direct electron transfer is not plausible (Alperin and Hoehler 2009). Krüger *et al* (2005) found lower *ex situ* rates for diffusion based samples than for seep-sediment samples under the same conditions and concluded that the lower rates were due to differences in the AOM community composition.

In seeps, hydrothermal vents and other non-diffusion based sediments, AOM rates are much higher due to higher methane concentrations and energy flux. In these environments, archaea are closely associated with sulfate-reducing partners forming the often observed big aggregates (Chapter 1, Fig 4). The high AOM rates cannot be explained by diffusion of an IEC, making direct electron transfer a more plausible explanation in these environments (Alperin and Hoehler 2010, Orcutt and Meile 2008). In sewage sludge reactors, methanogenic-sulfidogenic aggregates are formed spontaneously and the morphology resembles those of aggregates in mat-covered sediments on Hydrate Ridge. It was proposed that the methanogens initiate aggregation because of better attachment characteristics, and that the SRB colonize the methanogen core as the aggregate develops (Santegoeds et al 1999), as observed in the shell

type AOM and SR mediating aggregates (Chapter 1, Fig 4). In methanogenic-sulfidogenic aggregates, the methanogenic activity is mostly located in the core of the aggregate while SR was mostly occurring at the surface layer (Santegoeds et al 1999). Alperin and Hoehler postulated that in seep systems, the occurring ANME/SRB aggregates are actually methane producers that use the high fluxes of hydrogen or other fermentation products that derived from the decomposition of the chemosynthetic communities in these environments (Alperin and Hoehler 2010). Milucka *et al* (2012) proposed that the archaea perform both reverse methanogenesis and sulfate reduction, producing polysulfide that served as IEC for the associated SRB in an enrichment from Isis Mud Volcano sediment. This was consistent with another study with Black Sea sediment slurries (Deusner et al 2014) and with an isotopic sulfate fractionation study (Antler et al 2015).

Diversity of the associated partner bacteria

The diversity of the bacterial partners in AOM was discussed in chapter 1 and 4. A co-occurrence of ANME-2 archaea with SEEP-SRB1 bacteria and ANME-1 archaea with Eel-1 group members and SEEP-SRB2 bacteria was reported (discussed in chapter 2). However, in **chapter 2** we found ANME-2 archaea co-occurring with SEEP-SRB2 bacteria, which was also found in another study (Kleindienst et al 2012). The co-occurrence and possible relationship of Eel-1-group members with ANME-1 was noted before and the higher abundance of this group occurred at the SMTZ, indicating a relationship with AOM (Harrison et al 2009). We showed that the Eel-1 group members were not directly involved in AOM (discussed in chapter 2). The Eel-1 members are most closely related to bacteria present in benzene-degrading enrichment cultures (Phelps et al 1998) and to *Desulfobacterium anilini* (Schnell et al 1989) and are therefore probably involved in sulfate-mediated hydrocarbon degradation. Form the DSS clade, the SEEP-SRB1 subclade was described to be the predominant partner of ANME-2 in two enrichments originating from hydrothermal vents (Schreiber et al 2010). Recently, several other DSS related subgroups were found to be involved in degradation of non-methane short- and long-chain alkanes (Kleindienst et al 2014). Other sulfate-reducing partner bacteria of ANME, SEEP-SRB2, could be capable of performing other processes unrelated to AOM coupled to SR (Kleindienst et al 2012, Orcutt et al 2005, Vigneron et al 2013b). Future studies may lead to insight to understand which parameters in different environments determine the predominant sulfate-reducing bacterial partner in AOM and if these SRB could also be involved in the degradation of other hydrocarbons.
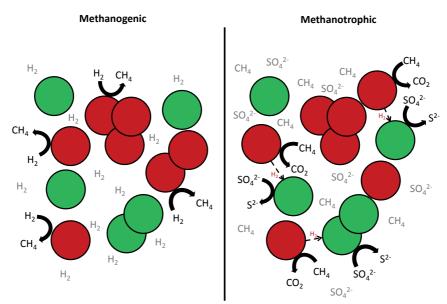
Figure 1 Model showing methanogenic conditions (left panel, high H_2 concentrations, no sulfate present) and methanotrophic conditions (right panel, low H_2 concentrations and high sulfate concentrations) in diffusive marine sediments, with the assumption that H_2 acts as interspecies electron carrier in methane oxidation coupled to sulfate reduction. Red spheres represent methanogens (left panel) and methanotrophs (right panel), green spheres are sulfate-reducing bacteria. Hydrogen could be replaced by any other compound of which *in situ* concentrations are low enough to make AOM feasible.

Future perspectives

Although AOM has been studied for more than 50 years, little is known on the metabolic pathways and the organisms involved and no consensus is reached in any of these aspects. An enrichment culture from Isis mud volcano appeared to be almost axenic after >8 years of continuous cultivation, with ANME-2/DSS consortia accounting for up to 95% of all cells (Milucka et al 2012). These cultures allow to perform physiological studies to get insights into the mechanisms of AOM, but also to investigate possible utilization of alternative substrates and electron acceptors besides methane and sulfate. Enrichment cultures from other environments, especially low flux diffusive sediments are also needed to investigate these aspects. Environments can force physiological differences in ANME and associated SRB due to thermodynamic constraints. In our laboratory, we accomplished to obtain a sediment-free AOM performing enrichment from Eckernförde bay (discussed in chapter 4) which would be suitable for these studies. Moreover, phylogenetically divergent ANME clades seem to show niche differentiation throughout marine sediments, also implying physiological differentiation. Understanding the mechanisms of electron transfer between the ANME and associated SRB would also allow to elucidate why AOM only seems to be performed by specialised clades and not by most methanogenic archaea. This phylogenetic separation seems to be existing partly in the associated SRB as well, but in some cases this syntrophy seems to be flexible and

7

more dependent on environmental factors (discussed in chapter 1 and 2). Experiments with pure strains of methanogens related to the ANME clades gave insights into the mechanism of trace methane oxidation. More experiments with co-cultures of methanogens and SRB where methane oxidation would be stimulated by applying thermodynamic constraints (i.e. high substrate and low product concentrations), could also give more insights into the mechanisms of AOM *in situ*.

Appendices

References
Summary
Nederlandse samenvatting
Co-author affiliations
Acknowledgements
About the author
List of publications
Sense diploma

References

– Achtnich C, Schuhmann A, Wind T, Conrad R (1995). Role of interspecies H_2 transfer to sulfate and ferric iron-reducing bacteria in acetate consumption in anoxic paddy soil. *FEMS Microbiol Ecol* **16:** 61-69.

– Aeckersberg F, Bak F, Widdel F (1991). Anaerobic oxidation of saturated-hydrocarbons to CO_2 by a new type of sulfate-reducing bacterium. *Arch Microbiol* **156:** 5-14.

– Alain K, Holler T, Musat F, Elvert M, Treude T, Krüger M (2006). Microbiological investigation of methane- and hydrocarbon-discharging mud volcanoes in the Carpathian Mountains, Romania. *Environ Microbiol* **8:** 574-590.

– Alperin MJ, Reeburgh WS, Whitaker MJ (1988). Carbon and hydrogen isotope fractionation resulting from anaerobic methane oxidation. *Glob Biochem Cycles* **2:** 279-288.

– Alperin MJ, Hoehler TM (2010). The ongoing mystery of sea-floor methane. *Science* **329:** 288-289.

– Alperin MJ, Hoehler TM (2009). Anaerobic methane oxidation by archaea/sulfate-reducing bacteria aggregates: 1. Thermodynamic and physical constraints. *Am J Sci* **309:** 869-957.

– Amos RT, Bekins BA, Cozzarelli IM, Voytek MA, Kirshtein JD, Jones EJ *et al* (2012). Evidence for iron-mediated anaerobic methane oxidation in a crude oil-contaminated aquifer. *Geobiology* **10:** 506-517.

– Antler G, Turchyn AV, Herut B, Sivan O (2015). A unique isotopic fingerprint of sulfate-driven anaerobic oxidation of methane. *Geology* published online on 26 May 2015 as doi:10.1130/G36688.1.

– Barnes RO, Goldberg ED (1976). Methane production and consumption in anoxic marine-sediments. *Geology* **4:** 297-300.

– Barnett PRO, Watson J, Connelly D (1984). A multiple corer for taking virtually undisturbed samples from shelf, bathyal and abyssal sediments. *Oceanol Acta* **7:** 399-408.

– Bartstra D (2003). Gasbronnen in Noord-Holland. Vereniging tot behoud van gasbronnen in Noord-Holland, Middenbeemster, doi:90-90-16912-1.

– Beal EJ, House CH, Orphan VJ (2009). Manganese- and iron-dependent marine methane oxidation. *Science* **325:** 184-187.

– Beal EJ, Claire MW, House CH (2011). High rates of anaerobic methanotrophy at low sulfate concentrations with implications for past and present methane levels. *Geobiology* **9:** 131-139.

– Beatty JT, Overmann J, Lince MT, Manske AK, Lang AS, Blankenship RE *et al* (2005). An obligately photosynthetic bacterial anaerobe from a deep-sea hydrothermal vent. *Proc Natl Acad Sci USA* **102:** 9306-9310.

– Bertram S, Blumenberg M, Michaelis W, Siegert M, Krüger M, Seifert R (2013). Methanogenic capabilities of ANME-archaea deduced from ^{13}C-labelling approaches. *Environ Microbiol* **15:** 2384-2393.

– Biddle JF, Lipp JS, Lever MA, Lloyd KG, Sørensen KB, Anderson R *et al* (2006). Heterotrophic archaea dominate sedimentary subsurface ecosystems off Peru. *Proc Natl Acad Sci USA* **103:** 3846-3851.

– Biddle JF, Cardman Z, Mendlovitz H, Albert DB, Lloyd KG, Boetius A *et al* (2012). Anaerobic oxidation of methane at different temperature regimes in Guaymas Basin hydrothermal sediments. *ISME J* **6:** 1018-1031.

– Blazewicz SJ, Petersen DG, Waldrop MP, Firestone MK (2012). Anaerobic oxidation of methane in tropical and boreal soils: ecological significance in terrestrial methane cycling. *J Geophys Res-Biogeo* **117:** G02033.

– Blodau C, Deppe M (2012). Humic acid addition lowers methane release in peats of the Mer Bleue bog, Canada. *Soil Biol Biochem* **52:** 96-98.

– Blumenberg M, Seifert R, Reitner J, Pape T, Michaelis W (2004). Membrane lipid patterns typify distinct anaerobic methanotrophic consortia. *Proc Natl Acad Sci USA* **101:** 11111-11116.

– Boetius A, Ravenschlag K, Schubert CJ, Rickert D, Widdel F, Gieseke A *et al* (2000). A marine microbial consortium apparently mediating anaerobic oxidation of methane. *Nature* **407:** 623-626.

– Boetius A, Suess E (2004). Hydrate Ridge: a natural laboratory for the study of microbial life fueled by methane from near-surface gas hydrates. *Chem Geol* **205:** 291-310.

– Bowles MW, Samarkin VA, Joye SB (2011). Improved measurement of microbial activity in deep-sea sediments at in situ pressure and methane concentration. *Limnol Oceanogr-Meth* **9:** 499-506.

– Bussmann I, Dando PR, Niven SJ, Suess E (1999). Groundwater seepage in the marine environment: role for mass flux and bacterial activity. *Mar Ecol Prog Ser* **178:** 169-177.

– Caldwell SL, Laidler JR, Brewer EA, Eberly JO, Sandborgh SC, Colwell FS (2008). Anaerobic oxidation of methane: mechanisms, bioenergetics, and the ecology of associated microorganisms. *Environ Sci Technol* **42:** 6791-6799.

– Camacho C, Coulouris G, Avagyan V, Ma N, Papadopoulos J, Bealer K, Madden T (2009). BLAST+:architecture and applications. *BMC Bioinformatics* **10:** 421.

– Caporaso JG, Kuczynski J, Stombaugh J, Bittinger K, Bushman FD, Costello EK *et al* (2010). QIIME allows analysis of high-throughput community sequencing data. *Nat Methods* **7:** 335-336.

– Chang YH, Cheng TW, Lai WJ, Tsai WY, Sun CH, Lin LH *et al* (2012). Microbial methane cycling in a terrestrial mud volcano in eastern Taiwan. *Environ Microbiol* **14:** 895-908.

– Cravo-Laureau C, Labat C, Joulian C, Matheron R, Hirschler-Rea A (2007). *Desulfatiferula olefinivorans* gen. nov. sp. nov., a long-chain n-alkane-degrading, sulfate-reducing bacterium. *Int J Syst Evol Microbiol* **57:** 2699-2702.

– Crowe SA, Katsev S, Leslie K, Sturm A, Magen C, Nomosatryo S *et al* (2011). The methane cycle in ferruginous Lake Matano. *Geobiology* **9:** 61-78.

– Daims H, Bruhl A, Amann R, Schleifer KH, Wagner M (1999). The domain-specific probe EUB338 is insufficient for the detection of all Bacteria: development and evaluation of a more comprehensive probe set. *Syst Appl Microbiol* **22:** 434-444.

– Dale AW, Regnier P, Van Cappellen P (2006). Bioenergetic controls on anaerobic oxidation of methane (AOM) in coastal marine sediments: a theoretical analysis. *Am J Sci* **306:** 246-294.

– Davis JB, Yarbroug HF (1965). Anaerobic oxidation of hydrocarbons by *Desulfovibrio desulfuricans*. *Chem Geol* **1:** 137-144.

– DeLong EF (2000). Resolving a methane mystery. *Nature* **407:** 577, 579.

– Demirel B (2014). Major pathway of methane formation from energy crops in agricultural biogas digesters. *Crit Rev Env Sci Tec* **44:** 199-222.

– DeSantis TZ, Hugenholtz P, Larsen N, Rojas M, Brodie EL, Keller K *et al* (2006). Greengenes, a chimera-checked 16S rRNA gene database and workbench compatible with ARB. *Appl Environ Microbiol* **72:** 5069-5072.

– Deusner C, Meyer V, Ferdelman TG (2010). High-pressure systems for gas-phase free continuous incubation of enriched marine microbial communities performing anaerobic oxidation of methane. *Biotechnol Bioeng* **105:** 524-533.

– Deusner C, Holler T, Arnold GL, Bernasconi SM, Formolo MJ, Brunner B (2014). Sulfur and oxygen isotope fractionation during sulfate reduction coupled to anaerobic oxidation of methane is dependent on methane concentration. *Earth Planet Sci Lett* **399:** 61-73.

– Deutzmann JS, Schink B (2011). Anaerobic oxidation of methane in sediments of Lake Constance, an oligotrophic freshwater lake. *Appl Environ Microbiol* **77:** 4429-4436.

– Egger M, Rasigraf O, Sapart CJ, Jilbert T, Jetten MS, Rockmann T *et al* (2015). Iron-mediated anaerobic oxidation of methane in brackish coastal sediments. *Environ Sci Technol* **49:** 277-283.

– Eller G, Kanel LK, Krüger M (2005). Cooccurrence of aerobic and anaerobic methane oxidation in the water column of lake plusssee. *Appl Environ Microbiol* **71:** 8925-8928.

– Elvert M, Hopmans EC, Treude T, Boetius A, Suess E (2005). Spatial variations of methanotrophic consortia at cold methane seeps: implications from a high-resolution molecular and isotopic approach. *Geobiolology* **3:** 195-209.

– Ettwig KF, Shima S, van de Pas-Schoonen KT, Kahnt J, Medema MH, op den Camp HJM *et al* (2008). Denitrifying bacteria anaerobically oxidize methane in the absence of archaea. *Environ Microbiol* **10:** 3164-3173.

– Ettwig KF, van Alen T, van de Pas-Schoonen KT, Jetten MSM, Strous M (2009). Enrichment and molecular detection of denitrifying methanotrophic bacteria of the NC10 Phylum. *Appl Environ Microbiol* **75:** 3656-3662.

– Ettwig KF, Butler MK, Le Paslier D, Pelletier E, Mangenot S, Kuypers MM *et al* (2010). Nitrite-driven anaerobic methane oxidation by oxygenic bacteria. *Nature* **464:** 543-548.

– Evers S, Weizenegger M, Ludwig W, Schink B, Schleifer KH (1993). The phylogenetic positions of *Pelobacter acetylenicus* and *Pelobacter propionicus*. *Syst Appl Microbiol* **16:** 216-218.

– Finke N, Hoehler TM, Jørgensen BB (2007). Hydrogen 'leakage' during methanogenesis from methanol and methylamine: implications for anaerobic carbon degradation pathways in aquatic sediments. *Environ Microbiol* **9:** 1060-1071.

– Flynn TM, Sanford RA, Ryu H, Bethke CM, Levine AD, Ashbolt NJ *et al* (2013). Functional microbial diversity explains groundwater chemistry in a pristine aquifer. *BMC Microbiol* **13:** 146-160.

– Friedrich MW (2005). Methyl-coenzyme M reductase genes: unique functional markers for methanogenic and anaerobic methane-oxidizing Archaea. *Method Enzymol* **397:** 428-442.

– Gantner S, Andersson AF, Alonso-Saez L, Bertilsson S (2011). Novel primers for 16S rRNA-based archaeal community analyses in environmental samples. *J Microbiol Meth* **84:** 12-18.

– Gauthier M, Bradley RL, Simek M (2015). More evidence that anaerobic oxidation of methane is prevalent in soils: is it time to upgrade our biogeochemical models? *Soil Biol Biochem* **80:** 167-174.

– Girguis PR, Orphan VJ, Hallam SJ, DeLong EF (2003). Growth and methane oxidation rates of anaerobic methanotrophic archaea in a continuous-flow bioreactor. *Appl Environ Microbiol* **69:** 5472-5482.

– Girguis PR, Cozen AE, DeLong EF (2005). Growth and population dynamics of anaerobic methane-oxidizing archaea and sulfate-reducing bacteria in a continuous-flow bioreactor. *Appl Environ Microbiol* **71:** 3725-3733.

– Gorlenko VM (1970). A new phototrophic green sulphur bacterium - *Prosthecochloris aestuarii* nov. gen. nov. spec. *J Basic Microb* **10:** 147-149.

– Green-Saxena A, Dekas AE, Dalleska NF, Orphan VJ (2014). Nitrate-based niche differentiation by distinct sulfate-reducing bacteria involved in the anaerobic oxidation of methane. *ISME J* **8:** 150-163.

– Grosskopf R, Janssen PH, Liesack W (1998). Diversity and structure of the methanogenic community in anoxic rice paddy soil microcosms as examined by cultivation and direct 16S rRNA gene sequence retrieval. *Appl Environ Microbiol* **64:** 960-969.

– Grossman EL, Cifuentes LA, Cozzarelli IM (2002). Anaerobic methane oxidation in a landfill-leachate plume. *Environ Sci Technol* **36:** 2436-2442.

– Gupta V, Smemo KA, Yavitt J, Fowle DA, Branfireun BA, Basiliko N (2013). Stable isotopes reveal widespread anaerobic methane oxidation across latitude and peatland type. *Environ Sci Technol* **47:** 8273-8279.

– Hageman SPW, van der Weijden RD, Weijma J, Buisman CJN (2013). Microbiological selenate to selenite conversion for selenium removal. *Water Res* **47:** 2118-2128.

– Hallam SJ, Putnam N, Preston CM, Detter JC, Rokhsar D, Richardson PM *et al* (2004). Reverse methanogenesis: testing the hypothesis with environmental genomics. *Science* **305:** 1457-1462.

– Hamady M, Walker JJ, Harris JK, Gold NJ, Knight R (2008). Error-correcting barcoded primers for pyrosequencing hundreds of samples in multiplex. *Nat Methods* **5:** 235-237.

– Hansen LB, Finster K, Fossing H, Iversen N (1998). Anaerobic methane oxidation in sulfate depleted sediments: effects of sulfate and molybdate additions. *Aquat Microbiol Ecol* **14:** 195-204.

– Harder J (1997). Anaerobic methane oxidation by bacteria employing ^{14}C-methane uncontaminated with ^{14}C-carbon monoxide. *Mar Geol* **137:** 13-23.

– Haroon MF, Hu SH, Shi Y, Imelfort M, Keller J, Hugenholtz P *et al* (2013). Anaerobic oxidation of methane coupled to nitrate reduction in a novel archaeal lineage. *Nature* **500:** 567-570.

– Harris JK, Caporaso JG, Walker JJ, Spear JR, Gold NJ, Robertson CE *et al* (2013). Phylogenetic stratigraphy in the Guerrero Negro hypersaline microbial mat. *ISME J* **7:** 50-60.

– Harrison BK, Zhang H, Berelson W, Orphan VJ (2009). Variations in archaeal and bacterial diversity associated with the sulfate-methane transition zone in continental margin sediments (Santa Barbara Basin, California). *Appl Environ Microbiol* **75:** 1487-1499.

– Heuer V, Elvert M, Tille S, Krummen M, Mollar XP, Hmelo LR (2006). Online δ^{13}C analysis of volatile fatty acids in sediment / porewater systems by liquid chromatography – isotope ratio mass spectrometry. *Limnol Oceanogr-Meth* **4:** 346–357.

– Higashioka Y, Kojima H, Nakagawa T, Sato S, Fukui M (2009). A novel n-alkane-degrading bacterium as a minor member of p-xylene degrading sulfate-reducing consortium. *Biodegradation* **20:** 383-390.

– Higashioka Y, Kojima H, Watanabe M, Fukui M (2013). *Desulfatitalea tepidiphila* gen. nov., sp. nov., a sulfate-reducing bacterium isolated from tidal flat sediment. *Int J Syst Evol Microbiol* **63:** 761–765.

– Hinrichs KU, Hayes JM, Sylva SP, Brewer PG, DeLong EF (1999). Methane-consuming archaebacteria in marine sediments. *Nature* **398:** 802-805.

– Hinrichs KU, Boetius A (2002). The anaerobic oxidation of methane: new insights in microbial ecology and biogeochemistry. In: Wefer G, Billett D, Hebbeln D, Jørgensen BB, Schlüter M, Van Weering T (eds) *Ocean Margin Systems* Springer-Verlag Berlin Heidelberg**,** pp 457-477.

– Hoehler TM, Alperin MJ, Albert DB, Martens CS (2001). Apparent minimum free energy requirements for methanogenic archaea and sulfate-reducing bacteria in an anoxic marine sediment. *FEMS Microbiol Ecol* **38:** 33-41.

– Hoehler TM, Alperin MJ, Albert DB, Martens CS (1994). Field and laboratory studies of methane oxidation in an anoxic marine sediment - evidence for a methanogen-sulfate reducer consortium. *Global Biogeochem Cy* **8:** 451-463.

– Holler T, Wegener G, Niemann H, Deusner C, Ferdelman TG, Boetius A *et al* (2011a). Carbon and sulfur back flux during anaerobic microbial oxidation of methane and coupled sulfate reduction. *Proc Natl Acad Sci USA* **108:** E1484-1490.

– Holler T, Widdel F, Knittel K, Amann R, Kellermann MY, Hinrichs KU *et al* (2011b). Thermophilic anaerobic oxidation of methane by marine microbial consortia. *ISME J* **5:** 1946-1956.

– Holmer M, Storkholm P (2001). Sulphate reduction and sulphur cycling in lake sediments: a review. *Freshwater Biol* **46:** 431-451.

– Hu SH, Zeng RJ, Burow LC, Lant P, Keller J, Yuan ZG (2009). Enrichment of denitrifying anaerobic methane oxidizing microorganisms. *Env Microbiol Rep* **1:** 377-384.

– Inagaki F, Suzuki M, Takai K, Oida H, Sakamoto T, Aoki K *et al* (2003). Microbial communities associated with geological horizons in coastal subseafloor sediments from the Sea of Okhotsk. *Appl Environ Microbiol* **69:** 7224-7235.

– Iversen N, Jørgensen BB (1985). Anaerobic methane oxidation rates at the sulfate methane transition in marine sediments from Kattegat and Skagerrak (Denmark). *Limnol Oceanogr* **30:** 944-955.

– Jaeggi T, Kortman GA, Moretti D, Chassard C, Holding P, Dostal A *et al* (2014). Iron fortification adversely affects the gut microbiome, increases pathogen abundance and induces intestinal inflammation in Kenyan infants. *Gut* **64:** 731-742.

– Jaekel U, Musat N, Adam B, Kuypers M, Grundmann O, Musat F (2013). Anaerobic degradation of propane and butane by sulfate-reducing bacteria enriched from marine hydrocarbon cold seeps. *ISME J* **7:** 885-895.

– Jaekel U, Zedelius J, Wilkes H, Musat F (2015). Anaerobic degradation of cyclohexane by sulfate-reducing bacteria from hydrocarbon-contaminated marine sediments. *Front Microbiol* **6:** 116.

– Jagersma CG, Meulepas RJ, Timmers PH, Szperl A, Lens PN, Stams AJ (2012). Enrichment of ANME-1 from Eckernförde Bay sediment on thiosulfate, methane and short-chain fatty acids. *J Biotechnol* **157:** 482-489.

– Jagersma GC, Meulepas RJW, Heikamp-de Jong I, Gieteling J, Klimiuk A, Schouten S *et al* (2009). Microbial diversity and community structure of a highly active anaerobic methane-oxidizing sulfate-reducing enrichment. *Environ Microbiol* **11:** 3223-3232.

– Joye SB, Boetius A, Orcutt BN, Montoya JP, Schulz HN, Erickson MJ *et al* (2004). The anaerobic oxidation of methane and sulfate reduction in sediments from Gulf of Mexico cold seeps. *Chem Geol* **205:** 219-238.

– Kallmeyer J, Boetius A (2004). Effects of temperature and pressure on sulfate reduction and anaerobic oxidation of methane in hydrothermal sediments of Guaymas Basin. *Appl Environ Microbiol* **70:** 1231-1233.

– Kappler A, Benz M, Schink B, Brune A (2004). Electron shuttling via humic acids in microbial iron(III) reduction in a freshwater sediment. *FEMS Microbiol Ecol* **47:** 85-92.

– Kendall MM, Wardlaw GD, Tang CF, Bonin AS, Liu YT, Valentine DL (2007). Diversity of archaea in marine sediments from Skan Bay, Alaska, including cultivated methanogens, and description of *Methanogenium boonei* sp. nov. *Appl Environ Microbiol* **73:** 407-414.

– Kleindienst S, Ramette A, Amann R, Knittel K (2012). Distribution and in situ abundance of sulfate-reducing bacteria in diverse marine hydrocarbon seep sediments. *Environ Microbiol* **14:** 2689-2710.

– Kleindienst S, Herbst FA, Stagars M, von Netzer F, von Bergen M, Seifert J *et al* (2014). Diverse sulfate-reducing bacteria of the Desulfosarcina/Desulfococcus clade are the key alkane degraders at marine seeps. *ISME J* **8:** 2029-2044.

– Klindworth A, Pruesse E, Schweer T, Peplies J, Quast C, Horn M *et al* (2013). Evaluation of general 16S ribosomal RNA gene PCR primers for classical and next-generation sequencing-based diversity studies. *Nucleic Acids Res* **41:** e1.

– Knab NJ, Cragg BA, Hornibrook ERC, Holmkvist L, Pancost RD, Borowski C *et al* (2009). Regulation of anaerobic methane oxidation in sediments of the Black Sea. *Biogeosciences* **6:** 1505-1518.

– Kniemeyer O, Musat F, Sievert SM, Knittel K, Wilkes H, Blumenberg M *et al* (2007). Anaerobic oxidation of short-chain hydrocarbons by marine sulphate-reducing bacteria. *Nature* **449:** 898-U810.

– Knittel K, Boetius A, Lemke A, Eilers H, Lochte K, Pfannkuche O *et al* (2003). Activity, distribution, and diversity of sulfate reducers and other bacteria in sediments above gas hydrate (Cascadia margin, Oregon). *Geomicrobiol J* **20:** 269-294.

– Knittel K, Lösekann T, Boetius A, Kort R, Amann R (2005). Diversity and distribution of methanotrophic archaea at cold seeps. *Appl Environ Microbiol* **71:** 467-479.

– Knittel K, Boetius A (2009). Anaerobic oxidation of methane: progress with an unknown process. *Annu Rev Microbiol* **63:** 311-334.

– Kobayashi T, Koide O, Mori K, Shimamura S, Matsuura T, Miura T *et al* (2008). Phylogenetic and enzymatic diversity of deep subseafloor aerobic microorganisms in organics- and methane-rich sediments off Shimokita Peninsula. *Extremophiles* **12:** 519-527.

– Krüger M, Meyerdierks A, Glöckner FO, Amann R, Widdel F, Kube M *et al* (2003). A conspicuous nickel protein in microbial mats that oxidize methane anaerobically. *Nature* **426:** 878-881.

– Krüger M, Treude T, Wolters H, Nauhaus K, Boetius A (2005). Microbial methane turnover in different marine habitats. *Palaeogeogr Palaeocl* **227:** 6-17.

– Krüger M, Wolters H, Gehre M, Joye SB, Richnow HH (2008a). Tracing the slow growth of anaerobic methane-oxidizing communities by (15)N-labelling techniques. *FEMS Microbiol Ecol* **63:** 401-411.

– Krüger M, Blumenberg M, Kasten S, Wieland A, Kanel L, Klock JH *et al* (2008b). A novel, multi-layered methanotrophic microbial mat system growing on the sediment of the Black Sea. *Environ Microbiol* **10:** 1934-1947.

– Ku HH (1966). Notes on use of propagation of error formulas. *J Res Nbs C Eng Inst* **70C:** 263-273.

– Kvist T, Ahring BK, Westermann P (2007). Archaeal diversity in Icelandic hot springs. *FEMS Microbiol Ecol* **59:** 71-80.

– Labrenz M, Grote J, Mammitzsch K, Boschker HTS, Laue M, Jost G, *et al* (2013). *Sulfurimonas gotlandica* sp. nov., a chemoautotrophic and psychrotolerant epsilonproteobacterium isolated from a pelagic redoxcline, and an emended description of the genus *Sulfurimonas*. *Int J Syst Evol Microbiol* **63:** 4141–4148.

– Lagier JC, Armougom F, Million M, Hugon P, Pagnier I, Robert C *et al* (2012). Microbial culturomics: paradigm shift in the human gut microbiome study. *Clin Microbiol Infec* **18:** 1185-1193.

– Lane DJ (1991). 16S/23S rRNA sequencing. In: Stackebrandt E and Goodfellow M (eds) *Nucleic acid techniques in bacterial systematics* Wiley & Sons, Chichester, United Kingdom, pp 115-175.

– Lee MJ, Zinder SH (1988). Isolation and characterization of a thermophilic bacterium which oxidizes acetate in syntrophic association with a methanogen and which grows acetogenically on H_2-CO_2. *Appl Environ Microbiol* **54:** 124-129.

– Lever MA, Rogers KL, Lloyd KG, Overmann J, Schink B, Thauer RK *et al* (2015). Life under extreme energy limitation: a synthesis of laboratory- and field-based investigations. *FEMS Microbiol Rev* **39:** 688-728.

– Lloyd KG, Lapham L, Teske A (2006). Anaerobic methane-oxidizing community of ANME-1b archaea in hypersaline Gulf of Mexico sediments. *Appl Environ Microbiol* **72:** 7218-7230.

– Lloyd KG, Alperin MJ, Teske A (2011). Environmental evidence for net methane production and oxidation in putative ANaerobic MEthanotrophic (ANME) archaea. *Environ Microbiol* **13:** 2548-2564.

– Lloyd KG, Schreiber L, Petersen DG, Kjeldsen KU, Lever MA, Steen AD *et al* (2013). Predominant archaea in marine sediments degrade detrital proteins. *Nature* **496:** 215-218.

– Lösekann T, Knittel K, Nadalig T, Fuchs B, Niemann H, Boetius A *et al* (2007). Diversity and abundance of aerobic and anaerobic methane oxidizers at the Haakon Mosby mud volcano, Barents Sea. *Appl Environ Microbiol* **73:** 3348-3362.

– Lovley DR, Goodwin S (1988). Hydrogen concentrations as an indicator of the predominant terminal electron-accepting reactions in aquatic sediments. *Geochim Cosmochim Ac* **52:** 2993-3003.

– Lovley DR, Phillips EJP (1994). Novel processes for anaerobic sulfate production from elemental sulfur by sulfate-reducing bacteria. *Appl Environ Microbiol* **60:** 2394-2399.

– Ludwig W, Strunk O, Westram R, Richter L, Meier H, Yadhukumar *et al* (2004). ARB: a software environment for sequence data. *Nucleic Acids Res* **32:** 1363-1371.

– Lyimo TJ, Pol A, Harhangi HR, Jetten MSM, Op den Camp HJM (2009). Anaerobic oxidation of dimethylsulfide and methanethiol in mangrove sediments is dominated by sulfate-reducing bacteria. *FEMS Microbiol Ecol* **70:** 483-492.

– Maignien L, Parkes RJ, Cragg B, Niemann H, Knittel K, Coulon S *et al* (2013). Anaerobic oxidation of methane in hypersaline cold seep sediments. *FEMS Microbiol Ecol* **83:** 214-231.

– Manske AK, Glaeser J, Kuypers MM, Overmann J (2005). Physiology and phylogeny of green sulfur bacteria forming a monospecific phototrophic assemblage at a depth of 100 meters in the Black Sea. *Appl Environ Microbiol* **71:** 8049-8060.

– Manz W, Eisenbrecher M, Neu TR, Szewzyk U (1998). Abundance and spatial organization of gram-negative sulfate-reducing bacteria in activated sludge investigated by in situ probing with specific 16S rRNA targeted oligonucleotides. *FEMS Microbiol Ecol* **25:** 43-61.

– Martens CS, Berner RA (1974). Methane production in interstitial waters of sulfate-depleted marine sediments. *Science* **185:** 1167-1169.

– Martens CS, Berner RA (1977). Interstitial water chemistry of anoxic Long Island Sound sediments 1. Dissolved-gases. *Limnol Oceanogr* **22:** 10-25.

– Martens CS, Albert DB, Alperin MJ (1998). Biogeochemical processes controlling methane in gassy coastal sediments - Part 1. A model coupling organic matter flux to gas production, oxidation and transport. *Cont Shelf Res* **18:** 1741-1770.

– Martin R, Heilig GHJ, Zoetendal EG, Smidt H, Rodriguez JM (2007). Diversity of the *Lactobacillus* group in breast milk and vagina of healthy women and potential role in the colonization of the infant gut. *J Appl Microbiol* **103:** 2638-2644.

– Mayr S, Latkoczy C, Krüger M, Günther D, Shima S, Thauer RK *et al* (2008). Structure of an F430 variant from archaea associated with anaerobic oxidation of methane. *J Am Chem Soc* **130:** 10758-10767.

– Meulepas RJW, Jagersma CG, Gieteling J, Buisman CJN, Stams AJM, Lens PNL (2009a). Enrichment of Anaerobic Methanotrophs in Sulfate-Reducing Membrane Bioreactors. *Biotechnol Bioeng* **104:** 458-470.

− Meulepas RJW, Jagersma CG, Khadem AF, Buisman CJN, Stams AJM, Lens PNL (2009b). Effect of environmental conditions on sulfate reduction with methane as electron donor by an Eckernförde Bay enrichment. *Environ Sci Technol* **43:** 6553-6559.

− Meulepas RJ, Jagersma CG, Zhang Y, Petrillo M, Cai H, Buisman CJ *et al* (2010a). Trace methane oxidation and the methane dependency of sulfate reduction in anaerobic granular sludge. *FEMS Microbiol Ecol* **72:** 261-271.

− Meulepas RJ, Jagersma CG, Khadem AF, Stams AJ, Lens PNL (2010b). Effect of methanogenic substrates on anaerobic oxidation of methane and sulfate reduction by an anaerobic methanotrophic enrichment. *Appl Microbiol Biotechnol* **87:** 1499-1506.

− Meulepas RJW, Stams AJM, Lens PNL (2010c). Biotechnological aspects of sulfate reduction with methane as electron donor. *Rev Environ Sci Bio* **9:** 59-78.

− Meyerdierks A, Kube M, Lombardot T, Knittel K, Bauer M, Glöckner FO *et al* (2005). Insights into the genomes of archaea mediating the anaerobic oxidation of methane. *Environ Microbiol* **7:** 1937-1951.

− Meyerdierks A, Kube M, Kostadinov I, Teeling H, Glöckner FO, Reinhardt R *et al* (2010). Metagenome and mRNA expression analyses of anaerobic methanotrophic archaea of the ANME-1 group. *Environ Microbiol* **12:** 422-439.

− Michaelis W, Seifert R, Nauhaus K, Treude T, Thiel V, Blumenberg M *et al* (2002). Microbial reefs in the Black Sea fueled by anaerobic oxidation of methane. *Science* **297:** 1013-1015.

− Mills HJ, Hodges C, Wilson K, MacDonald IR, Sobecky PA (2003). Microbial diversity in sediments associated with surface-breaching gas hydrate mounds in the Gulf of Mexico. *FEMS Microbiol Ecol* **46:** 39-52.

− Mills HJ, Martinez RJ, Story S, Sobecky PA (2005). Characterization of microbial community structure in Gulf of Mexico gas hydrates: Comparative analysis of DNA- and RNA-derived clone libraries. *Appl Environ Microbiol* **71:** 3235-3247.

− Milucka J, Ferdelman TG, Polerecky L, Franzke D, Wegener G, Schmid M *et al* (2012). Zero-valent sulphur is a key intermediate in marine methane oxidation. *Nature* **491:** 541-546.

− Miyashita A, Mochimaru H, Kazama H, Ohashi A, Yamaguchi T, Nunoura T *et al* (2009). Development of 16S rRNA gene-targeted primers for detection of archaeal anaerobic methanotrophs (ANMEs). *FEMS Microbiol Lett* **297:** 31-37.

− Moran JJ, House CH, Freeman KH, Ferry JG (2005). Trace methane oxidation studied in several Euryarchaeota under diverse conditions. *Archaea* **1:** 303-309.

− Moran JJ, House CH, Thomas B, Freeman KH (2007). Products of trace methane oxidation during nonmethyltrophic growth by *Methanosarcina*. *J Geophys Res-Biogeo* **112:** G02011.

− Moran JJ, Beal EJ, Vrentas JM, Orphan VJ, Freeman KH, House CH (2008). Methyl sulfides as intermediates in the anaerobic oxidation of methane. *Environ Microbiol* **10:** 162-173.

− Murray JW, Grundmanis V, Smethie WM (1978). Interstitial water chemistry in the sediments of Saanich Inlet. *Geochim Cosmochim Ac* **42:** 1011-1026.

− Muyzer G, De Waal EC, Uitterlinden AG (1993). Profiling of complex microbial populations by denaturing gradient gel electrophoresis analysis of polymerase chain reaction-amplified genes coding for 16S rRNA. *Appl Environ Microbiol* **59:** 695-700.

− Nauhaus K, Boetius A, Krüger M, Widdel F (2002). In vitro demonstration of anaerobic oxidation of methane coupled to sulphate reduction in sediment from a marine gas hydrate area. *Environ Microbiol* **4:** 296-305.

− Nauhaus K, Treude T, Boetius A, Krüger M (2005). Environmental regulation of the anaerobic oxidation of methane: a comparison of ANME-I and ANME-II communities. *Environ Microbiol* **7:** 98-106.

– Nauhaus K, Albrecht M, Elvert M, Boetius A, Widdel F (2007). In vitro cell growth of marine archaeal-bacterial consortia during anaerobic oxidation of methane with sulfate. *Environ Microbiol* **9:** 187-196.

– Niemann H, Lösekann T, de Beer D, Elvert M, Nadalig T, Knittel K *et al* (2006). Novel microbial communities of the Haakon Mosby mud volcano and their role as a methane sink. *Nature* **443:** 854-858.

– Niewöhner C, Hensen C, Kasten S, Zabel M, Schulz HD (1998). Deep sulfate reduction completely mediated by anaerobic methane oxidation in sediments of the upwelling area off Namibia. *Geochim Cosmochim Ac* **62:** 455-464.

– Nübel U, Engelen B, Felske A, Snaidr J, Wieshuber A, Amann RI *et al* (1996). Sequence heterogeneities of genes encoding 16S rRNAs in *Paenibacillus polymyxa* detected by temperature gradient gel electrophoresis. *J Bacteriol* **178:** 5636-5643.

– Nunoura T, Oida H, Toki T, Ashi J, Takai K, Horikoshi K (2006). Quantification of mcrA by quantitative fluorescent PCR in sediments from methane seep of the Nankai Trough. *FEMS Microbiol Ecol* **57:** 149-157.

– Orcutt B, Boetius A, Elvert M, Samarkin V, Joye SB (2005). Molecular biogeochemistry of sulfate reduction, methanogenesis and the anaerobic oxidation of methane at Gulf of Mexico cold seeps. *Geochim Cosmochim Ac* **69:** 5633-5633.

– Orcutt B, Samarkin V, Boetius A, Joye S (2008). On the relationship between methane production and oxidation by anaerobic methanotrophic communities from cold seeps of the Gulf of Mexico. *Environ Microbiol* **10:** 1108-1117.

– Orcutt B, Meile C (2008). Constraints on mechanisms and rates of anaerobic oxidation of methane by microbial consortia: process-based modeling of ANME-2 archaea and sulfate-reducing bacteria interactions. *Biogeosciences* **5:** 1587-1599.

– Orcutt BN, Joye SB, Kleindienst S, Knittel K, Ramette A, Reitz A *et al* (2010). Impact of natural oil and higher hydrocarbons on microbial diversity, distribution, and activity in Gulf of Mexico cold-seep sediments. *Deep-Sea Res Pt Ii* **57:** 2008-2021.

– Orphan VJ, House CH, Hinrichs KU, McKeegan KD, DeLong EF (2001a). Methane-consuming archaea revealed by directly coupled isotopic and phylogenetic analysis. *Science* **293:** 484-487.

– Orphan VJ, Hinrichs KU, Ussler W, Paull CK, Taylor LT, Sylva SP *et al* (2001b). Comparative analysis of methane-oxidizing archaea and sulfate-reducing bacteria in anoxic marine sediments. *Appl Environ Microbiol* **67:** 1922-1934.

– Orphan VJ, House CH, Hinrichs KU, McKeegan KD, DeLong EF (2002). Multiple archaeal groups mediate methane oxidation in anoxic cold seep sediments. *P Natl Acad Sci USA* **99:** 7663-7668.

– Orphan VJ, Ussler W, Naehr TH, House CH, Hinrichs KU, Paull CK (2004). Geological, geochemical, and microbiological heterogeneity of the seafloor around methane vents in the Eel River Basin, offshore California. *Chem Geol* **205:** 265-289.

– Orphan VJ, Turk KA, Green AM, House CH (2009). Patterns of 15N assimilation and growth of methanotrophic ANME-2 archaea and sulfate-reducing bacteria within structured syntrophic consortia revealed by FISH-SIMS. *Environ Microbiol* **11:** 1777-1791.

– Ozuolmez D, Na H, Lever MA, Kjeldsen KU, Jørgensen BB, Plugge CM (2015). Methanogenic archaea and sulfate-reducing bacteria co-cultured on acetate: teamwork or coexistence? *Front Microbiol* **6:** 492.

– Pachiadaki MG, Kallionaki A, Dahlmann A, De Lange GJ, Kormas KA (2011). Diversity and spatial distribution of prokaryotic communities along a sediment vertical profile of a deep-sea mud volcano. *Microb Ecol* **62:** 655-668.

– Panganiban AT, Jr., Patt TE, Hart W, Hanson RS (1979). Oxidation of methane in the absence of oxygen in lake water samples. *Appl Environ Microbiol* **37:** 303-309.

– Parkes RJ, Cragg BA, Banning N, Brock F, Webster G, Fry JC *et al* (2007). Biogeochemistry and biodiversity of methane cycling in subsurface marine sediments (Skagerrak, Denmark). *Environ Microbiol* **9:** 1146-1161.

– Paul K, Nonoh JO, Mikulski L, Brune A (2012). "Methanoplasmatales," Thermoplasmatales-related archaea in termite guts and other environments, are the seventh order of methanogens. *Appl Environ Microbiol* **78:** 8245-8253.

– Pernthaler A, Dekas AE, Brown CT, Goffredi SK, Embaye T, Orphan VJ (2008). Diverse syntrophic partnerships from deep-sea methane vents revealed by direct cell capture and metagenomics. *Proc Natl Acad Sci USA* **105:** 7052-7057.

– Phelps CD, Kerkhof LJ, Young LY (1998). Molecular characterization of a sulfate-reducing consortium which mineralizes benzene. *FEMS Microbiol Ecol* **27:** 269-279.

– Phelps TJ, Conrad R, Zeikus JG (1985). Sulfate-dependent interspecies H_2 transfer between *Methanosarcina barkeri* and *Desulfovibrio vulgaris* during coculture metabolism of acetate or methanol. *Appl Environ Microbiol* **50:** 589-594.

– Pruesse E, Quast C, Knittel K, Fuchs BM, Ludwig W, Peplies J *et al* (2007). SILVA: a comprehensive online resource for quality checked and aligned ribosomal RNA sequence data compatible with ARB. *Nucleic Acids Res* **35:** 7188-7196.

– Pruesse E, Peplies J, Glöckner FO (2012). SINA: Accurate high-throughput multiple sequence alignment of ribosomal RNA genes. *Bioinformatics* **28:** 1823-1829.

– Qu L, Zhu F, Hong X, Gao W, Chen J, Sun X (2011). *Sunxiuqinia elliptica* gen. nov., sp. nov., a member of the phylum *Bacteroidetes* isolated from sediment in a sea cucumber farm. *Int J Syst Evol Microbiol* **61:** 2885-2889.

– Quast C, Pruesse E, Yilmaz P, Gerken J, Schweer T, Yarza P *et al* (2013). The SILVA ribosomal RNA gene database project: improved data processing and web-based tools. *Nucl Acids Res* **41:** D590-D596.

– Raghoebarsing AA, Pol A, van de Pas-Schoonen KT, Smolders AJP, Ettwig KF, Rijpstra WIC *et al* (2006). A microbial consortium couples anaerobic methane oxidation to denitrification. *Nature* **440:** 918-921.

– Reeburgh WS (1976). Methane consumption in Cariaco Trench waters and sediments. *Earth Planet Sc Lett* **28:** 337-344.

– Reeburgh WS (1980). Anaerobic methane oxidation - rate depth distributions in Skan Bay sediments. *Earth Planet Sc Lett* **47:** 345-352.

– Reeburgh WS (2007). Oceanic methane biogeochemistry. *Chem Rev* **107:** 486-513.

– Riedinger N, Formolo MJ, Lyons TW, Henkel S, Beck A, Kasten S (2014). An inorganic geochemical argument for coupled anaerobic oxidation of methane and iron reduction in marine sediments. *Geobiology* **12:** 172-181.

– Roalkvam I, Jørgensen SL, Chen YF, Stokke R, Dahle H, Hocking WP *et al* (2011). New insight into stratification of anaerobic methanotrophs in cold seep sediments. *FEMS Microbiol Ecol* **78:** 233-243.

– Roalkvam I, Dahle H, Chen Y, Jørgensen SL, Haflidason H, Steen IH (2012). Fine-scale community structure analysis of ANME in Nyegga sediments with high and low methane flux. *Front Microbiol* **3:** 216.

– Rossel PA, Elvert M, Ramette A, Boetius A, Hinrichs KU (2011). Factors controlling the distribution of anaerobic methanotrophc communities in marine environments: evidence from intact polar membrane lipids. *Geochem Cosmochim Acta* **75:** 164-184.

− Santegoeds CM, Damgaard LR, Hesselink G, Zopfi J, Lens P, Muyzer G *et al* (1999). Distribution of sulfate-reducing and methanogenic bacteria in anaerobic aggregates determined by microsensor and molecular analyses. *Appl Environ Microbiol* **65:** 4618-4629.

− Schnell S, Bak F, Pfennig N (1989). Anaerobic degradation of aniline and dihydroxybenzenes by newly isolated sulfate-reducing bacteria and description of *Desulfobacterium anilini*. *Arch Microbiol* **152:** 556-563.

− Schreiber L, Holler T, Knittel K, Meyerdierks A, Amann R (2010). Identification of the dominant sulfate-reducing bacterial partner of anaerobic methanotrophs of the ANME-2 clade. *Environ Microbiol* **12:** 2327-2340.

− Schubert CJ, Vazquez F, Lösekann-Behrens T, Knittel K, Tonolla M, Boetius A (2011). Evidence for anaerobic oxidation of methane in sediments of a freshwater system (Lago di Cadagno). *FEMS Microbiol Ecol* **76:** 26-38.

− Schwertmann U, Cornell RM (1991). Ferrihydrite. In: Schwertmann, U and Cornell, RM (eds) *Iron oxides in the Laboratory: preparation and characterization*. WILEY-VCH Verlag GmbH, pp 103-112.

− Segarra KEA, Schubotz F, Samarkin V, Yoshinaga MY, Hinrichs KU, Joye SB (2015). High rates of anaerobic methane oxidation in freshwater wetlands reduce potential atmospheric methane emissions. *Nat Commun* **6:** 7477.

− Segarra KEA, Comerford C, Slaughter J, Joye SB (2013). Impact of electron acceptor availability on the anaerobic oxidation of methane in coastal freshwater and brackish wetland sediments. *Geochim Cosmochim Ac* **115:** 15-30.

− Seifert R, Nauhaus K, Blumenberg M, Krüger M, Michaelis W (2006). Methane dynamics in a microbial community of the Black Sea traced by stable carbon isotopes in vitro. *Org Geochem* **37:** 1411-1419.

− Shigematsu T, Tang YQ, Kobayashi T, Kawaguchi H, Morimura S, Kida K (2004). Effect of dilution rate on metabolic pathway shift between aceticlastic and nonaceticlastic methanogenesis in chemostat cultivation. *Appl Environ Microbiol* **70:** 4048-4052.

− Sivan O, Adler M, Pearson A, Gelman F, Bar-Or I, John SG *et al* (2011). Geochemical evidence for iron-mediated anaerobic oxidation of methane. *Limnol Oceanogr* **56:** 1536-1544.

− Slobodkin AI, Reysenbach AL, Slobodkina GB, Kolganova TV, Kostrikina NA, Bonch-Osmolovskaya EA (2013). *Dissulfuribacter thermophilus* gen. nov., sp. nov., a thermophilic, autotrophic, sulfur-disproportionating, deeply branching deltaproteobacterium from a deep-sea hydrothermal vent. *Int J Syst Evol Microbiol* **63 (PT 6):** 1967-1971.

− Smemo KA, Yavitt JB (2007). Evidence for anaerobic CH_4 oxidation in freshwater peatlands. *Geomicrobiol J* **24:** 583-597.

− Sørensen KB, Finster K, Ramsing NB (2001). Thermodynamic and kinetic requirements in anaerobic methane oxidizing consortia exclude hydrogen, acetate, and methanol as possible electron shuttles. *Microbial Ecol* **42:** 1-10.

− Sorokin YI (1957). On the ability of sulfate-reducing bacteria to utilize methane for the reduction of sulfates to hydrogen sulfide. *Presented by Academician VN Shaposhnikov, May 9, 1957***:** 713-715.

− Stams AJM, Vandijk JB, Dijkema C, Plugge CM (1993). Growth of syntrophic propionate-oxidizing bacteria with fumarate in the absence of methanogenic bacteria. *Appl Environ Microbiol* **59:** 1114-1119.

− Stams AJM, Plugge CM (2009). Electron transfer in syntrophic communities of anaerobic bacteria and archaea. *Nat Rev Microbiol* **7:** 568-577.

− Steudel R, Gobel T, Holdt G (1988). The molecular composition of hydrophilic sulfur sols prepared by acid decomposition of thiosulfate 1. *Z Naturforsch B* **43:** 203-218.

− Stokke R, Roalkvam I, Lanzen A, Haflidason H, Steen IH (2012). Integrated metagenomic and metaproteomic analyses of an ANME-1-dominated community in marine cold seep sediments. *Environ Microbiol* **14:** 1333-1346.

− Stookey LL (1970). Ferrozine - a new spectrophotometric reagent for iron. *Anal Chem* **42:** 779-781.

− Suzuki MT, Beja O, Taylor LT, Delong EF (2001). Phylogenetic analysis of ribosomal RNA operons from uncultivated coastal marine bacterioplankton. *Environ Microbiol* **3:** 323-331.

− Takeuchi M, Yoshioka H, Seo Y, Tanabe S, Tamaki H, Kamagata Y *et al* (2011). A distinct freshwater-adapted subgroup of ANME-1 dominates active archaeal communities in terrestrial subsurfaces in Japan. *Environ Microbiol* **13:** 3206-3218.

− Teske A, Hinrichs KU, Edgcomb V, de Vera Gomez A, Kysela D, Sylva SP *et al* (2002). Microbial diversity of hydrothermal sediments in the Guaymas Basin: evidence for anaerobic methanotrophic communities. *Appl Environ Microbiol* **68:** 1994-2007.

− Teske A, Sørensen KB (2008). Uncultured archaea in deep marine subsurface sediments: have we caught them all? *ISME J* **2:** 3-18.

− Thauer RK, Kaster AK, Seedorf H, Buckel W, Hedderich R (2008). Methanogenic archaea: ecologically relevant differences in energy conservation. *Nat Rev Microbiol* **6:** 579-591.

− Thauer RK (2011). Anaerobic oxidation of methane with sulfate: on the reversibility of the reactions that are catalyzed by enzymes also involved in methanogenesis from CO_2. *Curr Opin Microbiol* **14:** 292-299.

− Thomsen TR, Finster K, Ramsing NB (2001). Biogeochemical and molecular signatures of anaerobic methane oxidation in a marine sediment. *Appl Environ Microbiol* **67:** 1646-1656.

− Treude T, Niggemann J, Kallmeyer J, Wintersteller P, Schubert CJ, Boetius A *et al* (2005a). Anaerobic oxidation of methane and sulfate reduction along the Chilean continental margin. *Geochim Cosmochim Acta* **69:** 2767-2779.

− Treude T, Krüger M, Boetius A, Jørgensen BB (2005b). Environmental control on anaerobic oxidation of methane in the gassy sediments of Eckernförde Bay (German Baltic). *Limnol Oceanogr* **50:** 1771-1786.

− Treude T, Knittel K, Blumenberg M, Seifert R, Boetius A (2005c). Subsurface microbial methanotrophic mats in the Black Sea. *Appl Environ Microbiol* **71:** 6375-6378.

− Treude T, Orphan V, Knittel K, Gieseke A, House CH, Boetius A (2007). Consumption of methane and CO_2 by methanotrophic microbial mats from gas seeps of the anoxic Black Sea. *Appl Environ Microbiol* **73:** 2271-2283.

− Valentine DL, Blanton DC, Reeburgh WS (2000). Hydrogen production by methanogens under low-hydrogen conditions. *Arch Microbiol* **174:** 415-421.

− Valentine DL, Reeburgh WS (2000). New perspectives on anaerobic methane oxidation. *Environ Microbiol* **2:** 477-484.

− Valentine DL (2002). Biogeochemistry and microbial ecology of methane oxidation in anoxic environments: a review. *Anton Leeuw Int J G* **81:** 271-282.

− van Breukelen BM, Griffioen J (2004). Biogeochemical processes at the fringe of a landfill leachate pollution plume: potential for dissolved organic carbon, Fe(II), Mn(II), NH4, and CH_4 oxidation. *J Contam Hydrol* **73:** 181-205.

− van den Bogert B, de Vos WM, Zoetendal EG, Kleerebezem M (2011). Microarray analysis and barcoded pyrosequencing provide consistent microbial profiles depending on the source of human intestinal samples. *Appl Environ Microbiol* **77:** 2071-2080.

− van Diggelen JMH, Lamers LPM, van Dijk G, Schaafsma MJ, Roelofs JGM, Smolders AJP (2014). New insights into phosphorous mobilisation from sulphur-rich sediments: time-dependent effects of salinisation. *PloS one* **9:** e111106.

− Vanwonterghem I, Jensen PD, Dennis PG, Hugenholtz P, Rabaey K, Tyson GW (2014). Deterministic processes guide long-term synchronised population dynamics in replicate anaerobic digesters. *ISME J* **8:** 2015-2028.

− Vetriani C, Tran HV, Kerkhof LJ (2003). Fingerprinting microbial assemblages from the oxic/anoxic chemocline of the Black Sea. *Appl Environ Microbiol* **69:** 6481-6488.

− Vigneron A, Cruaud P, Pignet P, Caprais JC, Cambon-Bonavita MA, Godfroy A *et al* (2013a). Archaeal and anaerobic methane oxidizer communities in the Sonora Margin cold seeps, Guaymas Basin (Gulf of California). *ISME J* **7:** 1595-1608.

− Vigneron A, Cruaud P, Pignet P, Caprais JC, Gayet N, Cambon-Bonavita MA *et al* (2013b). Bacterial communities and syntrophic associations involved in anaerobic oxidation of methane process of the Sonora Margin cold seeps, Guaymas Basin. *Environ Microbiol* **16:** 2777-2790.

− Vossmeyer A, Deusner C, Kato C, Inagaki F, Ferdelman TG (2012). Substrate-specific pressure-dependence of microbial sulfate reduction in deep-sea cold seep sediments of the Japan Trench. *Front Microbiol* **3:** 253.

− Wang FP, Zhang Y, Chen Y, He Y, Qi J, Hinrichs KU *et al* (2014). Methanotrophic archaea possessing diverging methane-oxidizing and electron-transporting pathways. *ISME J* **8:** 1069-1078.

− Wang GZ, Spivack AJ, D'Hondt S (2010). Gibbs energies of reaction and microbial mutualism in anaerobic deep subseafloor sediments of ODP Site 1226. *Geochim Cosmochim Acta* **74:** 3938-3947.

− Wang Y, Qian PY (2009). Conservative fragments in bacterial 16S rRNA genes and primer design for 16S ribosomal DNA amplicons in metagenomic studies. *PloS one* **4:** e7401.

− Wankel SD, Adams MM, Johnston DT, Hansel CM, Joye SB, Girguis PR (2012). Anaerobic methane oxidation in metalliferous hydrothermal sediments: influence on carbon flux and decoupling from sulfate reduction. *Environ Microbiol* **14:** 2726-2740.

− Webster G, Sass H, Cragg BA, Gorra R, Knab NJ, Green CJ *et al* (2011). Enrichment and cultivation of prokaryotes associated with the sulphate-methane transition zone of diffusion-controlled sediments of Aarhus Bay, Denmark, under heterotrophic conditions. *FEMS Microbiol Ecol* **77:** 248-263.

− Wegener G, Boetius A (2009). An experimental study on short-term changes in the anaerobic oxidation of methane in response to varying methane and sulfate fluxes. *Biogeosciences* **6:** 867-876.

− Wright ES, Yilmaz LS, Noguera DR (2012). DECIPHER, a search-based approach to chimera identification for 16S rRNA sequences. *Appl Environ Microbiol* **78:** 717–725.

− Wu ZJ, Zhou HY, Peng XT, Chen GQ (2006). Anaerobic oxidation of methane: geochemical evidence from pore-water in coastal sediments of Qi'ao Island (Pearl River Estuary), southern China. *Chinese Sci Bull* **51:** 2006-2015.

− Yamamoto S, Alcauskas JB, Crozier TE (1976). Solubility of methane in distilled water and seawater. *J Chem Eng Data* **21:** 78-80.

− Yanagawa K, Sunamura M, Lever MA, Morono Y, Hiruta A, Ishizaki O *et al* (2011). Niche separation of methanotrophic archaea (ANME-1 and -2) in methane-seep sediments of the Eastern Japan Sea offshore Joetsu. *Geomicrobiol J* **28:** 118-129.

− Yoshinaga MY, Holler T, Goldhammer T, Wegener G, Pohlman JW, Brunner B *et al* (2014). Carbon isotope equilibration during sulphate-limited anaerobic oxidation of methane. *Nat Geosci* **7:** 190-194.

– Yoshioka H, Maruyama A, Nakamura T, Higashi Y, Fuse H, Sakata S *et al* (2010). Activities and distribution of methanogenic and methane-oxidizing microbes in marine sediments from the Cascadia Margin. *Geobiology* **8:** 223-233.

– Yu Y, Lee C, Kim J, Hwang S (2005). Group-specific primer and probe sets to detect methanogenic communities using quantitative real-time polymerase chain reaction. *Biotechnol Bioeng* **89:** 670-679.

– Yu ZT, Garcia-Gonzalez R, Schanbacher FL, Morrison M (2008). Evaluations of different hypervariable regions of archaeal 16S rRNA genes in profiling of methanogens denaturing by archaea-specific PCR and gradient gel electrophoresis. *Appl Environ Microbiol* **74:** 889-893.

– Zehnder AJ, Brock TD (1980). Anaerobic methane oxidation: occurrence and ecology. *Appl Environ Microbiol* **39:** 194-204.

– Zehnder AJB, Brock TD (1979). Methane formation and methane oxidation by methanogenic bacteria. *J Bacteriol* **137:** 420-432.

– Zhang GS, Jiang N, Liu XL, Dong XZ (2008). Methanogenesis from methanol at low temperatures by a novel psychrophilic methanogen, "*Methanolobus psychrophilus*" sp nov., prevalent in Zoige wetland of the Tibetan plateau. *Appl Environ Microbiol* **74:** 6114-6120.

– Zhang Y, Henriet JP, Bursens J, Boon N (2010). Stimulation of in vitro anaerobic oxidation of methane rate in a continuous high-pressure bioreactor. *Bioresour Technol* **101:** 3132-3138.

– Zhang Y, Maignien L, Zhao X, Wang F, Boon N (2011). Enrichment of a microbial community performing anaerobic oxidation of methane in a continuous high-pressure bioreactor. *BMC Microbiol* **11:** 137.

Summary

Anaerobic oxidation of methane (AOM) coupled to sulfate reduction (SR) is a widespread occurring process in anoxic marine sediments. The process is performed by ANaerobic MEthane oxidizing archaea (ANME) and associated sulfate reducing bacteria (SRB). The ANME presumably oxidize methane through reverse methanogenesis. The associated SRB were thought to reduce sulfate using an interspecies electron carrier (IEC) derived from AOM. The product of methane oxidation that is transferred to the SRB is either a less reduced compound that acts as IEC or electrons are transferred directly (through nanowires or pili) or indirectly (through extracellular quinones). However, recent evidence emerged that ANME could perform both methane oxidation and sulfate reduction to produce sulfur, where the SRB disproportionate the produced sulfur. Little is known on the physiology and ecology of these ANME and associated SRB. The main reasons for this are the difficulties in lab cultivation and to perform *in situ* studies.

Anaerobic methane oxidation is a process that is at the border of what is energetically possible for sustaining life, which makes it hard to cultivate the responsible organisms. Estimates of the Gibbs free energy yields are between -18 and -35 kJ mol^{-1} and growth rates between 1.1 and 7.5 months, depending on the environment. AOM therefore operates close to thermodynamic equilibrium and is highly dependent on substrate and product concentrations. In **chapter 2**, we obtained faster growth rates at elevated methane partial pressure as compared to ambient pressure. The increase in partial pressure increased the solubility of methane and thus the energy yield for the organisms. In **chapter 6**, we showed higher AOM activity and growth of ANME under thermodynamically favorable sulfate and sulfide concentrations. The problems in studying the process *in situ* in complex environments comes from difficulties in differentiation of reversible processes. In most studies, methane oxidation is monitored by labelled CO_2 formation from labelled methane. Methanogens can perform trace methane oxidation (TMO) during net methanogenesis, which also results in the production of labelled CO_2 from labelled methane. When AOM becomes less favorable, the anaerobic back flux of AOM becomes significant, leading to the production of measurable amounts of methane. In **chapter 2** and **chapter 3**, we were able to differentiate between AOM and TMO in long-term incubations.

Another challenge is related to the detection of ANME in complex environments. The phylogenetic distance between and within ANME clades is large. In **chapter 5**, we discussed the difficulties in primer and probe design for selective detection of ANME without targeting closely related methanogens. Furthermore, it is not known if even more ANME species and clades have yet to be discovered that are not detected with the primers and probes used thus far. In **chapter 3**, we found indications that besides ANME-2a/b, ANME-2d archaea were also able to perform AOM coupled to sulfate reduction in freshwater conditions. The finding of ANME-2a/b in freshwater shows that ANME archaea are ubiquitously distributed and not only occur in marine sediments. In **chapter 6**, we confirmed that different ANME clades show niche

separation based on the presence of methane and different sulfate and sulfide concentrations. In **chapter 2**, we obtained indications that ANME-2c grows at high methane partial pressure. More research on the ecophysiology could help in understanding occurrence and activity of ANME in different environments.

Many different SRB have been found so far to form close associations with ANME. Most fall within the *Desulfosarcina/Desulfococcus* (DSS) clade and only for two enrichment cultures the dominant partner of ANME-2a/b was determined to belong to a specific group with the DSS named SEEP-SRB1. In **chapter 2**, we found more evidence that a group outside the DSS clade, SEEP-SRB2, could also associate with ANME-2a/b and that Eel-1 members are not directly involved in AOM. In **chapter 4**, we enriched for SRB within the DSS clade on alternative substrates besides methane, but we were unable to show that these are involved in AOM. Therefore, more research on the sulfate-reducing partner is needed to understand the metabolic interactions between ANME and SRB.

Samenvatting

Anaerobe oxidatie van methaan (AOM) gekoppeld aan sulfaatreductie (SR) is een proces dat wijdverspreid voorkomt in zuurstofloze mariene sedimenten. Het proces wordt uitgevoerd door anaerobe methaan-oxiderende archaea (ANME) die samen leven met sulfaat-reducerende bacteriën (SRB). De ANME oxideren het methaan, waarschijnlijk door middel van omgekeerde methanogenese. De geassocieerde SRB reduceren sulfaat en gebruiken daarvoor de elektronen die vrijkomen bij methaanoxidatie. Voor de elektronenoverdracht wordt een inter-soortelijke elektron drager (IEC) gebruikt, maar het is niet duidelijk in welke vorm. Dit kan bijvoorbeeld een minder gereduceerde stof dan methaan zijn dat verder geoxideerd wordt door de SRB. Het kan ook dat elektronen direct (via nanodraden of pili) of indirect (via extraceullaire quinones) overgedragen worden. Recentelijk is er bewijs ontstaan dat ANME methaan oxideren én sulfaat reduceren, waarbij elementair zwavel wordt geproduceerd. De SRB nemen dit zwavel op als polysulfide en dismuteren het naar sulfaat en sulfide. Er is dus weinig bekend over de fysiologie en ecologie van ANME en de samenlevende SRB. De grootse redenen hiervoor zijn de moeilijkheden met het cultiveren in het lab en het bestuderen in de omgeving.

Anaerobe oxidatie van methaan is een proces dat zich voltrekt op de grens van wat energetisch mogelijk is om leven te onderhouden. De geschatte Gibbs vrije energie opbrengst van dit proces is tussen -18 en -35 kJ mol^{-1} en groeisnelheden zijn tussen 1.1 en 7.5 maanden, afhankelijk van de omgeving. AOM opereert dus zeer dicht bij het thermodynamisch evenwicht en is daarom zeer afhankelijk van substraat en product concentraties. In **hoofdstuk 2** zijn snellere groeisnelheden bereikt bij hogere partiële methaan druk vergeleken met atmosferische druk. Dit komt doordat verhoging van de druk de oplosbaarheid van methaan en dus de energie opbrengst voor de organismen verhoogt. In **hoofdstuk 6** laten we hogere AOM activiteit en groei van ANME zien onder thermodynamisch gunstige concentraties van sulfaat en sulfide. Het probleem voor het bestuderen van AOM in een complexe omgeving, komt doordat het moeilijk is om AOM te onderscheiden van andere processen die ook omkeerbaar zijn. In de meeste studies wordt methaanoxidatie bestudeerd door productie van stabiele isotoop gelabeld CO_2 uit methaan. Methaanvorming kan ook gelabeld CO_2 produceren tijdens 'spoor methaan oxidatie'. Daarnaast kan AOM, wanneer het energetisch minder gunstig is, ook omgekeerd worden en wordt er methaan gevormd tijdens AOM. Dit leidt tot meetbare hoeveelheden methaan. In **hoofdstuk 2** en **hoofdstuk 3** hebben we onderscheid weten te maken tussen AOM en 'spoor methaan-oxidatie'.

Een andere uitdaging is gerelateerd aan de detectie van ANME in complexe omgevingen. De fylogenetische afstand tussen, en binnen ANME groepen is groot. In **hoofdstuk 5** bediscussiëren we de moeilijkheden in primer en probe ontwikkeling voor selectieve detectie van ANME zonder nauw verwante methanogenen te detecteren. Daarnaast is het ook niet duidelijk of meer ANME soorten en groepen nog ontdekt moeten worden die niet gedetecteerd

worden met de primers en probes die tot dusverre bestaan. In **hoofdstuk 3** vonden we indicaties dat naast ANME-2a/b, ANME-2d archaea ook mogelijkerwijs AOM gekoppeld aan SR kunnen uitvoeren in zoetwater condities. De vinding van ANME-2a/b in zoetwater laat zien dat ANME archaea alom aanwezig zijn en niet alleen in marine sedimenten voorkomen. In **hoofdstuk 6** bevestigen we dat verschillende ANME groepen een niche verdeling laten zien dat gebaseerd is op de aanwezigheid van methaan en verschillende sulfaat- en sulfide concentraties. In **hoofdstuk 2** laten we zien dat ANME-2c onder hoge partiële methaan-druk groeit. Meer onderzoek naar de ecofysiologie zou kunnen helpen in het begrijpen van de aanwezigheid en activiteit van verschillende ANME archaea in verscheidenheid van omgevingen.

Veel verschillende SRB zijn gevonden die samen leven met ANME archaea. De meeste van deze SRB vallen in de *Desulfosarcina/Desulfococcus* (DSS) cluster. In twee ophopingsculturen is vastgesteld dat de dominante partner van ANME-2a/b een subgroep vormt in deze cluster, genaamd SEEP-SRB1. In **hoofdstuk 2** vonden we bewijs dat een groep buiten de DSS, genaamd SEEP-SRB2, ook associaties heeft met ANME-2a/b. Verder vonden we dat SRB leden behorende bij de 'Eel-1' niet direct betrokken zijn bij AOM. In **hoofdstuk 4** zijn ophopingculturen gemaakt van SRB binnen de DSS cluster op alternatieve substraten voor methaan. We hebben niet aan kunnen tonen of deze SRB betrokken zijn bij AOM. Daarom is er meer onderzoek nodig naar de sulfaat-reducerende partner van ANME om de metabolische interacties tussen ANME en de SRB te begrijpen.

Co-author affiliations

Alfons J. M. Stams, Caroline M. Plugge, H. C. Aura Widjaja-Greefkes, Martijn Diender, Fridtjof H. Treppke, Ahmad F. Khadem, Daan van Vliet, Minke van Rossum, Javier Ramiro-Garcia

Laboratory of Microbiology, Wageningen University, Dreijenplein 10, 6703 HB Wageningen, The Netherlands.

Alfons J. M. Stams

Centre of Biological Engineering, University of Minho, Braga, Portugal.

Javier Ramiro-Garcia

Laboratory of Systems and Synthetic Biology, Wageningen University, Wageningen, The Netherlands.

Caroline M. Plugge, Roel J. W. Meulepas

European Centre of Excellence for Sustainable Water Technology, Wetsus, Leeuwarden, The Netherlands.

Piet N. L. Lens

IHE: Pollution Prevention and Control Core, UNESCO-IHE, Delft, The Netherlands.

Diego A. Suarez Zuluaga, Jarno Gieteling , Roel J. W. Meulepas

Sub-Department of Environmental Technology, Wageningen University, Wageningen, The Netherlands.

Acknowledgements/Dankwoord

Ten eerste wil ik natuurlijk mijn begeleider en promotor Fons en co-promotor Caroline bedanken. Fons, je hart voor de pure wetenschap en de onvoorwaardelijke hulp die je mensen geeft dient als een groot voorbeeld voor mij. Je naderend pensioen betekent dat we een echte wetenschapper minder zullen hebben, waarvan er misschien al te weinig zijn. Caroline, jou als co-promotor in het project was onmisbaar. Ik heb erg veel gehad aan je 'hands-on' mentaliteit en je directheid in communicatie. Toen ik kwam solliciteren voor de PhD positie werd 25 jaar syntrophy tussen Fons en Caroline gevierd. Die syntrophy tussen Fons en Caroline is misschien net zo obligaat als in anaerobe methanotrophy. De expertise van Caroline en Fons sloten vaak naadloos aan tijdens het op -en neer gaan van manuscripten. Ik denk dat ik geen betere begeleiders heb kunnen wensen.

Diego, my partner in crime at Environmental Technology, thanks for all the joint meetings, (scientific) conversations, and joint experiments. I also enjoyed the sulphur conference and the beers and dinner we had. We have to do this more often!

Aura, samenwerken aan dit project met jou met de bijkomende qPCR frustraties heeft uiteindelijk zijn vruchten afgeworpen. Ik vond het een prettige tijd en het was fijn om te weten dat jij ook altijd uitkeek naar die 2 (of 3) dagen in de week dat je bij ons kwam werken. Ik wens je al het beste in de toekomst!

In het begin van het project was Roel als postdoc de ervaren wetenschapper die ons op het vakgebied kon inwerken. Zijn kennis en ervaring na zijn PhD bij Milieuwetenschappen met deze moeizame groeiers was ontzettend waardevol. Roel, bedankt voor alle hulp die essentieel was voor ons en ik hoop dat we in de toekomst nog eens samen mogen werken.

Christian als mijn voorganger op het project bij Microbiologie heeft me op het begin (en nog een flinke tijd erna) kunnen helpen met het ontcijferen van oude data en het vinden van incubaties die mogelijkerwijs na 4 jaar in de log fase van groei waren gekomen. Bedankt voor je geduld!

Naast de mensen die direct in het project betrokken waren, waren Wim en Ton onmisbaar tijdens het traject. Ton, bedankt voor het uitleggen van alle apparatuur en het geven van al het advies voor het fatsoenlijk cultiveren. Wim, ik sta ervan te kijken hoe je met alle vragen over computers tot kabels en openen van fietssloten altijd je geduld weet te behouden en bijna nooit een vraag met 'nee' hebt beantwoord. Geweldig.

Ook zonder Anja en Carolien was het me niet gelukt. Mede door mijn geordende administratie ben ik regelmatig binnen komen lopen waardoor Carolien (ik citeer) "mij zelfs gemist had na de vakantie". Ook hier moet ik zeggen dat ik onder de indruk ben van de eeuwige behulpzaamheid en geduld.

I would also like to thank everybody that was involved in this STW project for attending meetings and giving useful feedback on our results: Ron Winkler, Gerard Muyzer, Melike Balk, Paul Mason, Gijs van Heeringen, Henk Dijkman, Paula Gonzáles Contreras, Jacco Huisman, Jan Weijma en Cees Buisman.

Obviously, my dear office mates of office 0.012 cannot be left out in this list. Although we had many different people in our office throughout the years, I enjoyed the good times with all of you: Michael, Joanna, Rejoan Reza, Bryan, Petra, Nam, Susakul and Yuan. I especially need to thank the officemates that were there when I was in the last period of writing, since they had to cope with a 'less communicative' person: Nam, Yuan and Susakul: thanks for all the fun conversations.

Michael is degene waar ik de meeste tijd mee heb doorgebracht in het kantoor. Ik vond het ook erg tof om samen practicum te geven en ik hoop dat je toch echt leraar wordt, want dat zit in je bloed. Ik vond het prachtig dat we verschillende interesses hebben (daily dose of cuteness?) en (mede daardoor) veel konden lachen. Ook de stoelendans op je bruiloft ging goed, jammer dat ik verloor van een kind.

Here I want to refer to the thesis of Martin to thank the 'all-weather lunch group': Thomas, Michael, Martin and Bram. This group was occasionally accompanied by others, but the hardcore group never died.

Thanks to Anna Paulo and Teun Veuskens for the 'around-coffee-and-lunch-breaks' breaks where we conversed about standard deviations and other deviating topics. Teun, ook bedankt voor het samplen in Berkhout. Je bent erg handig en (zoals je toen zei) hoop ik dat je daar nog iets mee gaat doen.

Ineke en Hans, bedankt voor de hulp bij mijn eerste DNA extracties en DGGE's. Ineke, bedankt dat je tijd had om te graven in je labjournaals naar data van het oude project. Hans, bedankt voor de introductie in de klassieke muziek.

Obviously I want to thank everybody from MICFYS! You provided a good working atmosphere where we learned a lot from each other. Some people I need to thank personally such as Ana Luisa Arrantes for doing incubations with carbon monoxide and Michael, Vicente and Niko for doing the practical courses together. Vicente, good luck in Finland (stay in the sauna!) and Niko, a teacher is definitely in your blood!

Furthermore, I want to thank the sampling crew when we went to Arhus Bay, Denmark: Mark Lever, Kasper Kjeldsen, Hans Roy, Bo Barker Jørgenson, Derya, Martin and Caroline. Hyunsoo Na, thanks for the nice times before and after sampling in Denmark and in The Netherlands!

I also would like to thank the students that I worked with. I had a really good time in supervising you, especially when I saw that all of you performed great independently: Martijn, Fridtjof (aka Hauke), Daan and Minke.

I also greatly enjoyed the PhD trip to China. Teun, Sven, Ruud, Edze, Bas, Bram, Jing Zhang, Oylum, Mauricio, Elleke, Jimmy, Tessa and Michael significantly contributed to the quality of my time there. Also thanks to some of these people as usual suspects for the occasional visits to the international club.

Lastly, I want to thank all people not involved in the project or the Wageningen life but who were equally important to me:

Mijn bands 'General Midnight' (Kneel, Nick, Marijn, Martijn, Luuk) en 'Paksoi' (Johnny, Wessel, Theo, Harmen en mijn broer Ties) gaven me de mogelijkheid om even te ontsnappen aan mijn PhD. Compleet de gedachte verzetten lukte alleen maar als ik aan het drummen was. ONMISBAAR.

Yvette, bedankt voor alle gesprekken en tips over het AIO leven, vooral via gmail chat hebben we aardig wat uitgewisseld hierover. Je was toch een beetje het voorbeeld voor me!

Mijn vrienden, waarmee ik juist niet over werk hoefde te praten en waar ik altijd op kon rekenen voor vertier: mijn vrienden van de studietijd in Nijmegen, mijn goede oude Brabantse vrienden voor het leven, de Partizanen en mijn oud-huisgenoten van huize Spoorzicht. Bedankt allemaal!

Mijn ouders en broers (Ties en Jan): jullie hebben mij altijd gesteund en hebben me meer gegeven dan nodig. Pap en mam, bedankt voor alles. Jan, bedankt voor alle goede gesprekken aan de bar in Trianon, daar genoot ik altijd van. Ties, bedankt voor alle muzikale avondjes en de Pizza van Smaragdplein.

Irene, my biggest accomplishment during the PhD. Thanks for all the great times, the patience while I was writing the thesis, the great care with my time of sickness and with all your help in the background which in the end turns out to be quite a significant part. Je bent de beste.

About the author

Peer Hendrik Anton Timmers was born on January 13th, 1983 in "Heerlijkheid" Gemert, The Netherlands. In 2000, he obtained his "HAVO" diploma at the Commanderij College in Gemert, after which he studied to become a teacher in Biology at the HAN University of Applied Sciences in Nijmegen, The Netherlands. After one year, he obtained his propaedeutic diploma and went to study Biology at the Radboud University Nijmegen (RUN) in 2001. His first MSc internship research was done at the Department of (Ecological) Microbiology (RUN) in 2004, where he studied marine Crenarchaeotes that performed nitrification. Research was also done at the Royal Netherlands Institute for Sea Research (NIOZ) at Texel during that period.

Afterwards, the second MSc internship was done at the Netherlands Institute of Ecology of the Netherlands Royal Academy for Sciences (NIOO-KNAW), Centre for Terrestrial Ecology (CTE). He tested and validated phylogenetic microarrays for detection of soil bacteria and he conducted research on the bacterial composition of different soils in the Netherlands. Work was also done at the department of Microbiology from Wageningen University (WUR) and the Fungal Biodiversity Centre (CBS-KNAW) at Utrecht during this period. In February 2007, he obtained his master degree after which he worked for two years at Organon NV (which was renamed to Schering-Plough and MSD during that period). In 2010, he started his PhD research at the Laboratory of Microbiology at Wageningen University.

List of publications

Timmers PHA, Gieteling J, HC Aura Widjaja-Greefkes, Plugge CM, Stams AJM, Lens PNL, Meulepas RJW (2015). Growth of anaerobic methane-oxidizing archaea and sulfate-reducing bacteria in a high pressure membrane capsule bioreactor. *Appl Environ Microbiol* **81:** 1286-1296.

Timmers PHA, HC Aura Widjaja-Greefkes, Ramiro-Garcia J, Plugge CM, Stams AJM (2015). Growth and activity of ANME clades with different sulfate and sulfide concentrations in the presence of methane. *Front Microbiol* **6:** 988. doi: 10.3389/fmicb.2015.00988.

Timmers PHA, Suarez-Zuluaga D, van Rossem M, Diender M, Stams AJM, Plugge CM. Anaerobic oxidation of methane associated with sulfate reduction in a natural freshwater gas source, *accepted in The ISME Journal.*

Jagersma CG, Meulepas RJ, **Timmers PH**, Szperl A, Lens PN, Stams AJ (2012). Enrichment of ANME-1 from Eckernförde Bay sediment on thiosulfate, methane and short-chain fatty acids. *J Biotechnol* **157:** 482-489.

Suarez-Zuluaga D, Weijma J, **Timmers PHA**, Buisman CJN (2015). High rates of anaerobic oxidation of methane, ethane and propane coupled to thiosulfate reduction. *Environ Sci Pollut Res Int* **22:** 3697-3704.

Suarez-Zuluaga D, **Timmers PHA**, Plugge CM, Stams AJM, Buisman CJN, Weijma J. Thiosulphate conversion in a methane and acetate fed membrane bioreactor, *Environ Sci Pollut Res Int,* Oct 1, Epub ahead of print. doi: 10.1007/s11356-015-5344-3.

Wuchter, C, Abbas B, Coolen MJL, Herfort L, van Bleijskwijk J, **Timmers P**, Strous M, Teira E, Herndl G, Middelburg JJ, Schouten S, Sinnighe Damsté JS (2006). Archaeal nitrification in the ocean. *Proc Natl Acad Sci USA* **103:** 12317-12322.

Netherlands Research School for the
Socio-Economic and Natural Sciences of the Environment

D I P L O M A

For specialised PhD training

The Netherlands Research School for the
Socio-Economic and Natural Sciences of the Environment
(SENSE) declares that

Peer Timmers

born on 13 January 1983 in Gemert, The Netherlands

has successfully fulfilled all requirements of the
Educational Programme of SENSE.

Wageningen, 4 December 2015

the Chairman of the SENSE board

Prof. dr. Huub Rijnaarts

the SENSE Director of Education

Dr. Ad van Dommelen

The SENSE Research School has been accredited by the Royal Netherlands Academy of Arts and Sciences (KNAW)

K O N I N K L I J K E   N E D E R L A N D S E
A K A D E M I E   V A N   W E T E N S C H A P P E N

The SENSE Research School declares that **Mr Peer Timmers** has successfully fulfilled all requirements of the Educational PhD Programme of SENSE with a work load of 52.5 EC, including the following activities:

SENSE PhD Courses

o   Environmental Research in Context (2011)
o   Principles of Ecological Genomics (2011)
o   Research in Context Activity: Organising SENSE symposium 'Microbes for sustainability' (2012)

Other PhD and Advanced MSc Courses

o   Advanced Course Environmental Biotechnology, Delft University of Technology (2011)
o   Applied molecular microbiology, Wageningen University (2011)
o   Scientific writing, Wageningen University (2012)
o   Project and time management, Wageningen University (2013)

External training at a foreign research institute

o   ARB software course, Max Planck Institute for Marine Microbiology (MPI), Bremen, Germany (2012)

Management and Didactic Skills Training

o   Teaching practicals for BSc course 'Microbial Physiology' (2011-2014)
o   Teaching Research Methods for BSc and MSc students (2014-2015)
o   Supervising three MSc students and one BSc student (2012-2014)
o   Teaching Capita Selecta 'Methanotrophic pathway in Anaerobic methane oxidizing archaea / sulfate reducer consortium' (2012) and 'FISH on enrichment samples for detection of sulfate reducing bacteria' (2014)

Selection of Oral Presentations

o   *Anaerobic methane oxidation for biological sulfate reduction*. SENSE Symposium 'Microbes for sustainability', 4-5 April 2012, Wageningen, The Netherlands
o   *Growth and development of anaerobic methane oxidizing archaea and sulfate reducing bacteria in a high pressure membrane-capsule bioreactor*. Annual Conference of the Association for General and Applied Microbiology (VAAM) in collaboration with the Royal Netherlands Society of Microbiology (KNVM), 10-13 March 2013, Bremen, Germany
o   *Growth of anaerobic methane oxidizing archaea and sulfate reducing bacteria in a high pressure membrane-capsule bioreactor*. The International Society for Microbial Ecology (ISME) Symposium, 24-29 August 2014, Seoul, South-Korea

SENSE Coordinator PhD Education

Dr. ing. Monique Gulickx